1 Combined Loading

Learning Summary

1. Know how to use Mohr's circle to analyse a general state of plane stress (knowledge);
2. Recognise that the effect of combined loads on a component can be analysed by considering each load as initially having an independent effect (comprehension);
3. Employ the principle of superposition to determine the combined effect of these loads (application).

1.1 Introduction

Many engineering problems can be analysed as simple load situations e.g. uniaxial loading, beam bending, torsion etc. However, it is also very common in the real world for engineering components and structures to be subjected to several loads simultaneously. This is a **combined loading** situation and can be analysed by superposing the effects of the individual loads.

1.2 Mohr's Circle Recap

Mohr's circle for plane stress is a useful graphical technique for analysing plane stresses acting on an element in a material or structure. For combined loading situations, it is common to reduce the problem to such a plane stress problem and analyse using Mohr's circle. The analysis will give the principal stresses, the maximum shear stresses and the angles of the principal planes for the element. Figure 1.1 shows a shaft subjected to combined loading of a torque, T, and a compressive axial load, P.

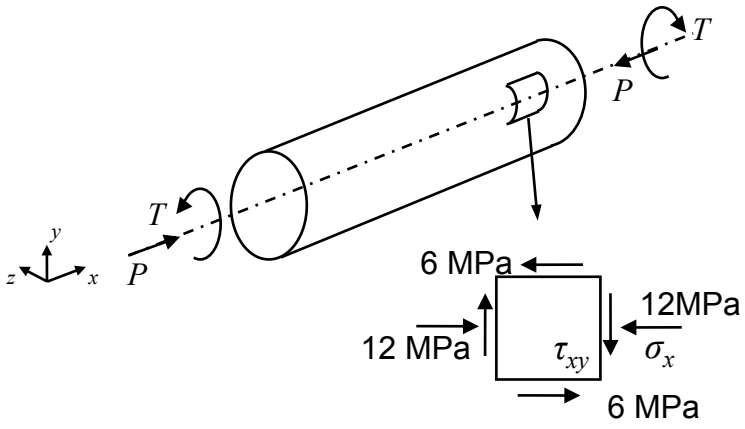

Figure 1.1

Let us assume that the loading gives rise to an axial stress of -12 MPa (i.e. compressive) and a shear stress of -6 MPa (i.e. causes element to rotate clockwise) acting on a surface element as shown in the figure. The Mohr's circle analysis is then as follows:

The known stresses on the element are:

σ_x = -12 MPa
σ_y = 0 MPa
τ_{xy} = -6 MPa
τ_{yx} = 6 MPa

Figure 1.2 shows the Mohr's circle for this stress system. To draw the circle, firstly draw the point **B**, which represents stresses on the x-plane (co-ordinates: -12, -6). Next draw point **E**, which represents stresses on the y-plane (co-ordinates: 0, +6). Join the two points with the line **BE**, which intersects the x-axis at the centre of the circle, **C**.

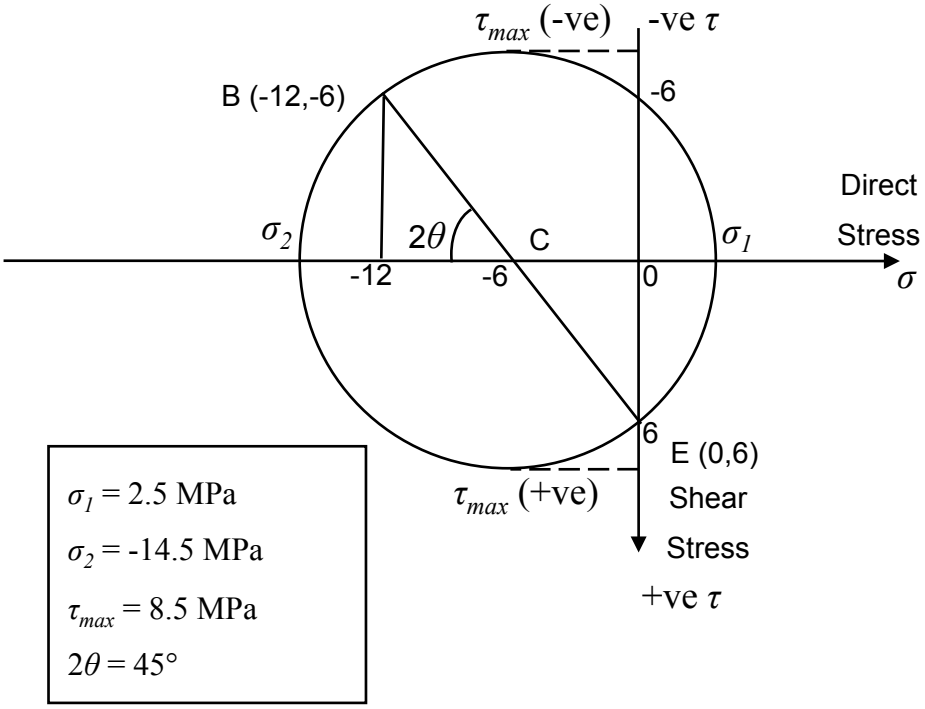

Figure 1.2

The circle can now be drawn and the following quantities measured:

σ_1 = 2.5 MPa

σ_2 = -14.5 MPa

τ_{max} = 8.5 MPa

2θ = 45°

On the element, the angle of the principal plane (P1) from the y-plane is θ = 22.5° anticlockwise as shown in Figure 1.2.

Alternatively, the important parameters in the circle can be calculated analytically as follows:

The centre of the circle is given by:

$$C = (\sigma_x + \sigma_y)/2 = -6$$

The radius of the circle is given by:

$$R = \sqrt{\left(\frac{\sigma_x - \sigma_y}{2}\right)^2 + \tau_{xy}{}^2} = 8.5$$

The Principal stresses are:

$\sigma_1 = C + R$ = 2.5 MPa

$\sigma_2 = C - R$ = -14.5 MPa

$\tau_{max} = R$ = 8.5 MPa

The angle of the principal planes:

$$\tan 2\theta = \frac{\tau_{xy}}{\left(\frac{\sigma_x - \sigma_y}{2}\right)} = 1$$

2θ = 45°

θ = 22.5°

If the analytical approach is taken (which does give the more accurate results), then it is always advisable to sketch the Mohr's circle in order to gain a clear understanding of the orientation of the principal planes and the maximum shear planes with respect to the x- or y-planes.

1.3 Superposition of Combined Loads

The Principal of Superposition states that:

$$\begin{bmatrix}\text{The total effect of } \underline{\text{combined}} \\ \text{loads applied to a body}\end{bmatrix} = \sum \begin{bmatrix}\text{The effects of the individual} \\ \text{loads applied } \underline{\text{separately}}\end{bmatrix}$$

[see volume 1 of 'Introduction to Mechanical Engineering']

Thus, when a body or structure is subjected to a combination of different types of loading simultaneously, we can consider the effect of each load on local stresses on an element separately. Stresses on the element can then be summed to determine the effect of the combined loading. A number of combined loading examples can be used to illustrate:

Combined bending and axial loads

Figure 1.3 shows a beam carrying a uniformly distributed load (UDL) along its span, while simultaneously being subjected to an axial force, F. Figure 1.3 shows how the effect of the combined loading, on the stress distribution through the thickness of the beam at the centre of its span, is determined. The effect of the UDL and the axial force are obtained separately and then summed to give the combined stress distribution in the beam. The symmetrical bending stress distribution about the neutral axis is essentially skewed to more by the effect of the axial stress

Combined bending and torsion

Figure 1.4 shows a similar beam to the above example, except now the beam carries a torque instead of the axial load. This loading situation is typical of a shaft with self-weight (UDL) transmitting a torque. In this case, the beam cross-section can be assumed to be solid circular with diameter d. The stresses at the centre of the span, at the bottom surface of the beam, are given by the usual bending and torsion equations as follows:

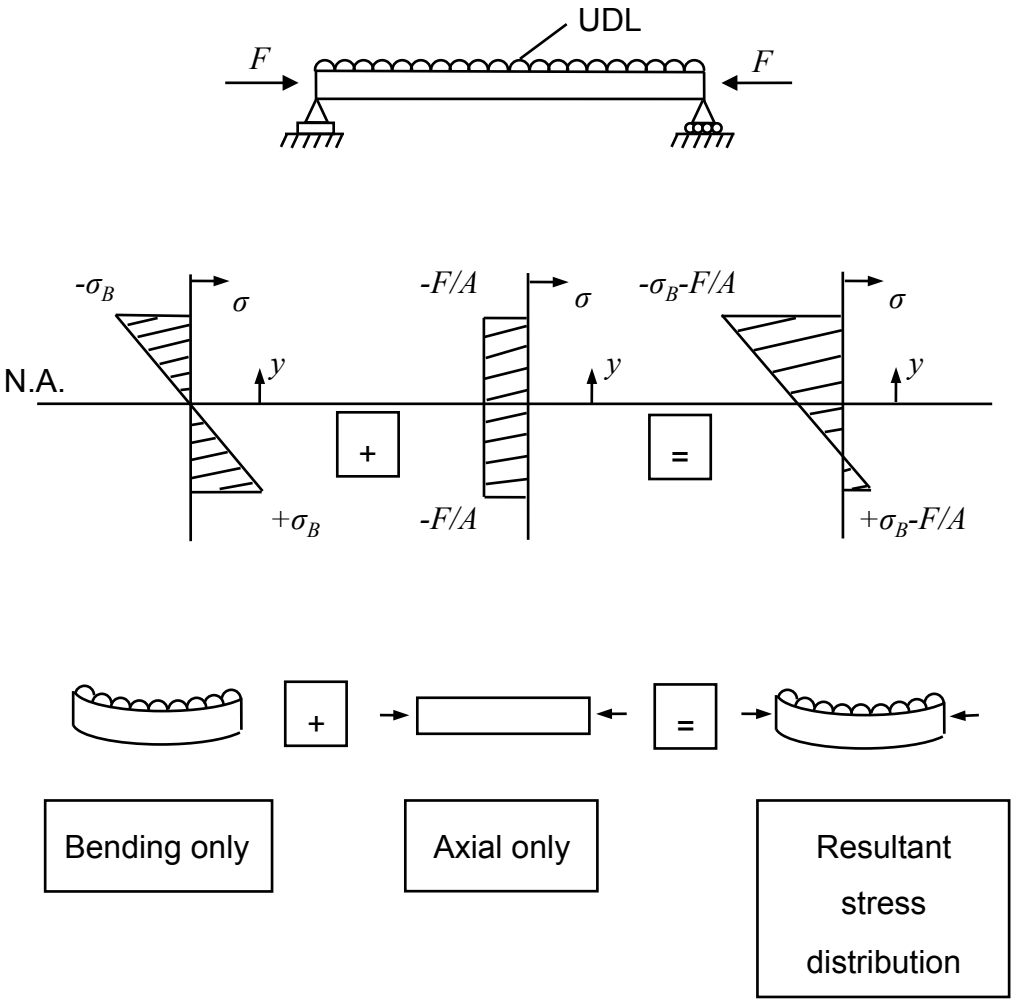
UDL
F
F
-σB
σ
y
N.A.
+σB
+
-F/A
σ
y
-F/A
=
-σB-F/A
σ
y
+σB-F/A
+
=
Bending only
Axial only
Resultant stress distribution

Figure 1.3

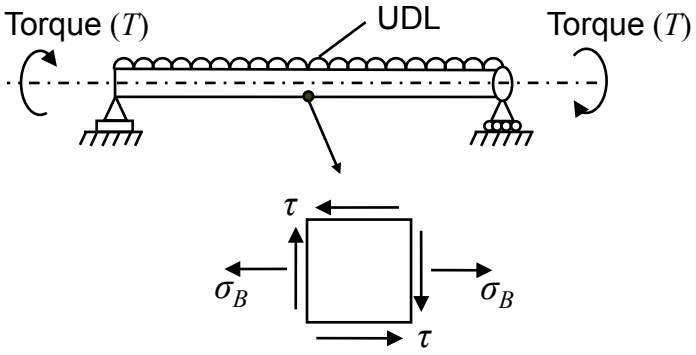

Figure 1.4

Arising from the UDL:

Bending stress (σ_B) $\sigma_B = \frac{My}{I}$ where y = d/2

Arising from the torque:

Torsional shear stress (τ) $\tau = \frac{Tr}{J}$ where r = d/2

These two stresses can be superposed and illustrated acting on an element at the surface of the beam, as shown in Figure 1.4**.**

Mohr's circle can now be used for this element to obtain the principal stresses and maximum shear stress at this position.

Combined pressure, axial and torsional loading

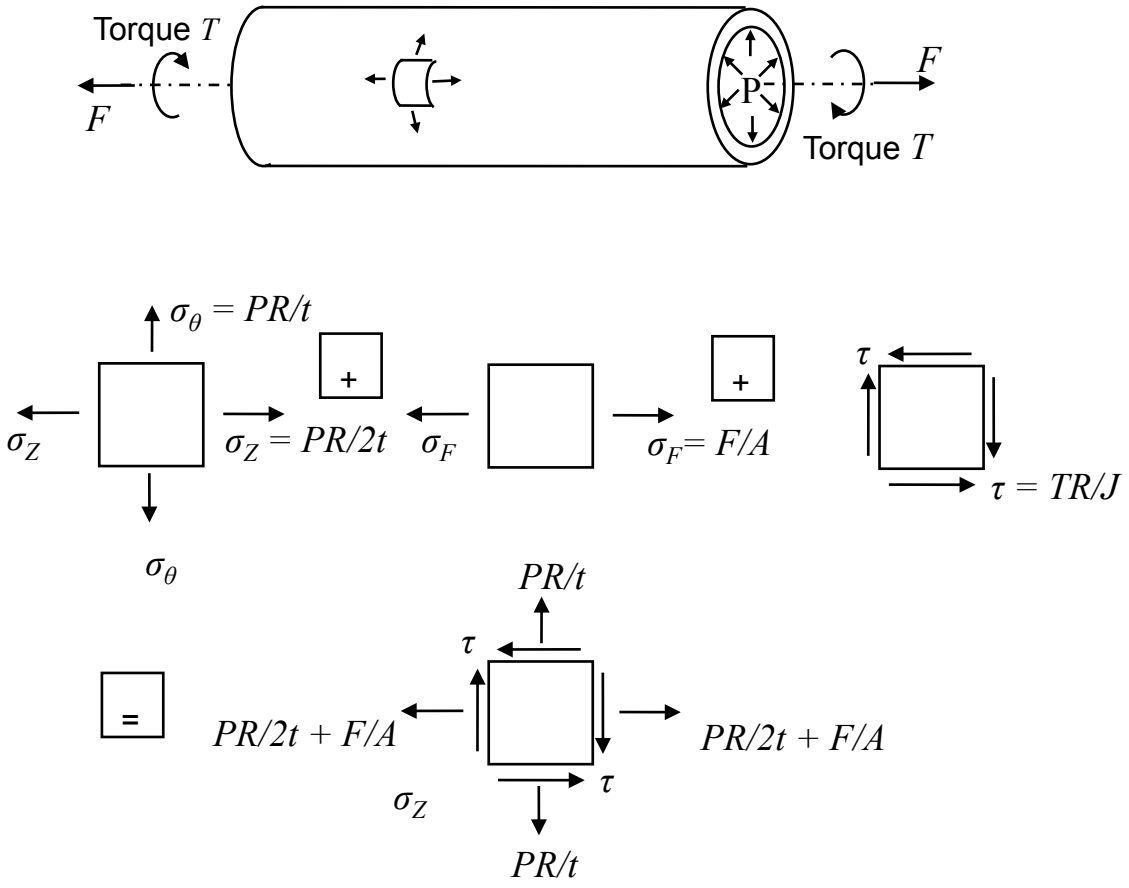

Figure 1.5

A combination of three loads can be illustrated by considering a thin-walled cylinder, as shown in Figure 1.5 subjected to an internal pressure, P, an axial tensile force, F, and a twisting torque, T. Figure 1.5 shows the stresses, arising from each load separately, acting on a surface element in the plane of the cylinder wall. Superposition of these three stresses are also shown on the element. Mohr's circle can again be used to obtain the principal stresses and maximum shear stress for the element.

1.4 Methodology for Combined Loading

The methodology for analysing components or structures under combined loading can now be summarised:

(i) Identify a 2D element at the location of interest in the component

(ii) Determine the stresses acting on the element arising from each individual load

(iii) Superpose the stresses from each individual load to obtain the combined stresses on the element

(iv) Use Mohr's circle to determine the principal stresses and the maximum shear stress on the element

1.5 Worked Example

Combined bending and torsion – offset loading on a cantilever

Figure 1.6 shows a solid circular cross-section cantilever beam, length, L, and diameter, d, fixed at one end. Attached at the free end of the beam is a crank arm which allows a vertical load, P, to be applied at an offset distance, a, from the axis of the cantilever.

Determine the maximum shear stress on the upper surface at the fixed support of the cantilever beam (position A).

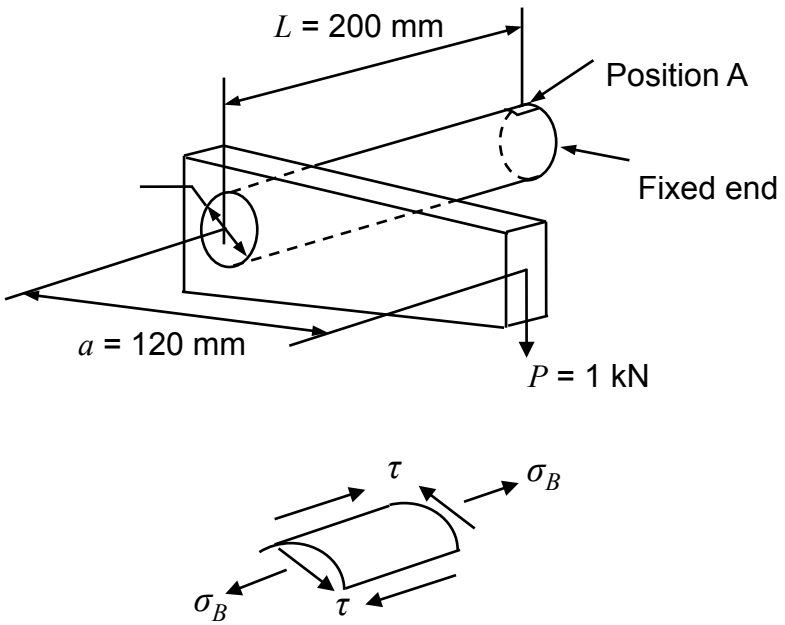

Figure 1.6

The following load and dimensions apply:

P = 1 kN

L = 200 mm

a = 120 mm

d = 30 mm

We consider the stresses acting on a small surface element at position A. The load gives rise to a bending moment and torsional moment at the cross-section at position A as follows:

Bending moment

$$M = PL$$

Torsional moment

$$T = Pa$$

These moments give rise to separate bending and shear stresses acting on the element at position A which can be superposed to give the total effect of the combined loading as shown in Figure 1.6 The stresses are:

Bending stress:

$$\sigma_B = \frac{My}{I} = \frac{PL\,d/2}{\pi d^4/64} = \frac{32PL}{\pi d^3} = \underline{75.45\ MPa}$$

Torsional shear stress

$$\tau = \frac{Tr}{J} = \frac{Pa\,d/2}{\pi d^4/32} = \frac{16Pa}{\pi d^3} = \underline{22.64\ MPa}$$

Mohr's circle can now be drawn for the element to determine the maximum shear stress, as shown in Figure 1.7. The co-ordinates of Point B on the circle (σ_B,τ) correspond to the stresses on the element in the longitudinal direction, i.e. along the cantilever. Point E corresponds to the stresses ($0,-\tau$) in the transverse direction to this. The line joining these two points defines the diameter of the circle and, where it crosses the σ-axis, the centre,

C. The circle can now be drawn and its radius measured to give the maximum shear stress as follows:

τ_{max} = Radius = <u>44 MPa</u>

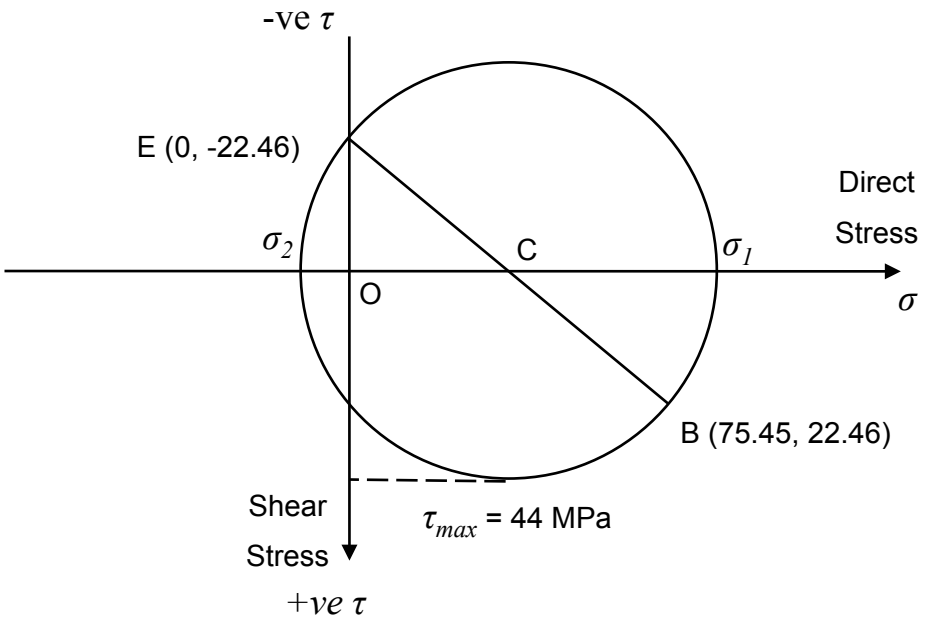

Figure 1.7

Alternatively, by calculation, given the element stresses:

σ_x = 75.45 MPa

σ_y = 0 MPa

τ_{xy} = 22.64 MPa

The maximum shear stress:

$$\tau_{max} = \text{Radius} = \sqrt{\left(\frac{\sigma_x - \sigma_y}{2}\right)^2 + \tau_{xy}^2}$$

$$= \sqrt{\left(\frac{75.45}{2}\right)^2 + 22.64^2}$$

= <u>44 MPa</u> as before

University of Nottingham
UK | CHINA | MALAYSIA

Mechanics of Solids – Deflection of Beams Notes

Learning Summary

1. Know how to derive the differential equation of the elastic line (i.e. deflection curve) of a beam (synthesis)
2. Be able to solve this equation by successive integration to yield the slope, $\frac{\mathrm{d}y}{\mathrm{d}x}$, and the deflection, y, of a beam at any position, x, along its span (application)
3. Employ Macaulay's method, also called the method of singularities, to solve for beam slopes and deflections where there are discontinuities in the bending moment distribution arising from discontinuous loading (application)
4. Recognise and use different singularity functions in the bending moment expression for different loading conditions including point loads, uniformly distributed loads and point bending moments (comprehension)
5. Employ Macaulay's method for statically indeterminate beams (application)

1. Introduction

Whereas the design of engineering structures and components is very often dictated by the strength of the materials used and consequently the stresses within the structure, often the limiting factor is the allowable deflection. This is particularly important for engineering artefacts made from materials of lower stiffness, e.g. aluminium, plastics, composites, etc., but may also be critical for high stiffness structures comprising slender members. It is therefore important, as part of the design process, to be able to calculate maximum deflections in a structure in addition to the position at which they occur.

Here, following the derivation of the fundamental deflection equation for a beam, a flexible procedure is introduced, called Macaulay's Method, which allows for slopes and deflections to be calculated at any position along a beam span. In particular, the method allows us to deal with different types of loading, such as point loads, uniformly distributed loads and point bending moments, including discontinuities in these loads. Although not the only method for calculating deflections, as we will see in the Strain Energy Methods section of the module, it is a particularly powerful and flexible method.

2. Equation of the Elastic Line

Taking a generic curve, $y = f(x)$, two arbitrary points, A and B, can be chosen, as shown in Figure 1.

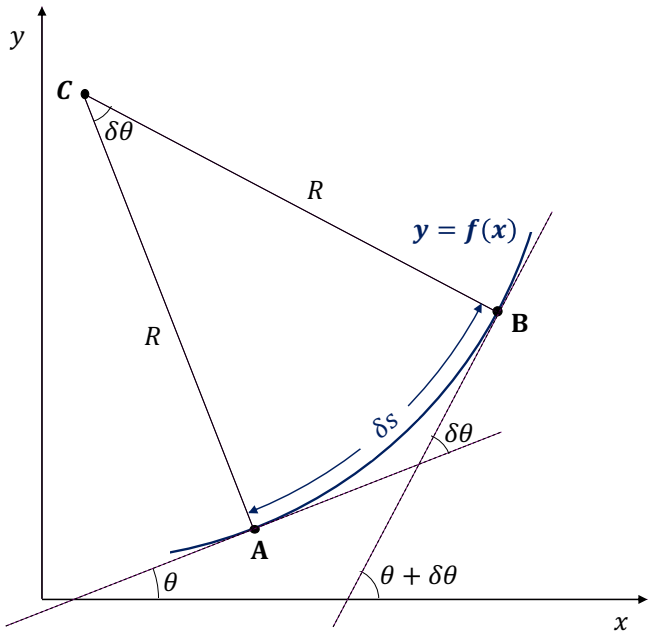

Figure 1

The gradients at these two arbitrary positions can be defined as:

$$\left(\frac{\mathrm{d}y}{\mathrm{d}x}\right)_{\mathrm{A}} = \tan\theta$$

and

$$\left(\frac{\mathrm{d}y}{\mathrm{d}x}\right)_{\mathrm{B}} = \tan\left(\theta + \delta\theta\right)$$

Letting the normals to the curve at points A and B meet at point C, if points A and B are close, the lengths AC and BC are similar. I.e.:

$$\mathrm{A}C \approx \mathrm{B}C \ (= R)$$

Length AB can therefore be thought of as a small arc of a circle of radius, R.

Note that angle ACB $= \delta\theta$, since, as the tangent turns through angle $\delta\theta$, so does the normal. Therefore arc AB $= \delta s = R\delta\theta$, which can be re-arranged to give:

$$\frac{1}{R} = \frac{\delta\theta}{\delta s}$$

As $\delta s \to 0$ (i.e. as points A and B become closer):

$$\frac{\delta\theta}{\delta s} \to \frac{\mathrm{d}\theta}{\mathrm{d}s}$$

$$\therefore \frac{1}{R} = \frac{\mathrm{d}\theta}{\mathrm{d}s} \tag{1}$$

It can be seen from Figure 2 that since δs is small, the arc AB $(= \delta s) \approx$ the chord AB.

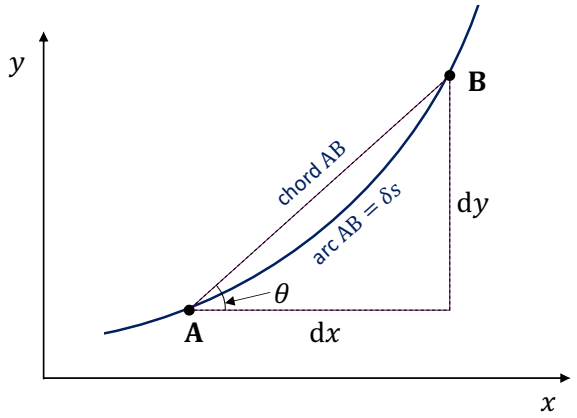

Figure 2

Therefore, when $\delta s \to 0$:

$$\frac{\mathrm{d}y}{\mathrm{d}x} = \tan\theta \tag{2}$$

and

$$\frac{\mathrm{d}x}{\mathrm{d}s} = \cos\theta \tag{3}$$

Differentiating equation (2) with respect to s gives:

$$\frac{\mathrm{d}}{\mathrm{d}s}\left(\frac{\mathrm{d}y}{\mathrm{d}x}\right) = \frac{\mathrm{d}}{\mathrm{d}s}(\tan\theta)$$

Multiplying the left-hand side of this equation by $\frac{\mathrm{d}x}{\mathrm{d}x}$, and the right-hand side by $\frac{\mathrm{d}\theta}{\mathrm{d}\theta}$ gives:

$$\frac{\mathrm{d}}{\mathrm{d}x}\left(\frac{\mathrm{d}y}{\mathrm{d}x}\right)\frac{\mathrm{d}x}{\mathrm{d}s} = \frac{\mathrm{d}}{\mathrm{d}\theta}(\tan\theta)\frac{\mathrm{d}\theta}{\mathrm{d}s}$$

Rearranging this and substituting in equation (3):

$$\frac{\mathrm{d}^2y}{\mathrm{d}x^2}(\cos\theta) = \sec^2\theta\frac{\mathrm{d}\theta}{\mathrm{d}s}$$

$$\therefore \frac{\mathrm{d}^2y}{\mathrm{d}x^2} = sec^3\theta \frac{\mathrm{d}\theta}{\mathrm{d}s} = \left(1 + \left(\frac{\mathrm{d}y}{\mathrm{d}x}\right)^2\right)^{3/2} \frac{\mathrm{d}\theta}{\mathrm{d}s} \quad (4)$$

where

$$\sec^3\theta = (\sec^2\theta)^{3/2} = (1 + \tan^2\theta)^{3/2} = \left(1 + \left(\frac{\mathrm{d}y}{\mathrm{d}x}\right)^2\right)^{3/2}$$

Rearranging equation (4):

$$\frac{\mathrm{d}\theta}{\mathrm{d}s} = \frac{\frac{\mathrm{d}^2y}{\mathrm{d}x^2}}{\left(1 + \left(\frac{\mathrm{d}y}{\mathrm{d}x}\right)^2\right)^{3/2}}$$

Substituting this into equation (1) gives:

$$\frac{1}{R} = \frac{\frac{\mathrm{d}^2y}{\mathrm{d}x^2}}{\left(1 + \left(\frac{\mathrm{d}y}{\mathrm{d}x}\right)^2\right)^{3/2}} \quad (5)$$

Application to a beam under bending

The section of a span of a beam, shown in Figure 3, is under pure bending, i.e. there is a constant bending moment along this section and no shear force.

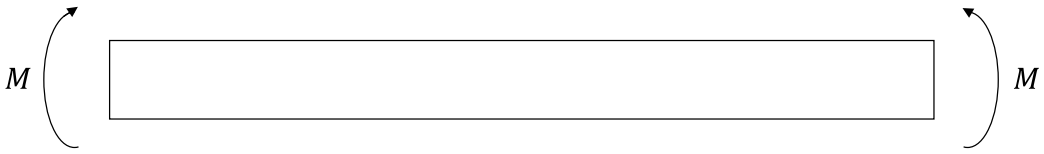

Figure 3

Under these pure bending conditions, the neutral axis (the axis on which there is zero stress) of the beam, also named the elastic line or deflection curve, is a circular arc with radius of curvature, R, as shown in Figure 4.

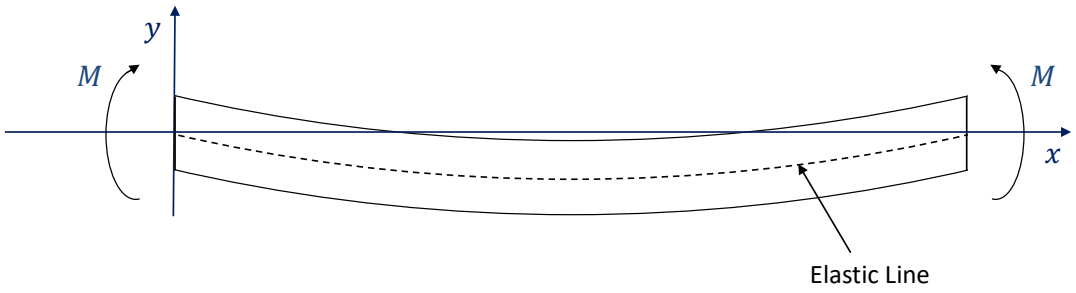

Figure 4

The transverse deflection of the elastic line is given by the co-ordinate, y, of any position along its length, x [n. b. do not confuse this 'y' definition for deflection with the 'y' denoting distance from the neutral axis in the beam bending equation, as shown in equation (6)]. The line denoting the neutral axis in Figure 4 is known as the 'elastic line' or the 'deflection curve' of the beam.

The elastic beam bending equation, which can be used to describe the bending moment, M, as a function of the radius of curvature, R, is:

$$\frac{M}{I} = \frac{\sigma}{y} = \frac{E}{R} \tag{6}$$

$$\therefore \frac{1}{R} = \frac{M}{EI}$$

where E is Young's modulus and I is 2nd moment of area.

Substituting this into equation (5), which also represents the shape of an arc, gives:

$$\frac{M}{EI} = \frac{\frac{\mathrm{d}^2 y}{\mathrm{d}x^2}}{\left(1 + \left(\frac{\mathrm{d}y}{\mathrm{d}x}\right)^2\right)^{3/2}} \tag{7}$$

For small deflections, $\frac{\mathrm{d}y}{\mathrm{d}x}$ is small. Therefore:

$$\left(1 + \left(\frac{\mathrm{d}y}{\mathrm{d}x}\right)^2\right)^{3/2} \approx 1$$

Equation (7) can therefore be simplified and rearranged to give:

$$\boldsymbol{EI\frac{\mathrm{d}^2 y}{\mathrm{d}x^2} = M} \tag{8}$$

This is the is the 2nd order differential equation of the elastic line, relating the deflection, y, to the applied bending moment, M, the Young's modulus, E, 2nd moment of area, I, and position along beam span, x. The product of E and I, i.e. EI, is termed the 'Flexural Rigidity' of the beam.

Successive integration of this equation, with respect to x, will yield the slope, $\frac{\mathrm{d}y}{\mathrm{d}x}$, and the deflection, y, as function of position, x, along the beam.

This equation has been derived for the case of pure bending, i.e. constant bending moment along the section, and does not take into account deflections due to shear. For long slender beams, shear deflections can be neglected.

A complication arises where discontinuities in M exist, such as where there are point loads and/or point bending moments or where there is an abrupt change in distributed loading. Various methods have been developed to solve such problems with discontinuities. Here we introduce and develop the procedure called Macaulay's Method, a versatile solution procedure which can handle most discontinuities we are likely to encounter.

3. Macaulay's Method (also termed the Method of Singularity Functions)

Named after the mathematician W. H. Macaulay, Macaulay's Method uses a mathematical technique to deal with discontinuous loading. The bending moment expression $M(x)$, i.e. M as a function of x, is replaced with the step function $M\langle x-a\rangle$, in which a defines the position at which a discontinuity arises.

Figure 5 shows a simply supported beam carrying a point load, P, at the centre of its length. This load gives rise to a discontinuity in the bending moment expression.

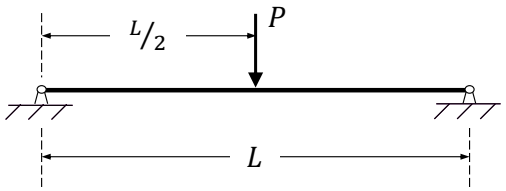

Figure 5

Figure 6 shows a free body diagram of this beam.

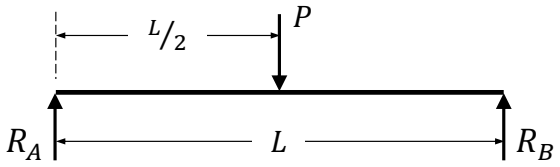

Figure 6

Considering each span between the loading discontinuity separately in order to determine expressions for bending moment, M.:

Span 1

Figure 7 shows the free body diagram of the beam sectioned within span 1 (i.e. before the loading discontinuity caused by P), taking the origin as the left-hand end. The unknown bending moment, M, and shear force, S, at this section, are shown in the diagram.

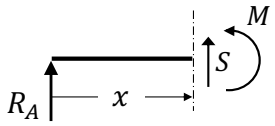

Figure 7

Taking moments about the section position in order to determine an expression for the bending moment, M, in span 1:

$$M = R_A x$$

Substituting this into equation (8):

$$EI\frac{\mathrm{d}^2 y}{\mathrm{d}x^2} = R_A x \tag{9}$$

Equation (9) applies to span 1 of the beam only.

Span 2

Figure 8 shows the free body diagram of the beam, now sectioned within span 2 (i.e. after the loading discontinuity caused by P). As before, the unknown bending moment, M, and shear force, S, at this section, are shown in the diagram.

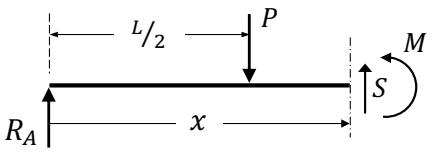

Figure 8

Taking moments about the section position in order to determine an expression for the bending moment, M, in span 2:

$$M + P\left(x - \frac{L}{2}\right) = R_A x$$

$$\therefore M = R_A x - P\left(x - \frac{L}{2}\right)$$

Substituting this into equation (8):

$$EI\frac{\mathrm{d}^2 y}{\mathrm{d}x^2} = R_A x - P\left(x - \frac{L}{2}\right) \tag{10}$$

Equation (10) applies to span 2 of the beam only.

It is interesting to note that the forms of equations (9) and (10) are similar, in that there is simply an extra term added to take account of the extra span of the beam (as we move past the loading discontinuity). In fact, due to this similarity, equation (10), i.e. the expression derived for the final span of the beam, can be applied to the full length of the beam by rewriting it in a slightly different form as follows:

$$EI\frac{\mathrm{d}^2 y}{\mathrm{d}x^2} = R_A x - P\langle x - \frac{L}{2}\rangle \tag{11}$$

Note the change of bracket shape. These ⟨ ⟩ brackets are termed 'Macaulay Brackets' and due to these, equation (11) is now applicable to any position, x, in the beam shown in Figure 5, if we adopt 'Macaulay's convention'. Macaulay's convention states that whenever a Macaulay bracketed term becomes negative, the entire term it is part of is set to zero.

Adopting this convention, the general 2nd order differential expression for the beam, shown by equation (11) for the beam shown in Figure 5, can be integrated with respect to x to give the slope, $\frac{\mathrm{d}y}{\mathrm{d}x}$, and integrated again to give the deflection, y, at any position x, along the length of the beam.

If, for example, the slope and deflection at the position of the point load shown in Figure 5 was required, the solution is as follows:

Application of equilibrium for the determination of the reaction forces at the support positions

Vertical Equilibrium:

$$P = R_A + R_B \tag{12}$$

Taking moments about the position of R_A:

$$R_B L = \frac{PL}{2}$$

$$\therefore R_B = \frac{P}{2}$$

Substituting this into equation (12):

$$R_A = \frac{P}{2} \tag{13}$$

Determination of expressions for slope, $\frac{\mathrm{d}y}{\mathrm{d}x}$, and deflection, y, as functions of x

Once the 2nd order differential expression for the beam has been determined, in this case as given by equation (11), integration with respect t to x gives:

$$EI\frac{\mathrm{d}y}{\mathrm{d}x} = \frac{R_A x^2}{2} - \frac{P\langle x - \frac{L}{2}\rangle^2}{2} + \mathrm{A} \tag{14}$$

where $\frac{\mathrm{d}y}{\mathrm{d}x}$ represents the slope at any position, x.

Integrating with respect to x again:

$$EIy = \frac{R_A x^3}{6} - \frac{P\langle x - \frac{L}{2}\rangle^3}{6} + \mathrm{A}x + \mathrm{B} \tag{15}$$

where y represents the deflection at any position, x.

Use of boundary conditions for the determination of the constants of integration

Boundary condition 1: at x = 0, y = 0 (i.e. at this support position there is no deflection)

Applying this to equation (15):

$$\mathrm{B} = 0$$

Note that the term related to P has been set to zero, as the contents of the Macaulay brackets is negative (i.e. $\langle 0 - \frac{L}{2}\rangle < 0$).

Boundary condition 2: at x = L, y = 0 (i.e. at this support position there is no deflection)

Applying this to equation (15):

$$0 = \frac{R_A L^3}{6} - \frac{P\left(\frac{L}{2}\right)^3}{6} + \mathrm{A}L$$

$$\therefore \mathrm{A} = \frac{L^2}{6}\left(\frac{P}{8} - R_A\right) \tag{16}$$

Note that for the term related to P, the Macaulay brackets have been changed to regular brackets, as Macaulay's convention has been applied and the contents of the Macaulay brackets is positive (i.e. $\langle L - \frac{L}{2} \rangle > 0$)).

Evaluation of slope and deflection at position of interest

As it is at $x = \frac{L}{2}$ that the slope and deflection is required, this value of x can be substituted into equations (14) and (15), and Macaulay's convention applied to give:

$$EI\frac{\mathrm{d}y}{\mathrm{d}x} = \frac{R_A L^2}{8} + \mathrm{A}$$

and

$$EIy = \frac{R_A L^3}{48} + \frac{\mathrm{A}L}{2}$$

Substituting the expressions for R_A and A, from equations (13) and (16), respectively, into these, and rearranging for $\frac{\mathrm{d}y}{\mathrm{d}x}$ and y, gives:

$$\frac{\mathrm{d}y}{\mathrm{d}x} = 0$$

and

$$y = -\frac{PL^3}{48EI} \qquad (17)$$

As the beam is loaded and supported symmetrically, it makes sense that the slope at the centre position is zero. Additionally, as the single applied load is downwards, it would be expected that the deflection at the centre position of the beam would also be downwards and therefore negative according to the sign convention defined in section 2 of these notes, i.e. y is positive in the upwards direction.

4. Alternative Loading Types

Uniformly distributed load

Consider a uniformly distributed load (UDL), w Nm^{-1}, acting over part of a beam's span, as shown in Figure 9. The UDL runs from distance a from the origin (left-hand end) of the beam, all the way to the right-hand end of the beam. A discontinuity occurs at the position where the UDL commences.

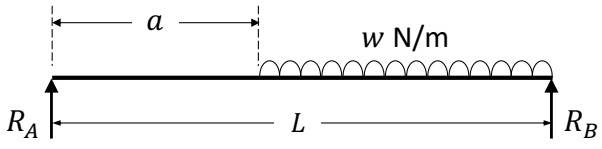

Figure 9

Figure 10 shows the resulting free-body diagram after sectioning the beam after the discontinuity.

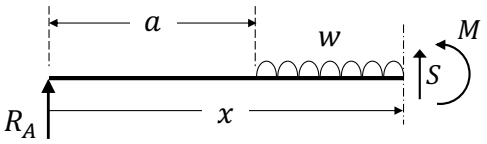

Figure 10

Taking moments about the section position:

$$M + \frac{w\langle x-a\rangle^2}{2} = R_A x \tag{18}$$

$$\therefore M = R_A x - \frac{w\langle x-a\rangle^2}{2}$$

And substituting this into equation (8) gives:

$$EI\frac{d^2y}{dx^2} = R_A x - \frac{w\langle x-a\rangle^2}{2}$$

As in section 3 of these notes, this 2nd order differential expression of the elastic line can now be integrated with respect to x in order to determine the slope, $\frac{\mathrm{d}y}{\mathrm{d}x}$, and again in order to determine the deflection, y, as functions of x. Boundary conditions are then used to determine the constants of integration before evaluation of the slope and/or deflection at any position, x, along the beam.

As can be seen from equation (18), when taking moment equilibrium, the contribution of the UDL is calculated by first turning the UDL, w (unit $\mathrm{Nm^{-1}}$), into a force (unit N) by multiplying it by the distance over which it acts, $x-a$ (unit m). This force is then turned into a moment by multiplying it by the distance to the centre position of the UDL, $\frac{\langle x-a\rangle}{2}$ (unit m). Note that Macaulay brackets are used in the length term in order to allow for Macaulay's method to be employed for the inclusion or elimination of the term depending on the position, x, being evaluated.

Discontinuous uniformly distributed load

A discontinuous UDL is shown in Figure 11.

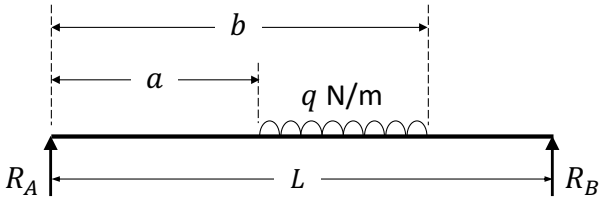

Figure 11

In this case, the UDL, q, runs from distance a from the origin (left-hand end) of the beam, up to distance b from the origin. Discontinuities therefore occur both at the position where the UDL commences, and at the position where it ends.

In order to progress towards a general bending moment expression for the beam, analogous to equation (18) for the continuous UDL, the applied discontinuous UDL, q, is extended to the end of the beam and an additional, negative, counterbalancing UDL superimposed over the newly extended part, as shown in Figure 12. The extended applied UDL, q, and the added counterbalancing UDL, $-q$, mathematically cancel each other out and therefore this gives a statically equivalent system to the original partially extended (discontinuous) UDL.

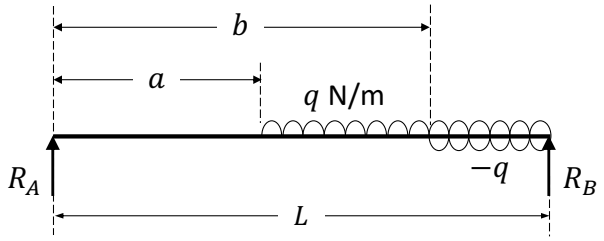

Figure 12

As before, the beam is then sectioned after the final discontinuity, and a free body diagram drawn, as shown in Figure 13.

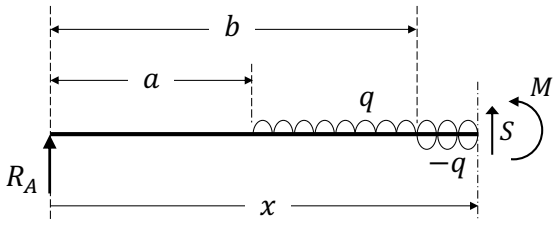

Figure 13

In the determination of a bending moment expression, each of the now continuous UDLs in Figure 13 are dealt with as in the determination of equation (18) from Figure 10. I.e.:

$$M + \frac{q\langle x-a\rangle^2}{2} = R_A x + \frac{q\langle x-b\rangle^2}{2}$$

$$\therefore M = R_A x + \frac{q\langle x-b\rangle^2}{2} - \frac{q\langle x-a\rangle^2}{2}$$

Substituting this into equation (8) gives:

$$EI\frac{\mathrm{d}^2y}{\mathrm{d}x^2} = R_A x + \frac{q\langle x-b\rangle^2}{2} - \frac{q\langle x-a\rangle^2}{2}$$

As before, this 2nd order differential expression of the elastic line can be integrated with respect to x in order to determine the slope, $\frac{dy}{dx}$, and again in order to determine the deflection, y, as functions of x, and boundary conditions used to determine the constants of integration before evaluation of the slope and/or deflection at any position, x, along the beam.

Point bending moment

Consider a point bending moment, M_o Nm, acting at a distance a from the left-hand side of a beam which is simply supported at both ends, as shown in Figure 14. This point bending moment gives rise to a discontinuity in the bending moment expression.

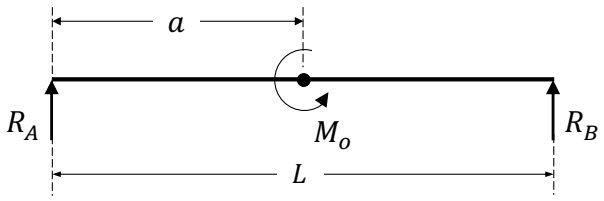

Figure 14

Figure 15 shows the resulting free-body diagram after sectioning the beam after the discontinuity.

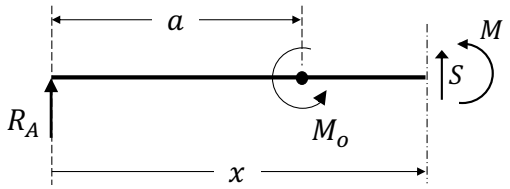

Figure 15

Taking moments about the section position:

$$M + M_o\langle x-a\rangle^0 = R_A x \tag{19}$$

$$\therefore M = R_A x - M_o\langle x-a\rangle^0$$

And substituting this into equation (8) gives:

$$EI\frac{\mathrm{d}^2y}{\mathrm{d}x^2} = R_A x - M_o\langle x-a\rangle^0 \tag{20}$$

Again, equation (20) can be integrated with respect to x in order to determine the slope, $\frac{\mathrm{d}y}{\mathrm{d}x}$, and again in order to determine the deflection, y, as functions of x, and boundary conditions used to determine the constants of integration before evaluation of the slope and/or deflection at any position, x, along the beam.

Note from equation (19), that the form of the discontinuity function for the point bending moment is $M_o\langle x-a\rangle^0$. This is the same as for a point load, except that the bracketed length is raised to the power zero. This is simply a mathematical convenience for facilitating Macaulay's method whilst maintaining the correct units of the moment, M_o. I.e. if a position in the beam where $x < a$ is considered for evaluation, then the contents of the Macaulay brackets is negative and the entire term set to zero. However, if a position in the beam where $x > a$ is considered for evaluation, then the contents of the Macaulay brackets is positive, and the term is included. As the length term, $\langle x-a\rangle^0$, is raised to the power of zero, it becomes 1, and so the term simplifies to M_o.

5. Summary of the Discontinuity Functions

We have seen that Macaulay's method can be used to find the slope and/or deflection at any position along a beam where point loads, uniformly distributed loads and/or point bending moments produce discontinuities in the bending moment expression. The method can also be used where there is a combination of these loads acting on a beam.

When developing the bending moment expression for a beam with load discontinuities, the singularity functions shown in Table 1 are used for each different type of load.

Table 1

Load Type	Singularity Function
Point Load, P	$P\langle x-a\rangle$
Continuous UDL, w – single discontinuity	$\frac{w\langle x-a\rangle^2}{2}$
Discontinuous UDL, q – double discontinuity	$\frac{q\langle x-b\rangle^2}{2} - \frac{q\langle x-a\rangle^2}{2}$
Point Bending Moment, M_o	$M_o\langle x-a\rangle^0$

Note that in these singularity functions, the exponent is 1 for a point load, 2 for a UDL and 0 for a point bending moment.

6. Worked Example – Beam with Point Load, Discontinuous Uniformly Distributed Load & Point Bending Moment

Problem

Figure 16 shows a steel simply supported beam of length, L = 1.5 m, carrying:

- a point bending moment, M_o = 3 kNm, at a distance of $\frac{L}{6}$ from the left-hand end
- a point load, P = 2 kN, at a distance of $\frac{L}{3}$ from the left-hand end
- a discontinuous uniformly distributed load, q = 4 kN/m, between distances of $\frac{L}{3}$ and $\frac{2L}{3}$ from the left-hand end

The Young's modulus, E, of the material is 200 GPa and the beam is of circular cross-section of diameter, D = 50 mm.

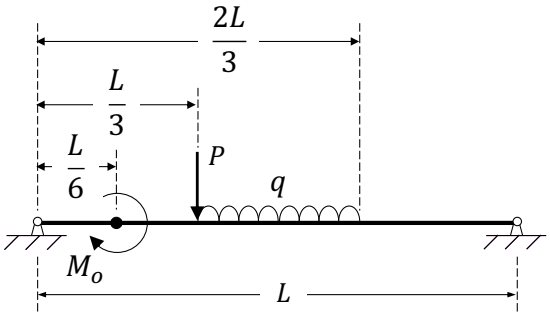

Figure 16

Use Macaulay's method to determine the slope and deflection of the beam at its centre position.

Solution

As the beam is of circular cross-section, the 2nd moment of area, I, is calculated as:

$$I = \frac{\pi D^4}{64} = \frac{\pi \times 0.05^4}{64} = 3.068 \times 10^{-7}\text{m}^4$$

Figure 17 shows a free-body-diagram of the beam which can be used to calculate the reaction forces.

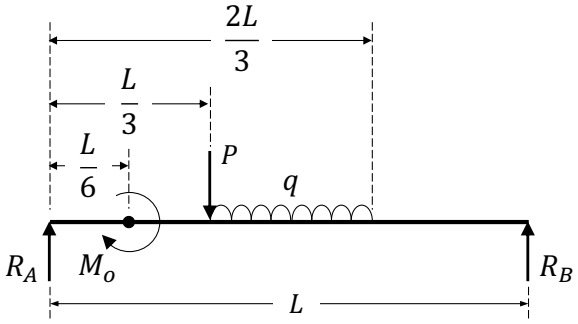

Figure 17

Taking vertical equilibrium:

$$R_A + R_B = P + \frac{qL}{3} \tag{21}$$

Taking moments about position A:

$$R_B L = M_o + \frac{PL}{3} + \frac{qL^2}{6}$$

$$\therefore R_B = \frac{M_o}{L} + \frac{P}{3} + \frac{qL}{6} = \frac{11}{3}\ \text{kN}$$

Substituting this into equation (21) and rearranging for R_A:

$$R_A = P + \frac{qL}{3} - R_B = \frac{1}{3}\ \text{kN}$$

Next, as there is a discontinuous uniformly distributed load, this needs to be extended to the end of the beam and an additional, negative, counterbalancing UDL superimposed over the newly extended part. Figure 18 shows the result of taking the left-hand end of the beam as the origin and sectioning the beam after the final discontinuity.

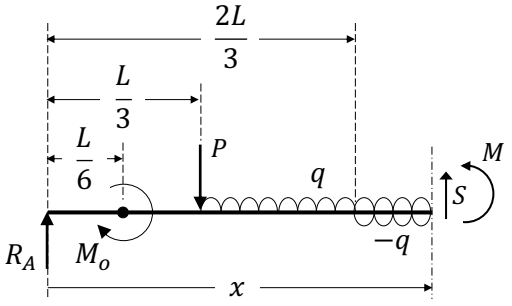

Figure 18

Taking moments about the section position (remembering to implement Macaulay's convention):

$$M + P\langle x - \frac{L}{3}\rangle + \frac{q\langle x - \frac{L}{3}\rangle^2}{2} = R_A x + M_o\langle x - \frac{L}{6}\rangle^0 + \frac{q\langle x - \frac{2L}{3}\rangle^2}{2}$$

$$\therefore M = M_o\langle x - \frac{L}{6}\rangle^0 + R_A x - P\langle x - \frac{L}{3}\rangle + \frac{q\langle x - \frac{2L}{3}\rangle^2}{2} - \frac{q\langle x - \frac{L}{3}\rangle^2}{2}$$

Substituting this into equation (8) gives:

$$EI\frac{\mathrm{d}^2y}{\mathrm{d}x^2} = M_o\langle x - \frac{L}{6}\rangle^0 + R_A x - P\langle x - \frac{L}{3}\rangle + \frac{q\langle x - \frac{2L}{3}\rangle^2}{2} - \frac{q\langle x - \frac{L}{3}\rangle^2}{2}$$

Integrating with respect to x to determine an expression for the slope:

$$EI\frac{\mathrm{d}y}{\mathrm{d}x} = M_o\langle x - \frac{L}{6}\rangle + \frac{R_A x^2}{2} - \frac{P\langle x - \frac{L}{3}\rangle^2}{2} + \frac{q\langle x - \frac{2L}{3}\rangle^3}{6} - \frac{q\langle x - \frac{L}{3}\rangle^3}{6} + A \quad (22)$$

Integrating with respect to x again to determine an expression for the deflection:

$$EIy = \frac{M_o\langle x - \frac{L}{6}\rangle^2}{2} + \frac{R_A x^3}{6} - \frac{P\langle x - \frac{L}{3}\rangle^3}{6} + \frac{q\langle x - \frac{2L}{3}\rangle^4}{24} - \frac{q\langle x - \frac{L}{3}\rangle^4}{24} + \mathrm{A}x + \mathrm{B} \quad (23)$$

Using boundary conditions for the determination of the constants of integration:

Boundary condition 1: at x = 0, y = 0 (i.e. at this support position there is no deflection)

Applying this to equation (23):

$$\mathrm{B} = 0$$

Boundary condition 2: at x = L, y = 0 (i.e. at this support position there is no deflection)

Applying this to equation (23) and substituting in values for M_o, P, q, L, R_A and B:

$$\mathrm{A} = -\frac{583}{432}$$

The slope and deflection at $x = \frac{L}{2}$ can now be evaluated by using equations (22) and (23), respectively.

Substituting $x = \frac{L}{2}$ into (22) and (23) and applying Macaulay's convention gives:

$$\frac{\mathrm{d}y}{\mathrm{d}x} = \frac{1}{EI}\left(\frac{M_o L}{3} + \frac{R_A L^2}{8} - \frac{PL^2}{72} - \frac{qL^3}{1296} + A\right)$$

and

$$y = \frac{1}{EI}\left(\frac{M_o L^2}{18} + \frac{R_A L^3}{48} - \frac{PL^3}{1296} - \frac{qL^4}{31104} + \frac{\mathrm{A}L}{2} + \mathrm{B}\right)$$

Note that in each of the above expressions, the term related to the added counterbalancing UDL, i.e. $\frac{q\langle x-\frac{2L}{3}\rangle^3}{6}$ and $\frac{q\langle x-\frac{2L}{3}\rangle^4}{24}$, respectively, has been removed as $x < c$ and so the contents of the Macaulay brackets in these terms is negative and so the terms are set to zero. In all of the other terms with Macaulay brackets, these have been replaced with regular brackets as the contents are positive and so Macaulay's convention has been satisfied.

Substituting in values of E, I, L, M_o, P, q, R_A, A and B gives:

$$\frac{\mathrm{d}y}{\mathrm{d}x} = 2.838 \times 10^{-3}\ \mathrm{rad}$$

and

$$y = -0.01026\ \mathrm{m} = -10.26\ \mathrm{mm}$$

7. Statically Indeterminate Problems

Macaulay's method can also be used to solve for the slopes and deflections of statically indeterminate beams. A beam is statically indeterminate when the reaction forces and/or bending moments cannot be determined by the equations of statics alone. An example of this is a clamped-clamped beam subjected to a point load, as shown in Figure 19.

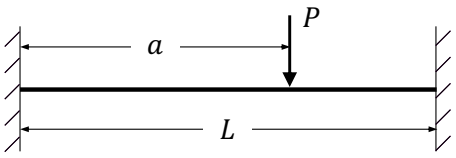

Figure 19

Figure 20 shows a free-body-diagram of the beam.

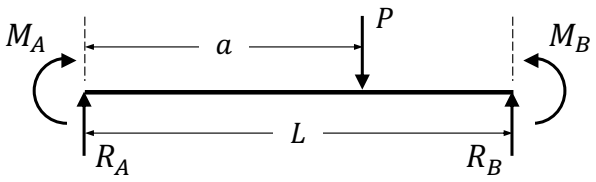

Figure 20

It can be seen from Figure 20 that the end reactions are R_A, M_A, R_B, and M_B; a reaction force and a reaction bending moment which restrain the displacement and rotation, respectively, at both ends of the beam. There are therefore four unknowns which cannot be solved for by equilibrium alone. We therefore continue as before, but this time without knowing the reactions.

Figure 21 shows the result of taking the left-hand end A as the origin and sectioning the beam after the discontinuity.

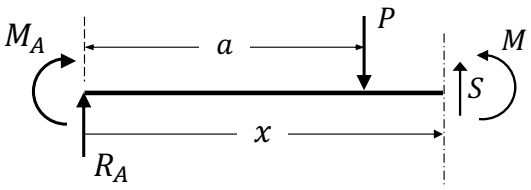

Figure 21

Taking moments about the section position:

$$M + P\langle x - a\rangle = R_A x + M_A$$

$$\therefore M = R_A x + M_A - P\langle x - a\rangle$$

Substituting this into equation (8):

$$EI\frac{\mathrm{d}^2 y}{\mathrm{d}x^2} = R_A x + M_A - P\langle x - a\rangle$$

Integrating with respect to x to determine an expression for the slope:

$$EI\frac{\mathrm{d}y}{\mathrm{d}x} = \frac{R_A x^2}{2} + M_A x - \frac{P\langle x - a\rangle^2}{2} + \mathrm{A} \tag{24}$$

Integrating with respect to x again to determine an expression for the deflection:

$$EIy = \frac{R_A x^3}{6} + \frac{M_A x^2}{2} - \frac{P\langle x-a\rangle^3}{6} + \mathrm{A}x + \mathrm{B} \tag{25}$$

Equations (24) and (25) contain four unknowns, namely M_A and R_A and the integration constants A and B. In this case we can use four boundary conditions to solve for these four unknowns.

Boundary condition 1: at x = 0, y = 0 (i.e. at this clamp position there is no deflection)

Applying this to equation (25):

$$\mathrm{B} = 0$$

Boundary condition 2: at x = 0, $\frac{\mathrm{d}y}{\mathrm{d}x}$ = 0 (i.e. at this clamp position there is no rotation)

Applying this to equation (24):

$$\mathrm{A} = 0$$

Boundary condition 3: at $x = L$, y = 0 (i.e. at this clamp position there is no deflection)

Applying this to equation (25):

$$0 = \frac{R_A L^3}{6} + \frac{M_A L^2}{2} - \frac{P(L-a)^3}{6} \tag{26}$$

Boundary condition 4: at $x = L$, $\frac{\mathrm{d}y}{\mathrm{d}x}$ = 0 (i.e. at this clamp position there is no rotation)

Applying this to equation (24):

$$0 = \frac{R_A L^2}{2} + M_A L - \frac{P(L-a)^2}{2}$$

$$\therefore M_A = \frac{P(L-a)^2 - R_A L^2}{2L} \tag{27}$$

Substituting equation (27) into equation (26):

$$R_A = \frac{P(L^3 - 3La^2 + 2a^3)}{L^3}$$

Substituting this into equation (27):

$$M_A = -\frac{Pa(L^2 - 2La + a^2)}{L^2}$$

Substituting these expressions for R_A and M_A into equations (24) and (25):

$$EI\frac{\mathrm{d}y}{\mathrm{d}x} = \frac{P(L^3 - 3La^2 + 2a^3)}{2L^3}x^2 - \frac{Pa(L^2 - 2La + a^2)}{L^2}x - \frac{P\langle x - a\rangle^2}{2} \tag{28}$$

and

$$EIy = \frac{P(L^3 - 3La^2 + 2a^3)}{6L^3}x^3 - \frac{Pa(L^2 - 2La + a^2)}{2L^2}x^2 - \frac{P\langle x - a\rangle^3}{6} \tag{29}$$

Special Case – Centrally Loaded Clamped-Clamped Beam

In the case of the beam shown in Figure 19 being loaded at the centre position, and evaluating for the slope and deflection at this position, i.e. $a = \frac{L}{2} = x$, equations (28) and (29) give:

$$\frac{\mathrm{d}y}{\mathrm{d}x} = 0$$

and

$$y = -\frac{PL^3}{192EI}$$

As this beam is loaded and supported symmetrically, it makes sense that the slope at the centre position is zero. Additionally, as the single applied load is downwards, it would be expected that the deflection at the centre of the beam would also be downwards and therefore negative (according to the sign convention defined in section 2 of these notes, i.e. y is positive in the upwards direction).

It is interesting to note that clamping the ends of a beam which is carrying a single point load at its centre position, results in a deflection which is 25% of the deflection of a simply supported equivalent (see equation (17)).

Mechanics of Solids – Elastic-Plastic Deformations Notes

Learning Summary

1. Know the shapes of uniaxial stress-strain curves and the elastic-perfectly-plastic approximation (knowledge);
2. Know the kinematic and isotropic material behaviour models used to represent cyclic loading behaviour (knowledge);
3. Understand elastic-plastic bending of beams (comprehension) and be able to use equilibrium, compatibility and σ-ε behaviour to solve these types of problems for deformation and stress state (application);
4. Understand elastic-plastic torsion of shafts (comprehension) and be able to use equilibrium, compatibility and τ-γ behaviour to solve these types of problems for deformation and stress state (application);
5. Be able to determine residual deformations and residual stresses in beams under bending and shafts under torsion (application).

1. Introduction

When materials are subjected to an increasing load (or stress), the strain response is often such that there is a linear (elastic) region in the stress-strain plot followed by a non-linear (plastic) region, as shown schematically in Figure 1. The ability to predict this material behaviour is extremely important, within many applications, in order to determine maximum allowable loads, that can be applied to components. These allowable loads are usually based on both the displacement this load causes as well as the remaining (residual) deformation upon unloading.

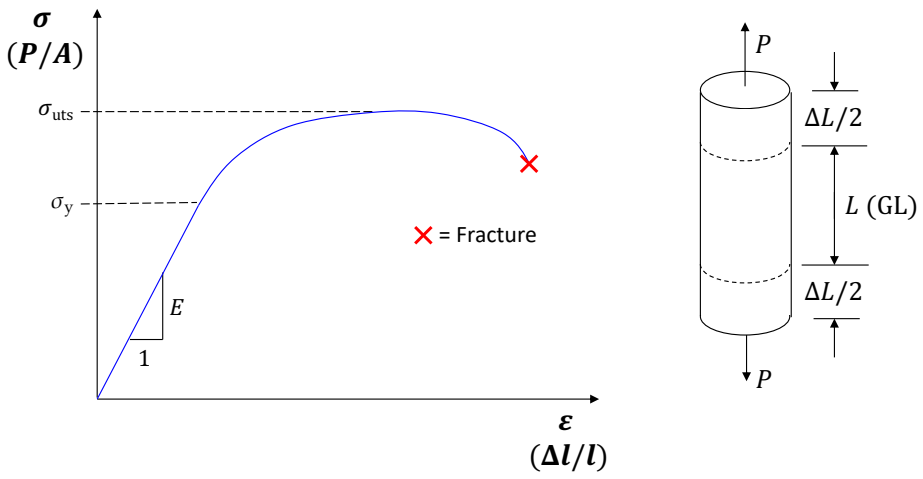

Figure 1

Several mathematical models can be used to estimate this material behaviour.

2. Elastic-Plastic Material Behaviour Models

Elastic-perfectly-plastic (EPP)

In this case, there is assumed to be no material hardening upon yield. I.e., once the yield stress, σ_y, is reached, further straining causes no further increase in stress, as shown in Figure 2.

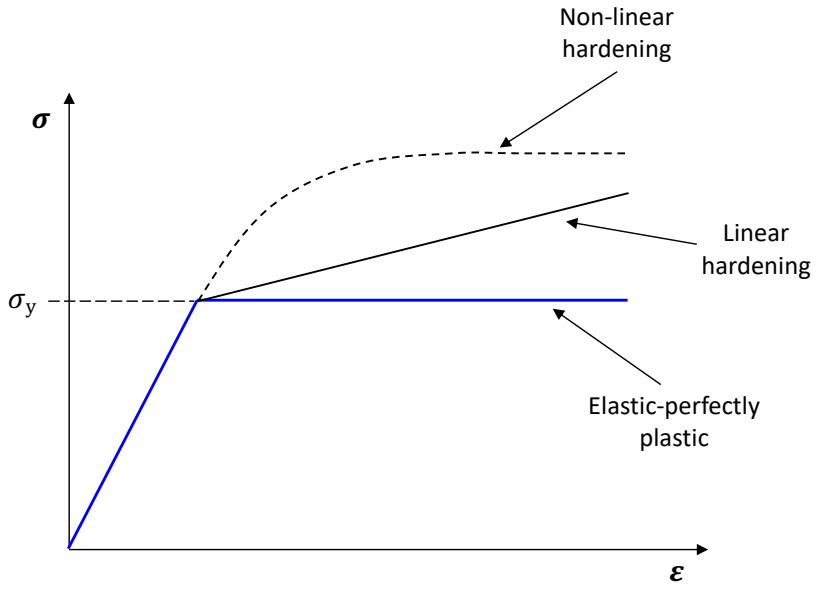

Figure 2

Figure 2 shows an EPP stress-strain curve for a material in tension. However, this behaviour is also applicable in compression. I.e., if the loading is reversed, the behaviour shown in Figure 2 can be extended to that shown in Figure 3, where it can be seen that the stress magnitude increases in compression until the compressive yield stress, $-\sigma_y$, is reached, after which no further change to the stress response occurs with increasing compressive strain magnitude.

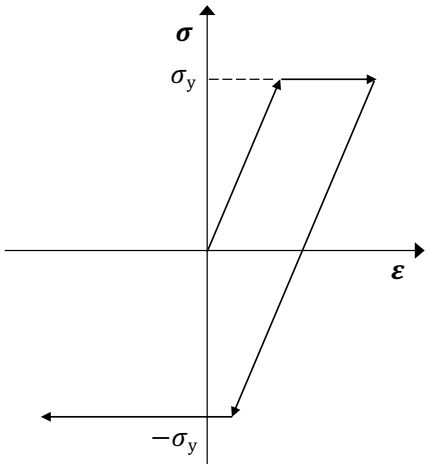

Figure 3

If the loading is then cycled between tension and compression, the material will continue to behave in the same way

(regardless of any previous plastic deformation) resulting in the hysteresis loop shown in Figure 4.

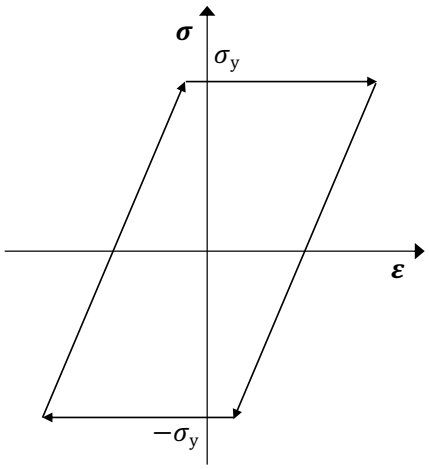

Figure 4

For EPP material behaviour, as loading conditions cause yielding (plasticity), there is no change to the yield surface, shown in Figure 5 (in blue for the von Mises yield criterion and in red for the Tresca yield criterion), in the principal stress-space.

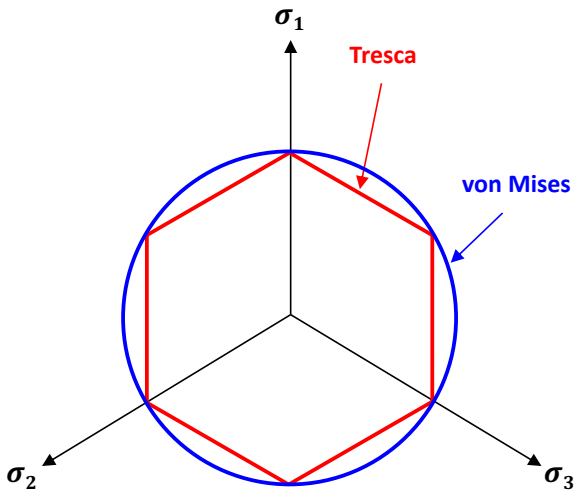

Figure 5

EPP, is a good material model for mild steel, for example, which demonstrates moderate plasticity.

Isotropic Hardening

For materials which harden, as shown in tension, for both linear and non-linear cases, in Figure 2, this hardening behaviour can also be observed as changes to the yield surface. For the case of isotropic hardening behaviour, when the loading state, shown by the red arrow in Figure 6a, reaches the point of causing yielding (plasticity), i.e., point a,

the yield surface will begin to grow. Point a, the yield point, is also shown on the equivalent stress-strain curve in Figure 6c. As the loading state is further increased to point b, as shown in Figure 6b and 6c, the yield surface remains centred at the same position, but its radius grows in all directions by an amount governed by the magnitude of the loading.

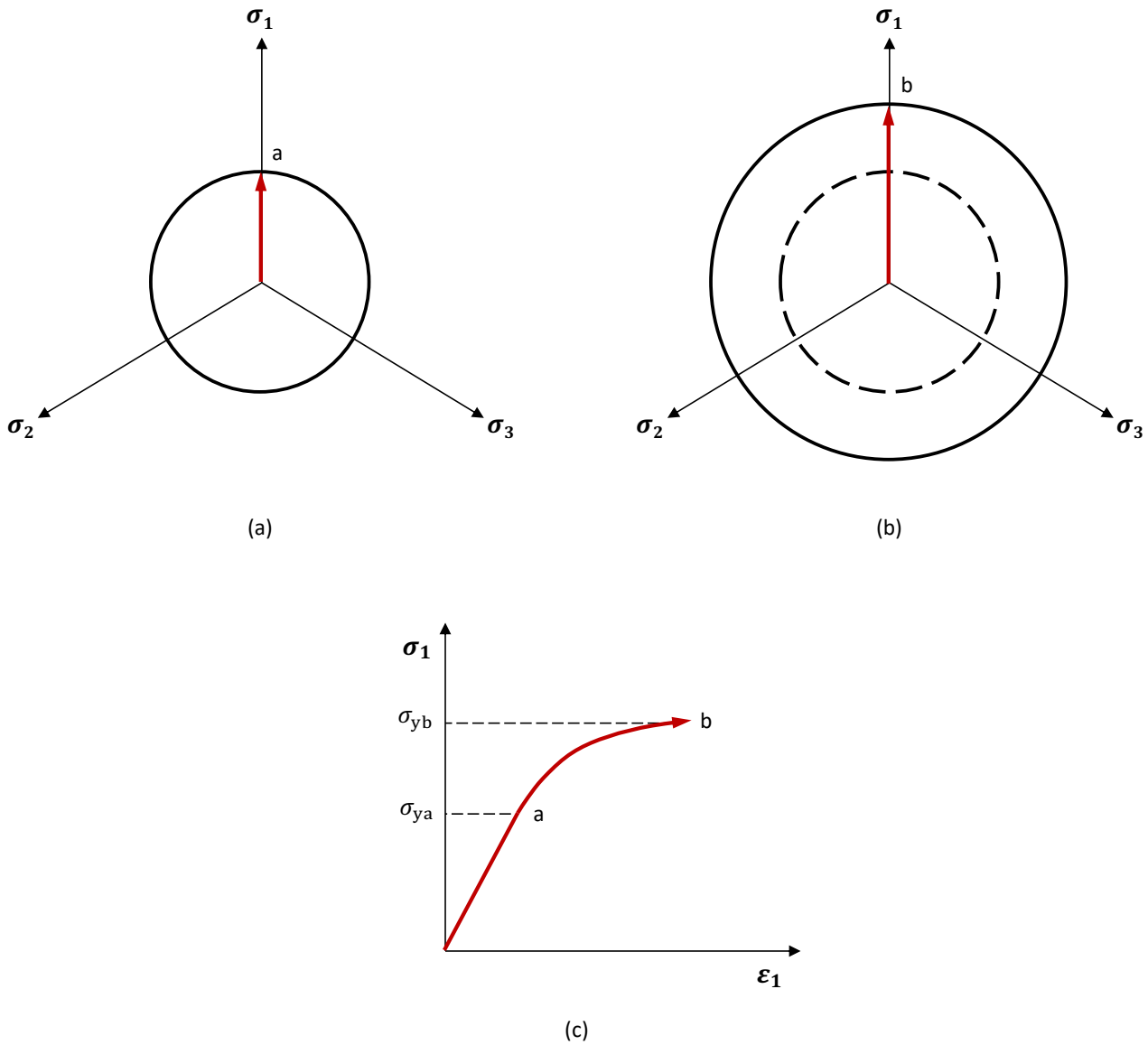

Figure 6

If the loading is then reversed, as shown in Figure 7a, further plasticity (and therefore hardening) does not occur until the magnitude of the reserved loading is such that the edge of the increased yield surface, point c, is reached. This can also be represented on the equivalent stress-strain curve, as shown in Figure 7c. This position of compressive yield is at a larger load magnitude than if loaded in this direction originally. This is due to the growth of the yield surface (isotropic hardening) during the prior tensile loading. As the compressive load magnitude is further increased to point d, as shown in Figure 7b and 7c, the yield surface again remains centred at the same position, but its radius grows further in all directions by an amount governed by the magnitude of the loading.

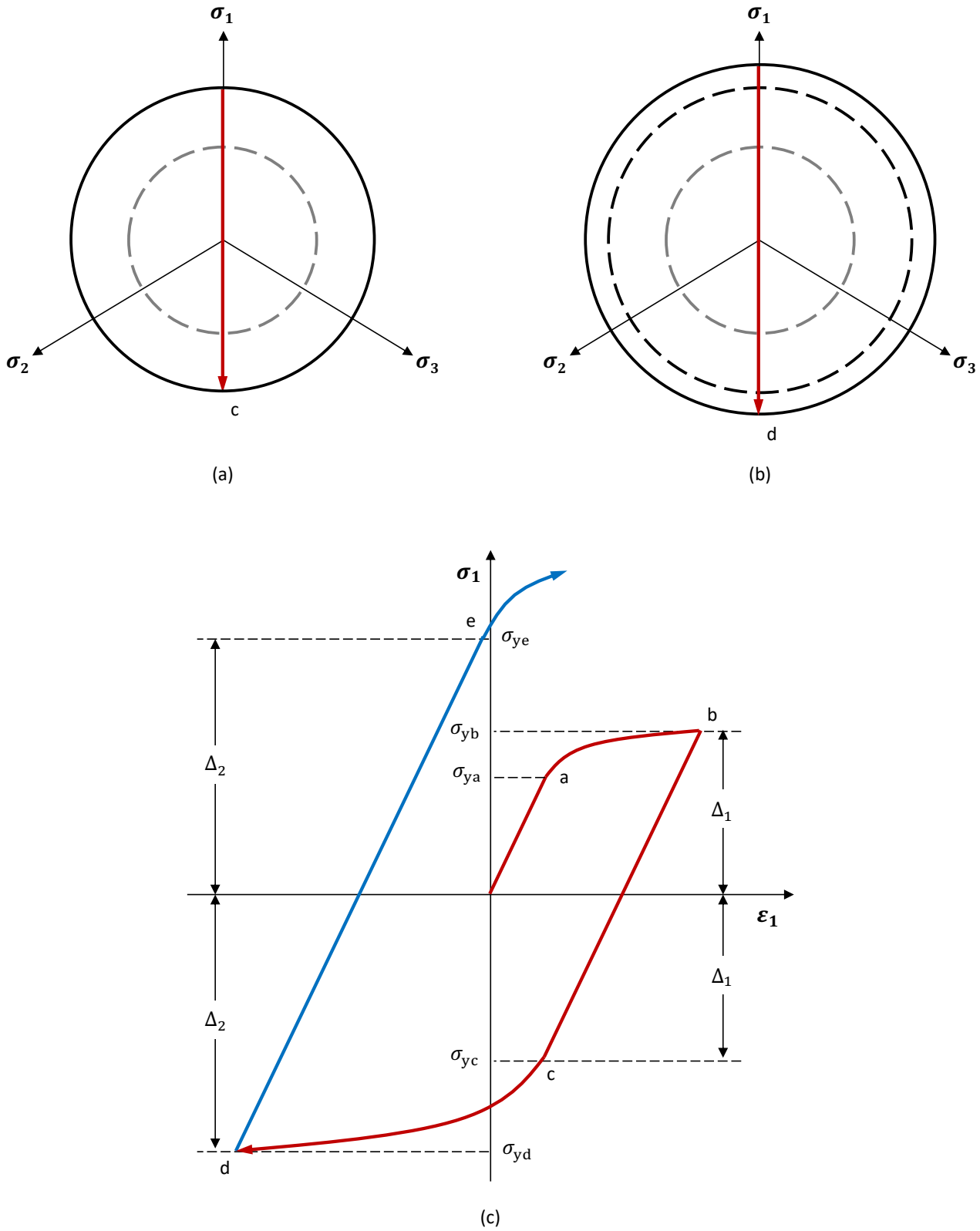

Figure 7

The blue loading curve shown in Figure 7c shows how the material would behave under a further tensile loading and shows that again, further plasticity (and therefore hardening) does not occur until the magnitude of the loading is such that the edge of the increased yield surface, point e, is reached.

Kinematic Hardening

In the case of kinematic hardening behaviour, when the loading state reaches the point of causing yielding within the material, i.e., point a in Figure 8a, the yield surface begins moves in the direction of the loading. Point a, the yield point, is also shown on the equivalent stress-strain curve in Figure 8c. As the load is further increased to point b, shown in Figure 8b and 8c, the yield surface remains the same size (diameter of $2\sigma_{ya}$) but moves in the direction of the loading by an amount governed by the magnitude of the loading.

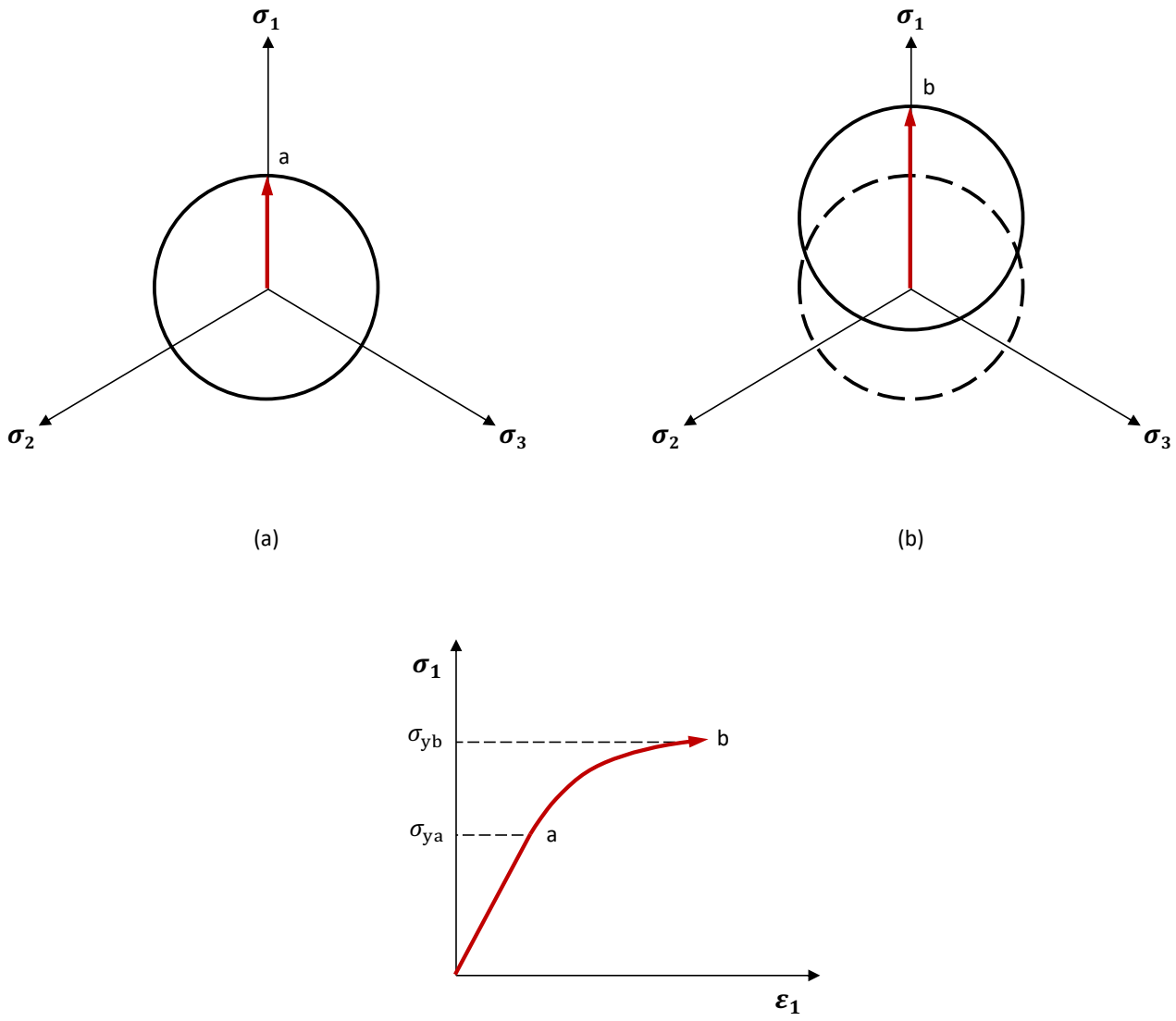

Figure 8

If the loading is then reversed, as shown in Figure 9a, further plasticity (and therefore hardening) will occur at position c. This can also be represented on the equivalent stress-strain curve, as shown in Figure 9c. This position of compressive yield is now at a lower load magnitude than if loaded in this direction originally, due to the movement of the yield surface (kinematic hardening) during the prior tensile loading. As the compressive load magnitude is further increased to point d, as shown in Figure 9b and 9c, the yield surface remains the same size, but its centre again moves in the direction of the loading by an amount governed by the magnitude of the loading.

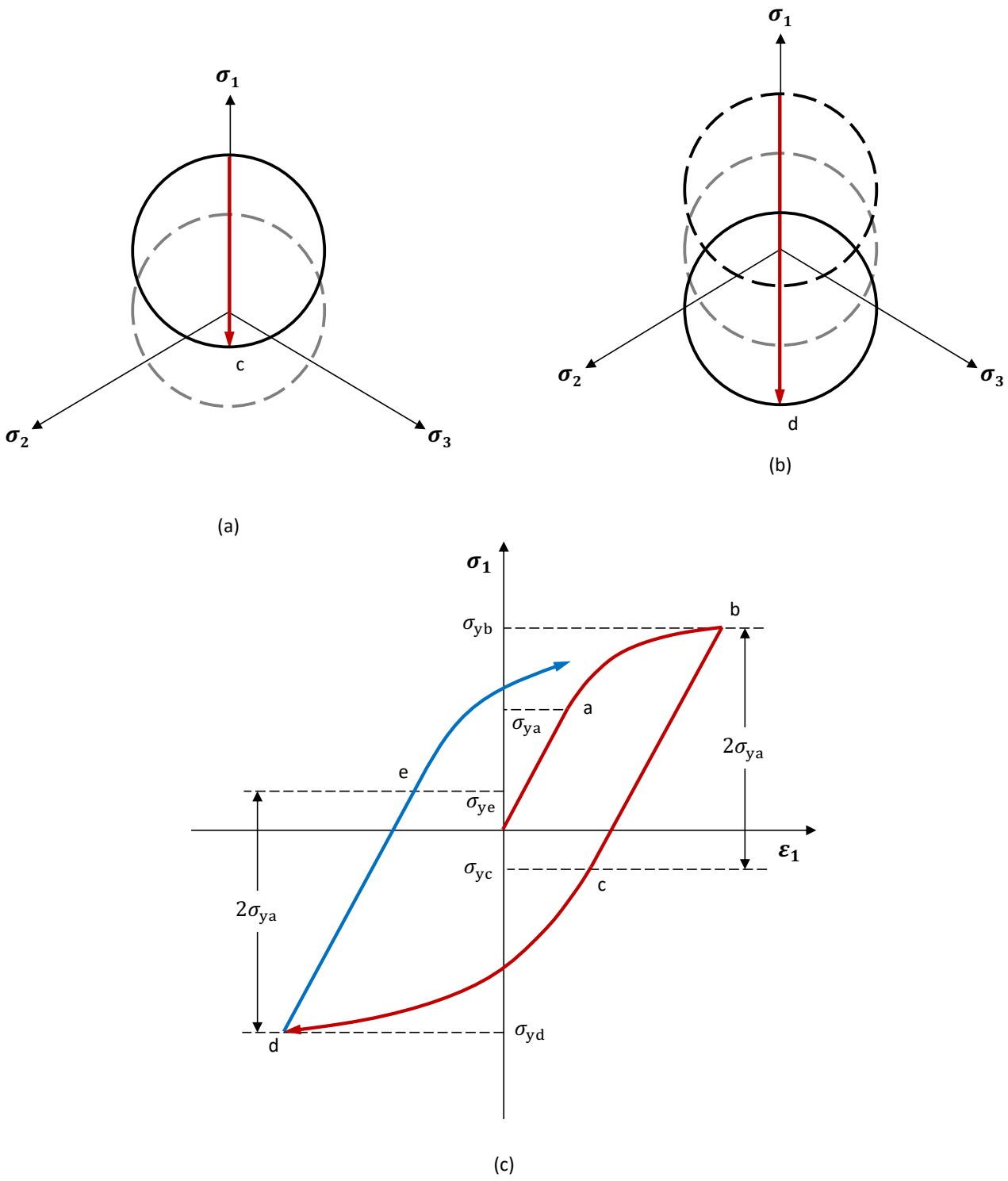

Figure 9

The blue loading curve shown in Figure 9c shows how the material would behave under a further tensile loading and shows that again, further plasticity (and therefore hardening) occurs at a lower stress magnitude, point e, than in the previous tensile and compressive loadings, due to the movement of the yield surface (kinematic hardening) during the prior compressive loading.

In the descriptions of isotropic and kinematic hardening above, the loading was chosen to be in the 1-direction, however, it is important to note that the applied loading could be in any direction, with the concepts described above

remaining valid. It should also be noted that in both cases, the von Mises yield criterion and non-linear hardening were chosen for demonstrative purposes, but the same concepts would apply in the case of the Tresca yield criterion and/or linear hardening, respectively.

In reality, it is not common for materials to harden in a purely isotropic or kinematic manner, but rather a mixture of these. There are material behaviour models (e.g., the unified visco-plasticity model) which account for both isotropic and kinematic hardening. Also, whereas isotropic and kinematic hardening represent growth and movement of the yield surface, respectively, other material hardening models represent a change in the shape of the yield surface.

In the following analyses related to the elastic-plastic deformation of components (e.g., beams in bending and torsion of shafts), only the EPP material behaviour model will be considered.

3. Elastic-Plastic Bending of Beams

Figure 10a shows a beam which is subjected to a bending moment, M. The rectangular cross-sectional area of the beam is shown in Figure 10b.

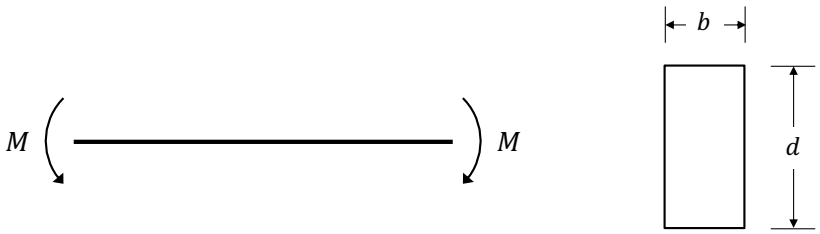

(a) (b)

Figure 10

Assuming that the magnitude of the bending moment is not high enough to cause plasticity (yielding) within the beam, the elastic beam bending equation can be used to describe the stress distribution, as a function of y (distance from the neutral axis), as:

$$\sigma = \frac{My}{I} \tag{1}$$

In this elastic case then, the stress distribution, as a function of y, throughout the cross-section, is linear, as shown in Figure 11.

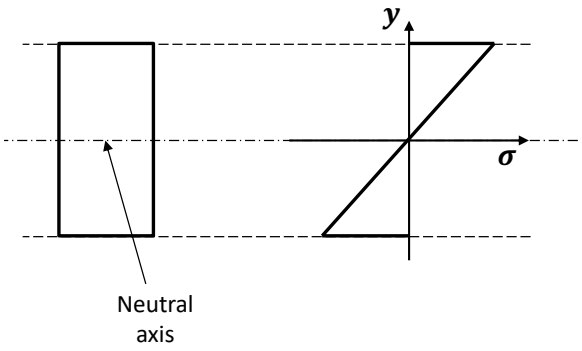

Figure 11

If the bending moment is increased to a magnitude which is just high enough to induce plasticity within the beam, this plasticity will occur at the positions furthest away from the neutral axis, i.e., at the positions of maximum y magnitude (top and bottom edges of the cross-section). As the bending moment is further increased, the plasticity spreads from the outer edges, to further within the cross-section (towards the neutral axis) as shown in Figure 12. As can be seen from Figure 12, the material behaviour demonstrated is elastic perfectly-plastic, as once the material has yielded, at $y > a$ and $y < -a$, no further increase in stress magnitude is observed.

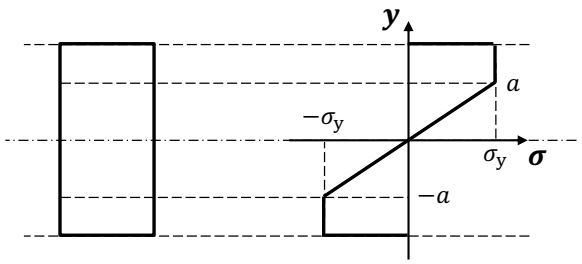

Figure 12

Moment equilibrium can be used to relate the applied bending moment, M, to the position as which yielding occurs, a, as:

$$M = \int_A y\sigma \mathrm{d}A \tag{2}$$

Equation (2) shows that the sum of the moments caused as a result of the stress, σ, in each unit of area, $\mathrm{d}A$, in the cross-section, must be equal to the applied bending moment, M. This can be seen in the right-hand side of the above equation as stress, σ, multiplied by area, A, gives force, F, and force multiplied by perpendicular distance, y, gives bending moment. I.e., for each unit of area, $\mathrm{d}A$:

$$\sigma \times \mathrm{d}A = \mathrm{dF}$$

and

$$\mathrm{d}F \times y = \mathrm{d}M$$

Equation (2) can be rewritten as:

$$M = \int_{-d/2}^{d/2} y\sigma b \mathrm{d}y \tag{3}$$

where b and d are the width (or breadth) and depth of the cross-section, respectively, as shown in Figure 10, and where:

$$\mathrm{d}A = b\mathrm{d}y$$

Recognising the symmetry about the neutral axis in the stress distribution magnitudes, equation (3) can be rewritten as:

$$M = 2\int_{0}^{d/2} y\sigma b \mathrm{d}y$$

Substituting the expressions for stress for each of the elastic ($0 > y > a$) and plastic ($a > y > {}^{d}/_{2}$) regions, i.e., $\sigma_{\mathrm{y}}\frac{y}{a}$ and σ_{y}, respectively, into this gives:

$$M = 2\int_{0}^{a} y\left(\sigma_{\mathrm{y}}\frac{y}{a}\right) b\mathrm{d}y + \int_{a}^{d/2} y\sigma_{\mathrm{y}} b\mathrm{d}y$$

$$= 2b\sigma_{\mathrm{y}}\left(\frac{d^2}{8} - \frac{a^2}{6}\right)$$

In order for the radius of curvature of the beam, R, due to the applied bending moment, M, to be calculated, both compatibility and a stress-strain relationship are required. As the region of the cross-section between $-a < y < a$ has only behaved elastically, the elastic beam bending equation can be applied. I.e.:

$$\frac{M}{I} = \frac{\sigma}{y} = \frac{E}{R}$$

$$\therefore \frac{y}{R} = \frac{\sigma}{E} = \varepsilon$$

$$\therefore R = \frac{y}{\varepsilon} \tag{4}$$

where ε is the strain related to the stress σ.

As the beam behaves as one body, the entirety of the beam (both the elastic and plastic regions) must share this common radius of curvature, R. This is the **compatibility requirement** mentioned above.

Again, as the region of the cross-section between $-a < y < a$ has only behaved elastically, Hooke's law applies here, and so:

$$\sigma = E\varepsilon$$

This is the required **stress-strain** relationship mentioned above.

Rearranging for ε and substituting this into equation (4):

$$R = \frac{Ey}{\sigma} \tag{5}$$

Substituting values for y and σ, from within the elastic region, into this equation, allows for R to be calculated. A convenient value of y to use is a (which is the outermost point of the elastic region), for which the corresponding value of σ is σ_y. Therefore:

$$R = \frac{Ea}{\sigma_y}$$

As plasticity has occurred within the beam during loading, on unloading the stress distribution and radius of curvature will not return to zero. Rather a residual stress distribution and residual radius of curvature will remain. If we assume that the stress change which occurs on unloading is purely elastic, then the stress change, $\Delta\sigma$, can be calculated from equation (1) as:

$$\Delta\sigma = \frac{\Delta M y}{I}$$

The maximum stress change, $\Delta\sigma_{\max}$, will therefore occur at $y_{\max}$, and so:

$$\Delta\sigma_{\max} = \frac{\Delta M \times y_{\max}}{I} = \frac{-M \times \pm {}^{d}/_{2}}{I}$$

where the change in bending moment on unloading, ΔM, is $-M$ and $y_{\max} = \pm {}^{d}/_{2}$.

Therefore, at $y = {}^{d}/_{2}$ (top edge):

$$\Delta\sigma_{(y={}^{d}/_{2})} = \frac{-Md}{2I}$$

and at $y = -{}^{d}/_{2}$ (bottom edge):

$$\Delta\sigma_{(y=-{}^{d}/_{2})} = \frac{Md}{2I}$$

As the unloading behaviour has been assumed to be elastic, the stress variation between these two values, relating to the top and bottom edges, will be linear, as shown by the unloading part of Figure 13.

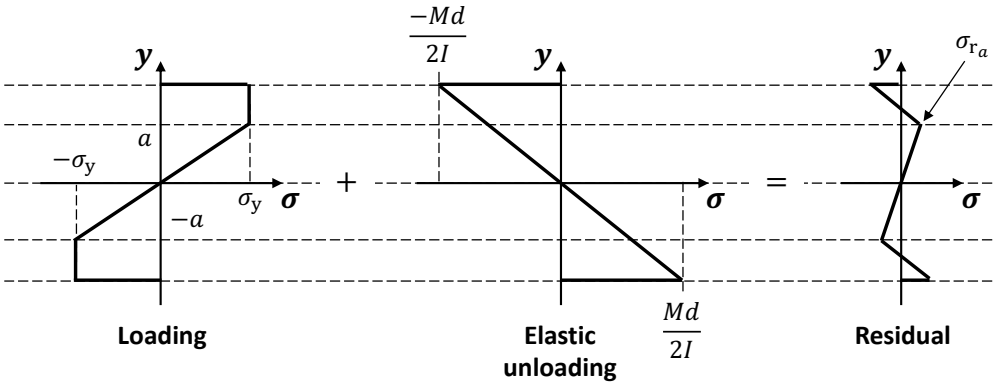

Figure 13

Figure 13 also shows that by summing the loaded stress distribution on the cross-section with the stress change which occurs on unloading, the residual stress distribution can be obtained.

It is clear that the residual stresses are well below the yield stress, so reverse yielding does not occur, and therefore the elastic unloading assumption made, is correct.

This residual stress distribution will be accompanied by a residual radius of curvature, which can be calculated by substituting unloaded beam values for y and σ into equation (5), which again relate to a position that has only been subjected to elastic behaviour. As before (under loaded conditions), a convenient value of y to use is a (which is the outermost point of the elastic region), for which the corresponding value of σ can be taken from the residual stress distribution given in Figure 13 and is shown labelled as σ_{r_a} (i.e., the residual stress, σ_r, at position a).

On releasing the moment, the radius of curvature increases. This change of curvature is called 'spring back' and is particularly important when bending beams to specified radii of curvature.

4. Worked Example – Elastic-Perfectly Plastic I-Beam Subjected to a Pure Bending Moment

Problem

Figure 14 shows the cross-section of a straight I-beam which is subjected to a pure bending moment, M.

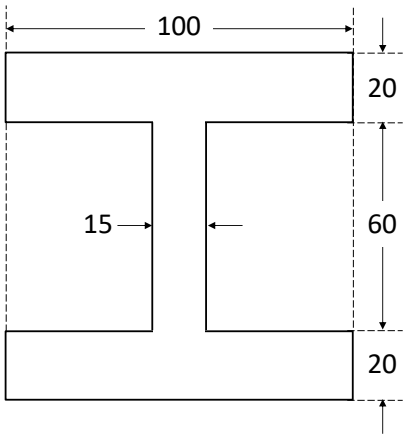

All dimensions in mm

Figure 14

Calculate:

a. the maximum allowable value of M if the web of the section is not to be subjected to any plasticity.
b. the stress distribution and radius of curvature upon the application of M
c. the stress distribution and radius of curvature upon unloading

The material can be assumed to be elastic-perfectly-plastic with a yield stress, $\sigma_y = 215$ MPa, and Young's Modulus, $E = 200$ GPa.

Solution

As it is known that the full depths of each flange are allowed to yield, but the web is to remain fully elastic, the resulting stress distribution due to the application of the maximum allowable bending moment, M, is as shown in Figure 15.

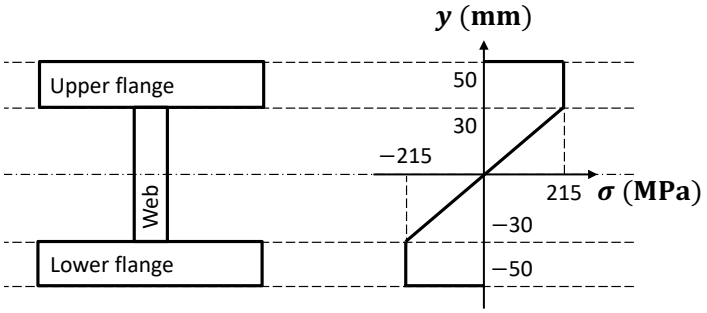

Figure 15

Moment Equilibrium

Balancing the moments due to stresses in the elastic and plastic regions with the applied moment:

$$M = \int_A y\sigma dA$$

$$= \int_{-d/2}^{d/2} y\sigma b \mathrm{d}y$$

Due to the symmetry of the stress distribution magnitude about the neutral axis and substituting in the elastic and plastic terms for σ, this can be rewritten as:

$$M = 2\left(\int_0^a y\left(\sigma_y \frac{y}{a}\right) b_w \mathrm{d}y + \int_a^{d/2} y\sigma_y b_f \mathrm{d}y\right)$$

$$= 2\sigma_y\left(\frac{b_w}{a}\int_0^a y^2 \mathrm{d}y + b_f \int_a^{d/2} y \mathrm{d}y\right)$$

where b_w and b_f are the widths of the web and flange sections of the beam, respectively, and a is the value of y where the cross-section transitions from the web to the flange.

Therefore,

$$M = 2\sigma_y\left(\frac{b_w}{a}\left[\frac{y^3}{3}\right]_0^a + b_f\left[\frac{y^2}{2}\right]_a^{d/2}\right)$$

$$= 2\sigma_y\left(b_w\frac{a^2}{3} + b_f\left(\frac{d^2}{8} - \frac{a^2}{2}\right)\right)$$

$$\therefore \boldsymbol{M = 36{,}335{,}000\ \mathrm{Nmm} = 36.34\ \mathrm{kNm}}$$

Compatibility

As the region of the cross-section between $-a < y < a$ has only behaved elastically, the elastic beam bending equation can be applied and rearranged to give:

$$R = \frac{y}{\varepsilon}$$

As the beam behaves as one body, this expression for R can be applied to any value of y.

Stress-Strain Relationship

Again, as the region of the cross-section between $-a < y < a$ has only behaved elastically, Hooke's law applies here, which can be substituted into the above expression for R to give:

$$R = \frac{Ey}{\sigma}$$

Substituting values for y and σ from the outermost point of the elastic region gives:

$$R_{\text{load}} = \frac{Ea}{\sigma_y}$$

$$\therefore \boldsymbol{R_{\text{load}} = 27,906.98\ \text{mm} = 27.91\ \text{m}}$$

Unloading

Assuming that the stress change caused by unloading is purely elastic, then from the elastic beam bending equation:

$$\Delta\sigma = \frac{\Delta M \times y}{I}$$

Therefore, at the top and bottom edges:

$$\Delta\sigma_{(y=d/2)} = \frac{-M \times d/2}{I} = \frac{-Md}{2I} = \frac{-36{,}335{,}000 \times 100}{2 \times 6{,}803{,}333.33} = -267.04\ \text{MPa}$$

and

$$\Delta\sigma_{(y=-d/2)} = \frac{-M \times -d/2}{I} = \frac{Md}{2I} = 267.04\ \text{MPa}$$

Where:

$$I = \left(\frac{bd^3}{12}\right)_{outer} - \left(\frac{bd^3}{12}\right)_{gaps} = \frac{100 \times 100^3}{12} - 2\left(\frac{42.5 \times 60^3}{12}\right) = 8{,}333{,}333.33\ \text{mm}^4 - 1{,}530{,}000\ \text{mm}^4$$

$$= 6{,}803{,}333.33\ \text{mm}^4$$

Since the unloading behaviour has been assumed to be elastic, the stress variation between these two values, relating to the top and bottom edges, will be linear, as shown in the unloading section of Figure 16.

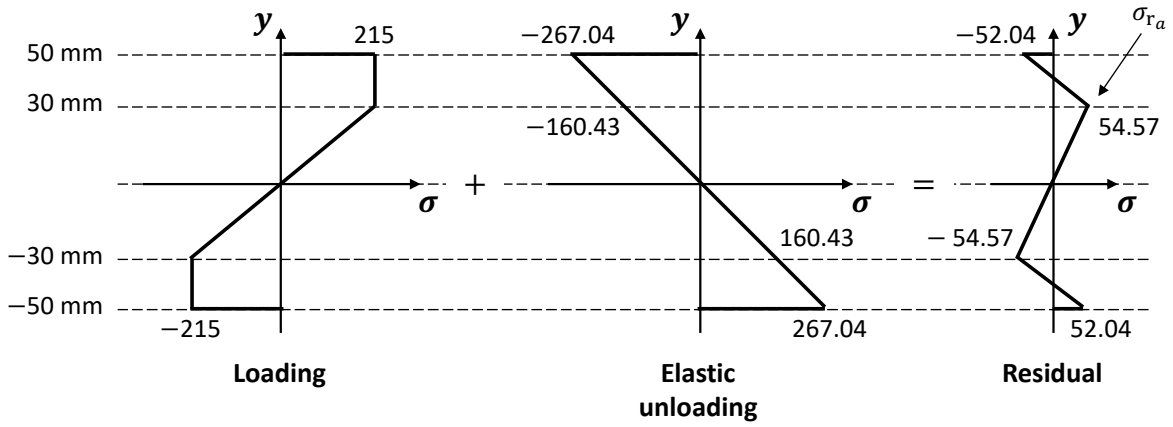

Figure 16

The equation of the linear unloading relationship is:

$$y = m\sigma + c \tag{6}$$

where, as the line passes through the origin:

$$c = 0$$

and the gradient, m, can be calculated by choosing a corresponding set of y and σ values, e.g., those applicable to the top edge, i.e., $y = 50$ mm and $\sigma = -267.04$ MPa and substituting these into equation (6) as:

$$\therefore 50 = m \times -267.04$$

$$\therefore m = -0.187$$

This value for m allows for the interpolation of the unloading stress distribution to determine the σ value at $y = 30$ mm, from equation (6) as:

$$30 = -0.187\sigma$$

$$\therefore \sigma = -160.43$$

The loading and unloading stress distributions can now be summed together in order to determine the residual stress distribution as follows.

At $y = 50$ mm:

$$\sigma_{r_{50}} = \sigma_{\text{load}_{50}} + \sigma_{\text{unload}_{50}} = 215 \text{ MPa} - 267.04 \text{ MPa} = -52.04 \text{ MPa}$$

At $y = 30$ mm:

$$\sigma_{r_{30}} = \sigma_{\text{load}_{30}} + \sigma_{\text{unload}_{30}} = 215 \text{ MPa} - 160.43 \text{ MPa} = 54.57 \text{ MPa}$$

At $y = 0$ mm:

$$\sigma_{r_0} = \sigma_{\text{load}_0} + \sigma_{\text{unload}_0} = 0 \text{ MPa} - 0 \text{ MPa} = 0 \text{ MPa}$$

At $y = -30$ mm:

$$\sigma_{r_{-30}} = \sigma_{\text{load}_{-30}} + \sigma_{\text{unload}_{-30}} = -215 \text{ MPa} + 160.43 \text{ MPa} = -54.57 \text{ MPa}$$

At $y = -50$ mm:

$$\sigma_{r_{-50}} = \sigma_{\text{load}_{-50}} + \sigma_{\text{unload}_{-50}} = -215 \text{ MPa} + 267.04 \text{ MPa} = 52.04 \text{ MPa}$$

The residual section of Figure 16 shows this in graphical form.

As the residual stresses are well below the yield stress (±215 MPa), reverse yielding will not occur, and therefore the elastic unloading assumption made, is correct.

This residual stress distribution will be accompanied by a residual radius of curvature, which can be calculated by substituting unloaded beam values for y and σ into the same equation as above for the loaded equivalent, which again relate to a position that has only been subjected to elastic behaviour. As before (under loaded conditions), a convenient value of y to use is $a = 30$ mm (which is the outermost point of the elastic region), for which the corresponding value of σ can be seen, from Figure 16, to be 54.57 MPa. I.e.:

$$R_{\text{unload}} = \frac{Ea}{\sigma_{\text{r}_a}}$$

$$\therefore \boldsymbol{R_{\text{unload}} = 109,950.52 \text{ mm} = 109.95 \text{ m}}$$

5. Elastic-Plastic Torsion of Shafts

Figure 17a shows a shaft which is subjected to a torque, T. The circular cross-sectional area of the shaft is shown in Figure 17b.

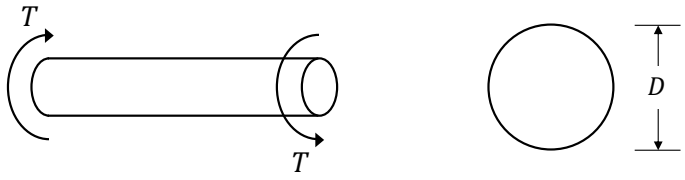

(a) (b)

Figure 17

Assuming that the magnitude of the torque is not high enough to cause plasticity (yielding) within the shaft, the elastic shaft torsion equation can be used to describe the shear stress distribution, as a function of r (radius of the shaft), as:

$$\tau = \frac{Tr}{J} \tag{7}$$

In this elastic case then, the shear stress distribution, as a function of r, throughout the cross-section is linear, as shown in Figure 18.

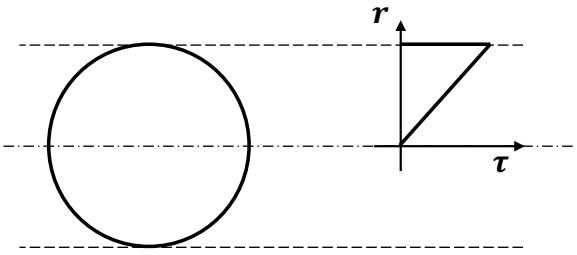

Figure 18

If the torque is increased to a magnitude which is just high enough to induce plasticity in the shaft, this plasticity will occur at the positions furthest away from the centre of the cross-section, i.e., at the positions of maximum r magnitude (circumference of the cross-section). As the torque is further increased, the plasticity spreads from the outer edge, to further within the cross-section (towards the centre) as shown in Figure 19. As can be seen from Figure 19, the material behaviour demonstrated is elastic perfectly-plastic, as once the material has yielded, at $r > a$, no further increase in stress magnitude is observed.

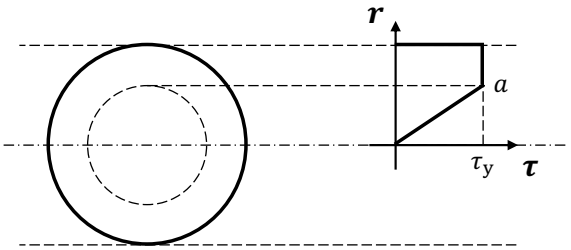

Figure 19

Torque equilibrium can be used to relate the applied torsion, T, to the position as which yielding occurs, a, as:

$$T = \int_A r\tau dA \tag{8}$$

Equation (8) shows that the sum of the torques caused as a result of the shear stress, τ, in each unit of area, $\mathrm{d}A$, in the cross-section, must be equal to the applied torque, T. This can be seen in the right-hand side of the above equation as shear stress, τ, multiplied by area, A, gives units of force, and force multiplied by perpendicular distance, r, gives torque.

Equation (8) can be rewritten as:

$$T = 2\pi \int_0^R \tau r^2 \mathrm{d}r \tag{9}$$

where R is the outer radius of the cross-section, and:

$$\mathrm{d}A = 2\pi r \mathrm{d}r$$

Substituting the expressions for shear stress for each of the elastic ($0 > r > a$) and plastic ($a > r > R$) regions, i.e., $\tau_y \frac{r}{a}$ and τ_y, respectively, into equation (9) gives:

$$T = 2\pi \int_0^a \left(\tau_y \frac{r}{a}\right) r^2 \mathrm{d}r + 2\pi \int_a^R \tau_y r^2 \mathrm{d}r$$

$$= 2\pi\tau_y \left(\frac{R^3}{3} - \frac{a^3}{12}\right)$$

In order for the twist, θ, of the shaft, due to the applied torque, T, to be calculated, both compatibility and a shear stress-shear strain relationship are required. As the region of the cross-section between $0 < r < a$ has only behaved elastically, the elastic shaft torsion equation can be applied. I.e.:

$$\frac{T}{J} = \frac{\tau}{r} = \frac{G\theta}{L}$$

$$\therefore \frac{r\theta}{L} = \gamma \left(= \frac{\tau}{G}\right)$$

$$\therefore \theta = \frac{\gamma L}{r} \tag{10}$$

where γ is the shear strain related to the shear stress τ.

As the shaft behaves as one body, the entirety of the shaft (both the elastic and plastic regions) must share this common twist, θ. This is the **compatibility requirement** mentioned above.

Again, as the region of the cross-section between $0 < r < a$ has only behaved elastically, Hooke's law applies here, therefore:

$$\tau = G\gamma$$

This is the required **shear stress-shear strain** relationship mentioned above. Rearranging for γ and substituting this into equation (10):

$$\theta = \frac{\tau L}{Gr} \tag{11}$$

Substituting values for r and τ, from within the elastic region, into this equation, allows for θ to be calculated. A convenient value of r to use is a (which is the outermost point of the elastic region), for which the corresponding value of τ is τ_{y}. Therefore:

$$\theta = \frac{\tau_y L}{Ga}$$

As plasticity has occurred within the shaft during loading, on unloading the shear stress distribution and twist will not return to zero. Rather a residual shear stress distribution and residual twist will remain. If we assume that the shear stress change which occurs on unloading is purely elastic, then the shear stress change, $\Delta\tau$, can be calculated from equation (7) as:

$$\Delta\tau = \frac{\Delta T \times r}{J}$$

The maximum shear stress change, $\Delta\tau_{\max}$, will therefore occur at $r_{\max}$, and so:

$$\Delta\tau_{\max} = \frac{\Delta T \times r_{\max}}{J} = \frac{-TR}{J}$$

where the change in torque on unloading, ΔT, is $-T$ and $r_{\max} = R$.

As the unloading behaviour has been assumed to be elastic, the shear stress variation through the cross-section will be linear, as shown by the unloading part of Figure 20.

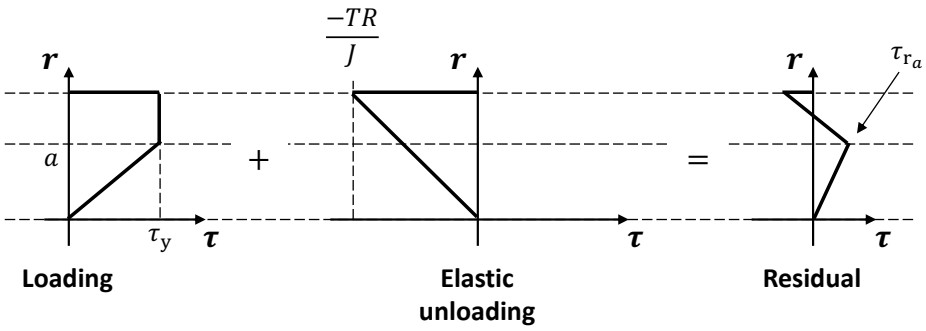

Figure 20

Figure 20 also shows that by summing the loaded shear stress distribution on the cross-section with the shear stress change which occurs on unloading, the residual shear stress distribution can be obtained.

It is clear that the residual shear stresses are well below the yield shear stress, so reverse yielding does not occur, and therefore the elastic unloading assumption made, is correct.

This residual shear stress distribution will be accompanied by a residual shaft twist, which can be calculated by substituting unloaded beam values for r and τ into equation (11), which again relate to a position that has only been subjected to elastic behaviour. As before (under loaded conditions), a convenient value of r to use is a (which is the outermost point of the elastic region), for which the corresponding value of τ can be taken from the residual shear stress distribution given in Figure 20 and is shown labelled as τ_{r_a} (i.e., the residual shear stress, τ_{r}, at position a).

1 Fatigue and Fracture

Learning Summary

1. Know the various stages leading to fatigue failure (knowledge);
2. Know the basis of the total life and of the damage tolerant approaches to estimating the number of cycles to failure (knowledge);
3. Be able to include the effects of mean and alternating stress on cycles to failure using the Gerber, modified Goodman and Soderberg methods (application);
4. Be able to include the effect of a stress concentration on fatigue life (application);
5. Be able to apply the S-N design procedure for fatigue life (application);
6. Know the meaning of linear-elastic fracture mechanics (LEFM) (knowledge);
7. Know what the three crack tip loading modes are (knowledge);
8. Be able to use the energy and stress intensity factor (Westergaard crack tip stress field) approaches to LEFM (application);
9. Know the meaning of small-scale yielding and fracture toughness (knowledge);
10. Understand the Paris equation for fatigue crack growth and the effects of the mean and alternating components of the stress intensity factor (knowledge/comprehension).

1.1 Fatigue

1.1.1 Introduction

Fatigue failure of components and structures results from cyclic (or repeated) loading and from the associated cyclic stresses and strains, as opposed to failure due to monotonic or static stresses or strains, such as buckling or plastic collapse due to excessive plastic deformation yielding. The topic of fatigue is extremely important in mechanical engineering, since machines have moving parts, which in turn give rise to stresses and strains which may vary with time, typically in a repetitive fashion. For example, the axle of a car which will transmit a time-varying torque, that changes from zero to some finite value when the car is put into gear and driven (and back to zero again when the car is taken out of gear).

An important design consideration, with respect to fatigue, is the fact that fatigue failure can occur at stresses which are well below the ultimate tensile strength of the material and often below the yield strength.

1.1.2 Basic phenomena

The failure mechanism for an initially un-cracked component with a smooth (polished) surface can be split into three parts, namely crack initiation, crack propagation and final fracture, as follows:

(i) Stage I crack growth: The micro-structural phenomenon which causes the initiation of a fatigue cracks is the development of persistent slip bands at the surfaces of the specimen. These persistent slip bands are the result of dislocations moving along crystallographic planes leading to both slip band intrusions and extrusions on the surface. These act as excellent stress concentrations and can thus lead to crack initiation. Crystallographic slip is primarily controlled by shear stresses rather than normal stresses so that fatigue cracks initially tend to grow in a plane of maximum shear stress range. This stage leads to short cracks, usually only of the order of a few grains.

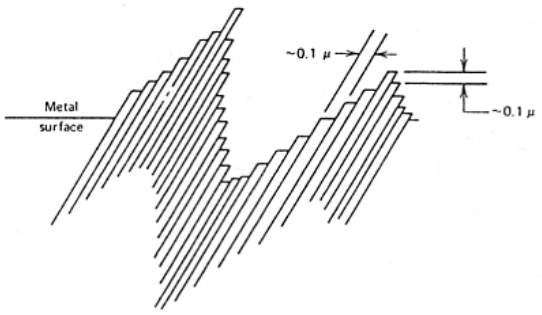

Figure 1.1: Persistent slip bands in ductile metals subjected to cyclic stress

(ii) Stage II crack growth: As cycling continues, the fatigue cracks tend to coalesce and grow along planes of maximum tensile stress range.

(iii) Final fracture; this occurs when the crack reaches a critical length and results in either ductile tearing (plastic collapse) at one extreme, or cleavage (brittle fracture) at the other extreme.

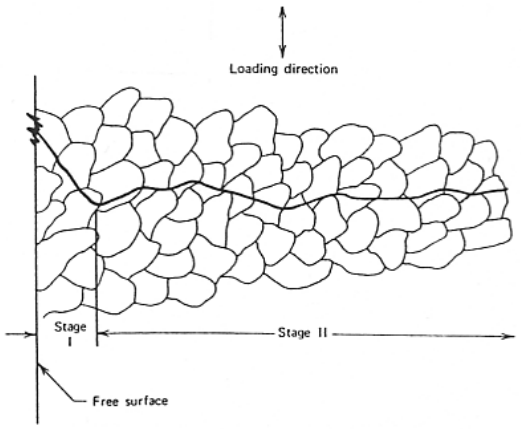

Figure 1.2: Schematic of stages I and II transcrystalline microscopic fatigue crack growth.

1.1.3 Fatigue Life Analysis

In order to allow for fatigue in the analysis and design of components, a number of different approaches are adopted; two of these approaches are described here. The more traditional approach is what is now referred to as the *total life approach* (see section 1.1.4), based on laboratory tests, which are carried out under either stress- or strain-controlled loading conditions on idealised specimens. These tests furnish the number of loading cycles to the initiation of a 'measurable' crack as a function of applied stress or strain parameters. The 'measurability' is dictated by the resolution accuracy of the crack detection method employed. A typical 'measurable' crack is about 0.75 mm to 1 mm. The challenge of fatigue design is then to relate these test results to actual component lives under real loading conditions. The second approach is known as the *damage tolerant approach* (see section 1.2.5). This approach is based on the inclusion of fatigue as a crack growth process, taking account of the fact that all components have inherent flaws or cracks. The development of fracture mechanics techniques to predict crack growth has facilitated this approach as a competing technique to the total life approach. Both of the approaches have advantages and disadvantages; the former has more appeal to design engineers while the latter is more often used by material scientists and researchers. Nonetheless, even in routine design, the damage tolerant approach is gaining popularity.

1.1.4 Total life approach

The total life approach is based on the results of stress- and strain-controlled cyclic testing of laboratory test specimens of material, in order to obtain the numbers of cycles to failure

as a function of the applied alternating stress, for example. Figure 1.3 shows a rotating bending test machine set-up. This is a constant load amplitude machine since the load doesn't change even with crack growth. The specimens usually have finely polished surfaces to minimise surface roughness effects, which would particularly affect Stage I growth. In this approach, no distinction is made between crack initiation and propagation. Stress concentration effects can be studied by machining in grooves, notches or holes.

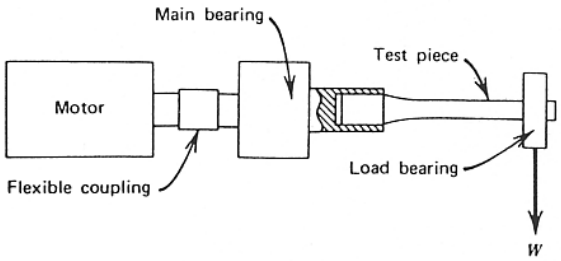

Figure 1.3: Rotating bending moment test apparatus for fully-reversed fatigue loading.

Traditionally, most fatigue testing was based on fully-reversed (i.e. zero mean stress, $S_m = 0$), stress-controlled conditions and the fatigue design data was presented in the form of *S*-*N* curves (see Figure 1.6), which are either semi-log or log-log plots of alternating stress, S_a, against the measured number of cycles to failure, *N*, where failure is defined as fracture. Some of the important stress parameters for cyclic loading are shown in Figure 1.4.

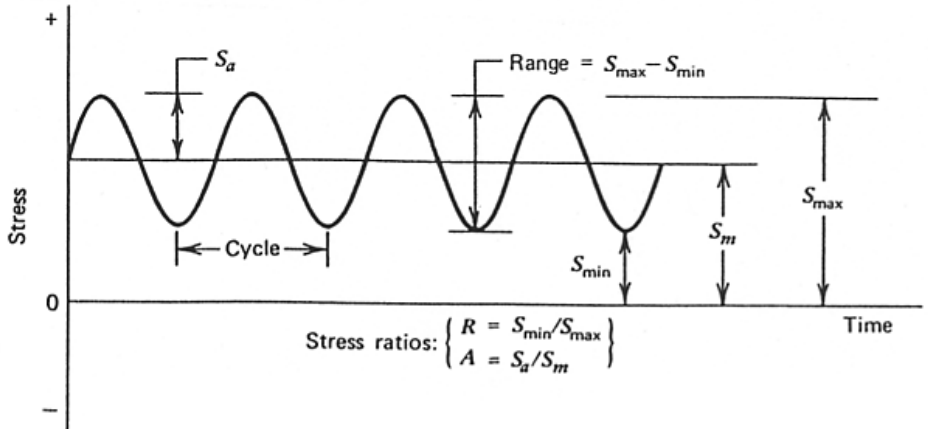

Figure 1.4: Notation used to describe constant load fatigue test cycles.

Figure 1.5 contains schematic representations of two typical *S*-*N* curves obtained from load (or stress)-controlled tests on smooth specimens. Figure 1.5(a) shows a continuously

sloping curve, while Figure 1.5(b) shows a discontinuity or “knee” in the curve. A “knee” is only found in a few materials (notably low strength steels) between 10^6 and 10^7 cycles under non-corrosive conditions. The curves are normally drawn through the median life value (of the scatter in N) and thus represents 50 percent expected failure. The *fatigue life*, N, is the number of cycles of stress (or strain) range of a specified character that a given specimen sustains before failure of a specified nature occurs. *Fatigue strength* is a hypothetical value of stress range at failure for exactly N cycles as obtained from an S-N curve. The *fatigue limit* (sometimes called the *endurance limit*) is the limiting value of the median fatigue strength as N becomes very large, e.g. $>10^8$ cycles.

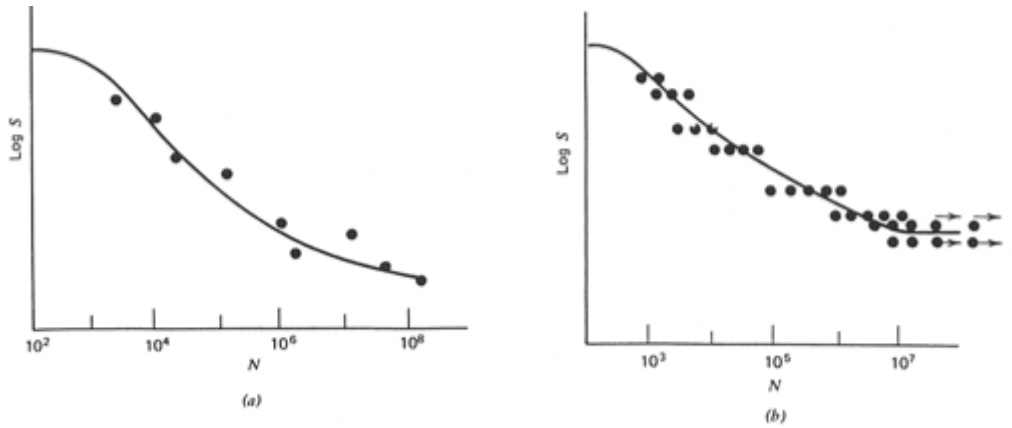

Figure 1.5: Typical S-N diagrams.

1.1.5 Effect of mean stress

The alternating stress, S_a, and the mean stress, S_m, are defined in Figure 1.4. Early investigators of fatigue assumed that only the alternating stress affected the fatigue life of a cyclically-loaded component. However, it has since been established that the mean stress has a significant effect on fatigue behaviour, as shown in Figure 1.6. It can be seen that tensile mean stresses are detrimental while compressive mean stresses are beneficial in comparison to zero mean stresses.

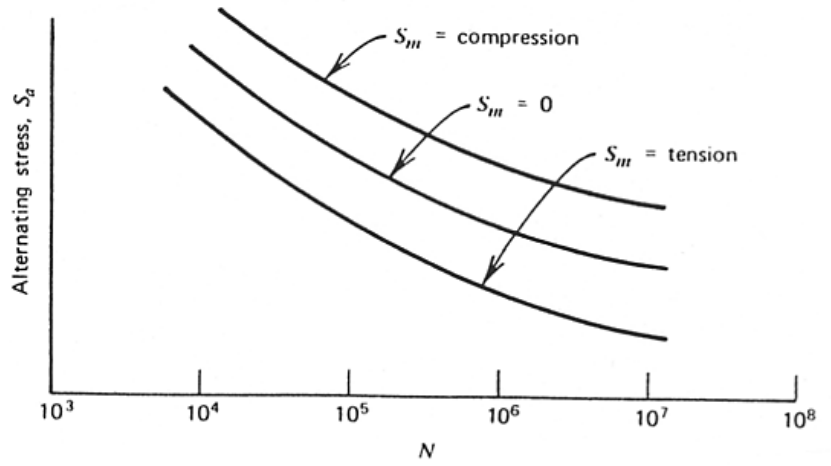

Figure 1.6: The effect of mean stress on fatigue life.

The effect of mean stress is commonly represented as a plot of S_a versus S_m for a given fatigue life. Attempts have been made to develop this relationship into general relations. Three of these common relations between allowable alternating stress for a given life as a function of mean stress, are shown in Figure 1.7.

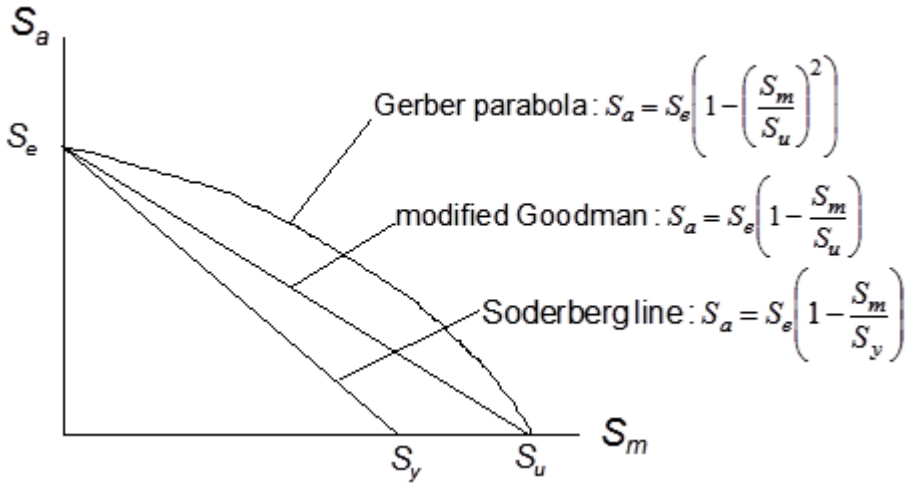

Figure 1.7: Gerber, modified Goodman and Soderberg relationships between S_a and S_m.

The modified Goodman line assumes a linear relationship between the allowable S_a and the corresponding mean stress S_m, where the slope and intercepts are defined by the fatigue strength, S_e, and the material UTS, S_u, respectively. The Gerber parabola employs the same end-points but, in this case, the relation is defined by a parabola. Finally, the Soderberg line again assumes a linear relation, but this time the mean stress axis end-point is taken as the yield stress, S_y. The modified Goodman line, for example, can be

extended into the compressive mean stress region to give increasing allowable alternating stress with increasing compressive mean stress, but this is normally taken to be horizontal for design purposes and for conservatism.

1.1.6 Effect of stress concentrations

Ever since the first occurrences of fatigue failure, it has been recognised that such failures are most commonly associated with notch-type features in components. It is impossible to avoid notches in engineering structures, although the effects of such notches can be reduced through appropriate design. The stress concentration associated with notch-type features leads typically to local plastic strain which eventually leads to fatigue cracking. Consequently, the estimation of stress concentration factors associated with various types of notches and geometrical discontinuities has received a lot of attention. This is typically expressed in terms of an elastic stress concentration factor (SCF), K_t, which is simply the relationship between the maximum local stress and an appropriate nominal stress, as follows:

$$K_t = \frac{\sigma_{\max}^{el}}{\sigma_{nom}}$$

It was once thought that the fatigue strength of a notched component could be predicted as the strength of a smooth component divided by the SCF. However, this is not the case. The reduction is, in fact, often less than K_t and is defined by the *fatigue notch factor,* K_f, which is defined as the ratio of the smooth fatigue strength to the notched fatigue strength as follows:

$$K_f = \frac{S_{a,smooth}}{S_{a,notch}}$$

However, this fatigue notch factor is also found to vary with both alternating and mean stress level and thus with number of cycles to failure. Figure 1.8 shows the effect of a notch, with an SCF of 3.4, on the fatigue behaviour of a wrought aluminium alloy, where the smooth lines are for the smooth specimen and the dotted lines are for the notched

specimen.

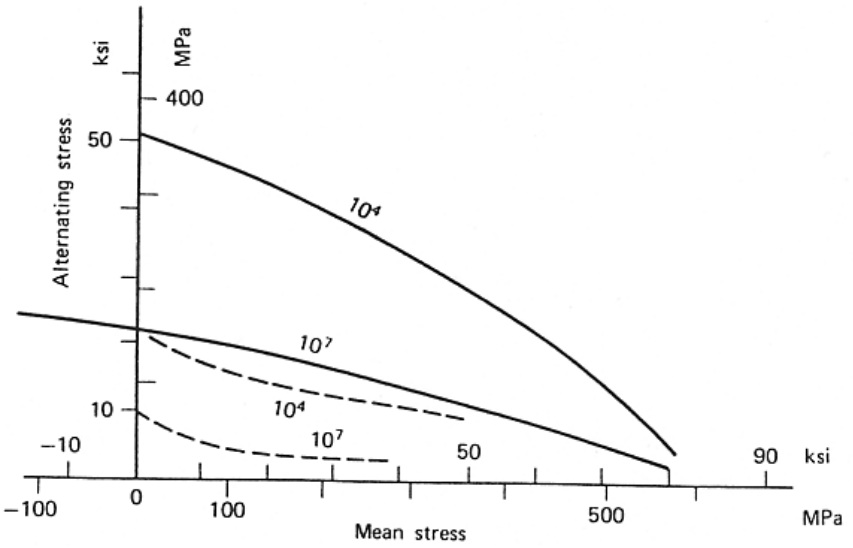

Figure 1.8: Constant life diagrams for a wrought aluminium alloy for both smooth and notched specimens (SCF = 3.4).

Table 1.1 shows how the fatigue notch factor changes with mean stress level and fatigue life. Clearly, the fatigue notch factor increases from 3.2 to 5.7 from 10^4 cycles to 10^7 cycles at 172 MPa mean stress, but remains unchanged between these lives at 2.3 for zero mean stress.

Table 1.1: Fatigue notch factor change with mean stress and fatigue life

Mean stress	10^4 cycles	10^7 cycles
0 MPa	51/22 = 2.3	22/9 = 2.3
172 MPa	42/13 = 3.2	17/3 = 5.7

1.1.7 *S-N* Design Procedure for Fatigue

Constant life diagrams plotted as S_a versus S_m, also called Goodman diagrams, as shown in Figure 1.9, can be used in design to give safe estimates of fatigue life and loads.

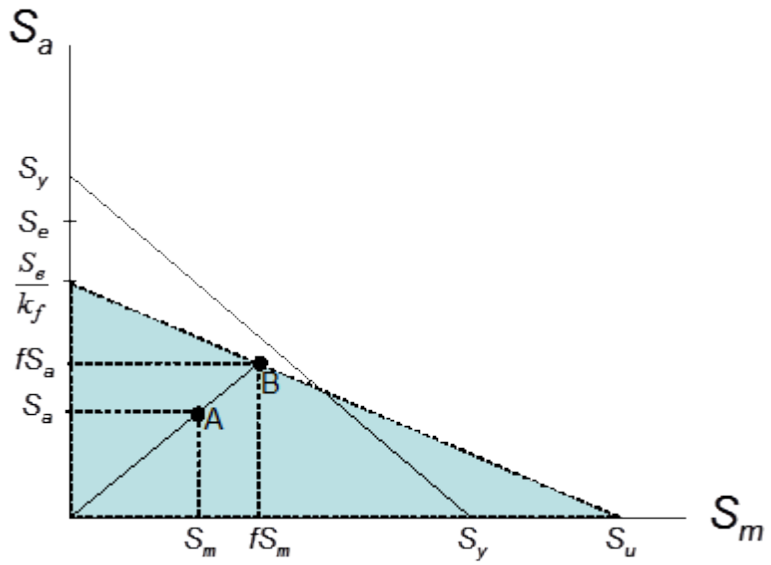

Figure 1.9: Goodman diagram.

(i) The Goodman line connects the endurance limit, S_e (or long life fatigue strength), to the U.T.S., S_u

(ii) The fatigue strength for zero mean stress is reduced by the fatigue notch factor, K_f. The stress concentration factor, K_t is used if K_f is not known.

(iii) For static loading of a ductile component with a stress concentration, failure still occurs when the mean stress is equal to the U.T.S. Failure at intermediate values of mean stress is assumed to be given by the dotted line.

(iv) In order to avoid yield of the whole cross-section of the component, the maximum nominal stress must be less than the yield stress, S_y , i.e. $S_m + S_a < S_y$
This relationship gives the yield line joining S_y to S_y.

(v) The region of the diagram nearest to the origin is the 'safe' region (can also be extended to include compressive yield).

(vi) A component is assessed by plotting the point corresponding to the nominal alternating stress, S_a, and the nominal mean stress, S_m, i.e. not the maximum values associated with the notch. The factor of safety is determined from the position of the point relative to the safe/fail boundary.
i.e. factor of safety F = OB/OA

from similar triangles $$\frac{S_a}{\left(\frac{S_u}{F} - S_m\right)} = \frac{S_e}{k_f S_u}$$

$$\frac{1}{F} = \frac{S_a k_f}{S_e} + \frac{S_m}{S_u}$$

A procedure similar to that described above for long life can also be used to design for a specified number of cycles. In this case the endurance limit and the fatigue notch factor are replaced by the fatigue strength and the fatigue notch factor for the specified number of cycles.

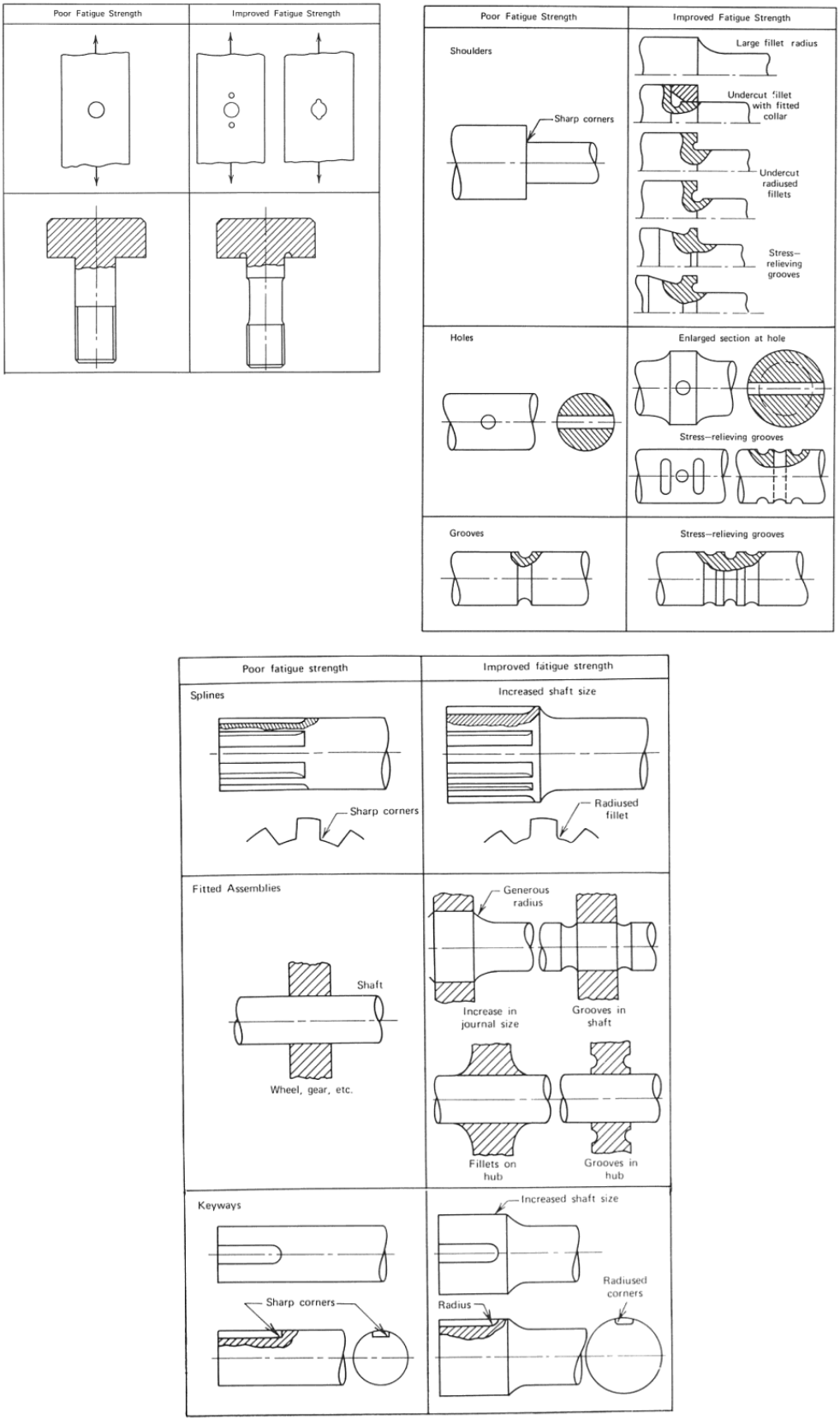

Figure 1.10: Examples of geometries/components with poor and improved fatigue strength.

1.2 Linear Elastic Fracture Mechanics (LEFM)

1.2.1 Introduction

Consider the stress concentration factor for an elliptical hole in a large, linear-elastic plate subjected to a remote, uniaxial stress.

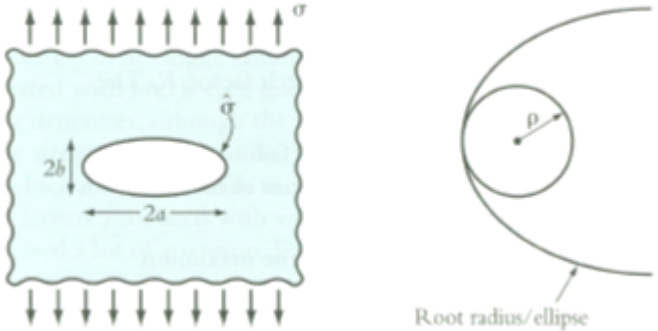

Figure 1.11: Elliptical hole in an infinite plate root radius ellipse

It can be shown that the stress concentration factor is as follows:

$$K_t = \frac{\sigma_{\max}^{el}}{\sigma} = 1 + \frac{2a}{b}$$

Thus, as $b \to 0$, the elliptical hole degenerates to a crack, and $\frac{a}{b} \to \infty$, so that the notch stress also goes to infinity (i.e. becomes singular), $K_t \to \infty$, provided the material behaviour remains linear elastic.

The root radius for an ellipse is given by

$$\rho = \frac{b^2}{a} \qquad \therefore\ b = \sqrt{a\rho}$$

so that

$$\frac{\hat{\sigma}}{\sigma} = 1 + 2\sqrt{\frac{a}{\rho}}$$

and again, as the notch tip radius goes to zero, i.e. $\rho \to 0$, the notch tip stress again goes to infinity,

$$\frac{\hat{\sigma}}{\sigma} \to 2\sqrt{\frac{a}{\rho}} \to \infty$$

The singular (infinite) state of stress at a crack tip is one of the fundamental and most important aspects of fracture mechanics.

1.2.2 Basis of the energy approach to fracture mechanics

Griffith (1921) studied the brittle fracture of glass and adopted an energy approach to solve the problem. He reasoned that unstable crack propagation occurs only if an increment of crack growth, d*a*, results in more strain energy being released than is absorbed by the creation of the new crack surfaces. This can be re-expressed as the change in strain energy *U*, due to crack extension, being greater than the energy absorbed by the creation of the new crack surfaces. Thus, if we designate the surface energy per unit area of the crack γ_S, then the surface energy associated with a crack of length 2*a* in a body of thickness *B* (as shown in the Figure 1.12) is given by:

$$W_S = 4aB\gamma_S$$

Detailed stress analysis of an elliptical hole in an infinite elastic plate has established that the strain energy in such a body is

$$W_p = -\frac{\pi a^2 \sigma^2 B}{E'}$$

where σ is the remote stress (away from the hole) and where, for plane strain and plane stress, respectively,

$$E' = \frac{E}{1-\nu^2} \quad \text{and } E' = E$$

The total system energy is thus

$$W = -\frac{\pi a^2 \sigma^2 B}{E'} + 4aB\gamma_s$$

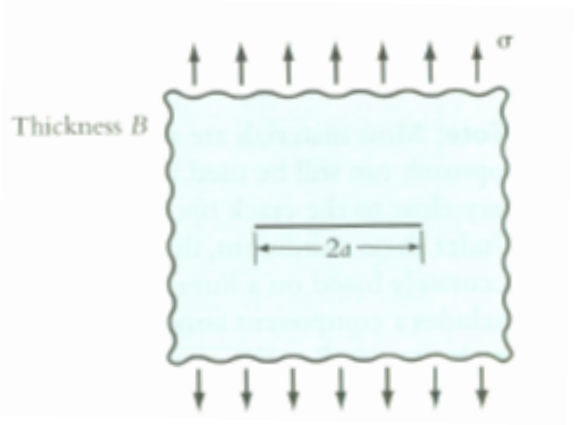

Figure 1.12: Crack in Infinite Plate

According to Griffith, the critical condition for the onset of crack growth is

$$\frac{dU}{dA} = -\frac{\pi a \sigma^2}{E'} + 2\gamma_s = 0$$

Therefore:

$$\frac{\pi a \sigma^2}{E'} = 2\gamma_s$$

where $A = 2aB$ is the crack area and dA denotes an incremental increase in crack area. The total surface area of the two crack surfaces is 2A. This relationship is conventionally re-expressed as

$$G = G_c$$

where G is called the *strain energy release rate*, the *crack tip driving force* or the *crack extension force*. G_c is a material property, which is known as the *critical strain energy release rate*, the *toughness* or the *critical crack extension force*. A high value of G_c means that it is difficult to cause unstable crack growth in the material whereas a low value means it is easy to make a crack grow unstably. Thus, copper, for example, has a value of $G_c \approx 10^6$ Jm^{-2}, whereas glass has a value of $G_c \approx 10$ Jm^{-2}. The following relationships for plane stress and plane strain, respectively, follow from the above:

$$G = \frac{\pi a \sigma^2}{E} \text{ (plane stress)}$$

$$G = \frac{(1-\nu^2)}{E} \pi a \sigma^2 \text{ (plane strain)}$$

Note that plane stress and plane strain are two contrasting two-dimensional assumptions which permit simplification of three-dimensional problems to two-dimensional ones. Plane stress corresponds physically to thin plate type situations while plane strain corresponds to thick plate type situations. Plane strain testing of fracture leads to lower values of G_c, so that the material property value of G_c for design purposes is taken as the plane strain value and is designated as G_{Ic}.

The critical stress, which causes a crack to propagate in an unstable fashion, giving fracture, is governed by the following relationships

$$\sigma\sqrt{\pi a} = \sqrt{EG_c} \text{ (plane stress)}$$

$$\sigma\sqrt{\pi a} = \sqrt{\frac{EG_c}{1-\nu^2}} \text{ (plane strain)}$$

Since the term on the right-hand side of these equations is a material constant and since the term on the left hand side is so common, it is usually abbreviated to the symbol, *K*, which is referred to as the *stress intensity factor* and the equations can be re-expressed as:

$$K = K_c$$

where K_c is called the *critical stress intensity factor* or the *fracture toughness*. Thus

$$K_c = \sqrt{EG_c}$$

In summary,

$K = \sigma\sqrt{\pi a}$ is called the *stress intensity factor*

K_c is called the fracture *toughness* of *critical stress intensity factor*

G_c is called the *toughness* or the *critical strain energy release rate*.

Note

Most materials are not linear elastic up to failure. However, the energy approach can still be used if the plastic strain is restricted to a region very close to the crack tip; this is referred to as *small scale yielding*. Under these conditions, the energy release rate can still be reasonably accurately based on a linear elastic analysis. Also, G_c or G_{Ic} now includes a component associated with plastic deformation of the crack tip as well as the creation of the surfaces. So far, we have only considered the so-called Mode I loading case. There are actually three different loading modes considered in fracture mechanics, as shown in Figure 1.13.

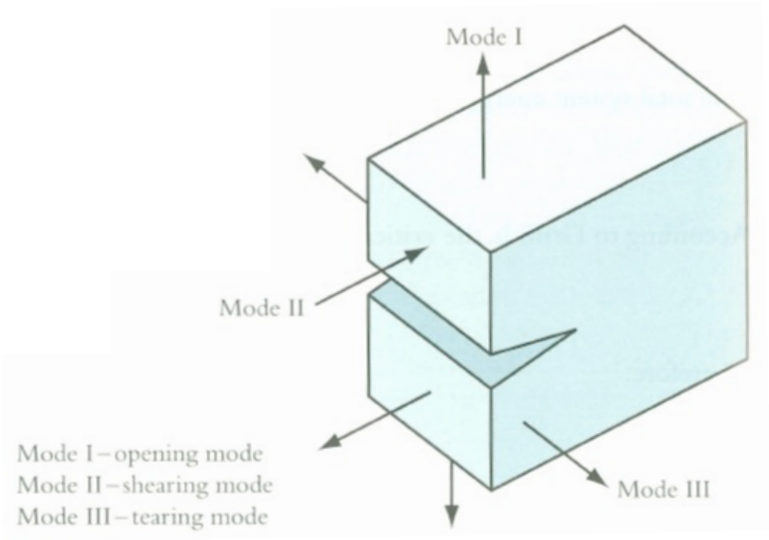

Figure 1.13: Crack tip loading modes

In general, the energy release rate under mixed-mode loading is given by

$$G_{total} = G_I + G_{II} + G_{III}$$

1.2.3 Elastic crack tip stress fields

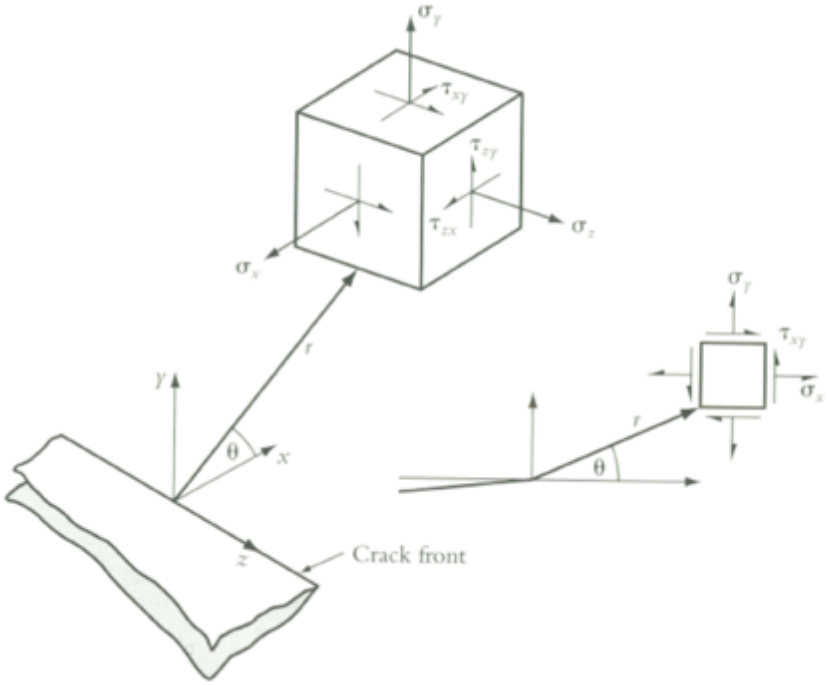

Figure 1.14. Crack tip stress fields

Westergaard (1939) established the following equations for the elastic stress field in the vicinity of a crack tip:

$$\sigma_x = \frac{K_I}{\sqrt{2\pi r}}\cos\left(\frac{\theta}{2}\right)\left[1-\sin\left(\frac{\theta}{2}\right)\sin\left(\frac{3\theta}{2}\right)\right] + \text{non}-\text{singular terms}$$

$$\sigma_y = \frac{K_I}{\sqrt{2\pi r}}\cos\left(\frac{\theta}{2}\right)\left[1+\sin\left(\frac{\theta}{2}\right)\sin\left(\frac{3\theta}{2}\right)\right] + \text{non}-\text{singular terms}$$

$$\tau_{xy} = \frac{K_I}{\sqrt{2\pi r}}\sin\left(\frac{\theta}{2}\right)\cos\left(\frac{\theta}{2}\right)\cos\left(\frac{3\theta}{2}\right) + \text{non}-\text{singular terms}$$

$$\tau_{zx} = \tau_{zy} = 0;\ \sigma_z = 0\ (\text{plane stress});\ \sigma_z = \nu(\sigma_x + \sigma_y)\ (\text{plane strain})$$

K_I is the Mode-I stress-intensity factor (units $N/m^{3/2}$) which defines the magnitude of the elastic stress field in the vicinity of the crack tip. Similar expressions exist, in terms of K_{II} and K_{III}, for the Mode II and III loading situations. For mixed-mode loading, the stress fields can be added together directly. It can be seen that K_I, K_{II} and K_{III} characterize the entire stress field (and hence the strain fields) in the vicinity of the crack tip. It therefore seems reasonable to assume that, for Mode I loading for example, failure will occur when K_I reaches a critical value K_c (K_{Ic} under plane strain conditions).

The energy approach and the stress intensity approach are equivalent. Generally, for plane stress:

$$G_{total} = G_I + G_{II} + G_{III} = \frac{1}{E}(K_I^2 + K_{II}^2 + K_{III}^2)$$

and for plane strain:

$\frac{1}{E}$ is replaced by $\frac{(1-\nu^2)}{E}$.

Generally, for geometries with finite boundaries, the following expression is employed for stress intensity factor

$$K_I = Y\sigma\sqrt{\pi a}$$

and similarly for K_{II} and K_{III}, where Y is a function of the crack and component dimensions.

Table 1.2: Typical Fracture Toughness Values

Material	$\sigma_y \left(MN/m^2\right)$	$K_{Ic}\left(MN/m^{3/2}\right)$
Mild Steel	220	140 to 200
Pressure Vessel Steel (HY130)	1700	170
Aluminium Alloys	100 to 600	45 to 23
Cast Iron	200 to 1000	20 to 6

Solutions for Y can be found in the literature for a wide range of geometries and loadings, e.g.

1. H Tada, P Paris and G Irwin, "The stress analysis of cracks handbook", DEL Research Corporation, Hellertown, Pennsylvania, 1973.
2. G P Rooke and D J Cartwright, "Compendium of stress intensity factors", HMSO, 1975.
3. Y Murakami (Editor), "Stress-intensity factors handbook", Pergamon Press, Oxford 1987, (2 volumes).

1.2.4 The effect of finite boundaries on expressions for stress intensity factors

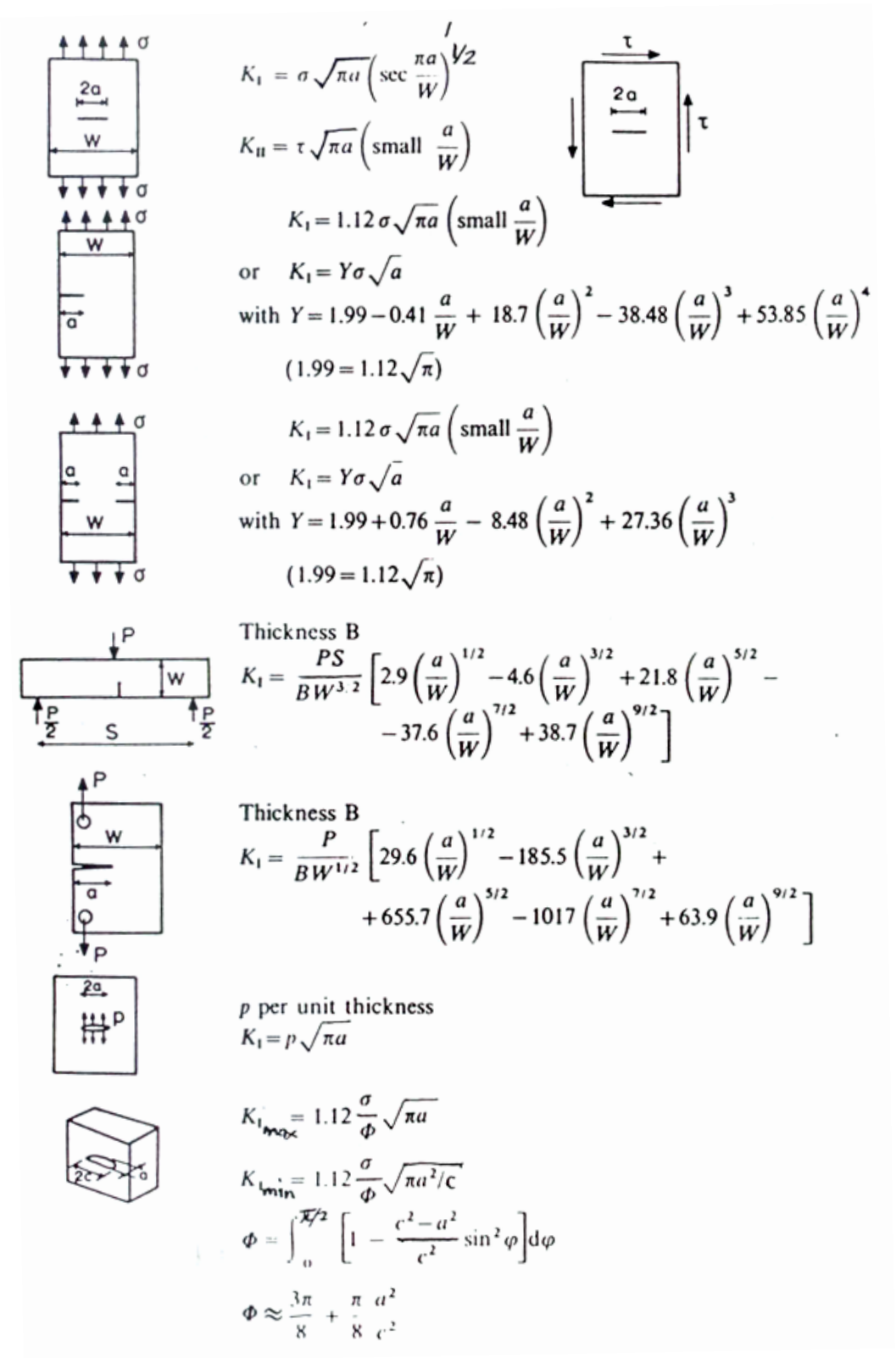

Figure 1.15. Stress intensity factors for finite bodies.

Example

A large high carbon steel plate with a thumbnail crack, shown in Figure 1.16, for which

$$K_{\max} = 1.2\sigma\sqrt{\pi a}$$

has a fracture toughness of 72MN/m$^{3/2}$ and σ_y = 1450 MPa.

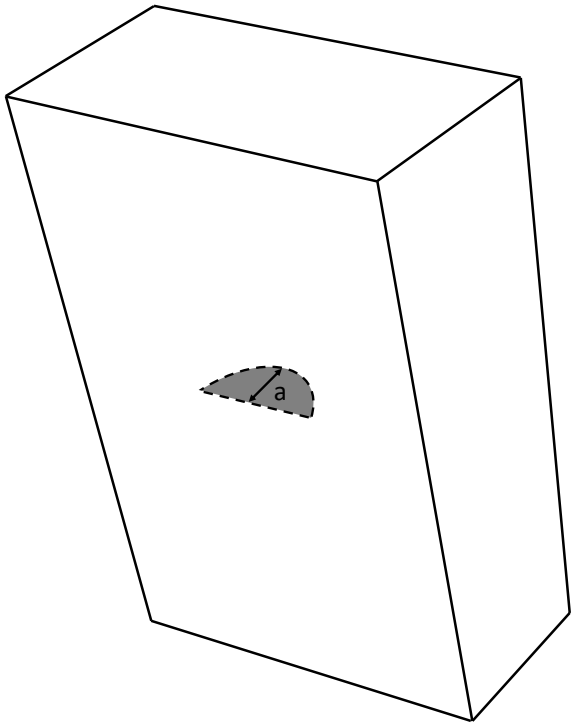

Figure 1.16: Thumbnail crack geometry.

If $\sigma = \frac{2}{3}\sigma_y$, determine the critical initial crack size assuming linear elastic material.

Solution

At fracture, with

$$\sigma = \frac{2}{3}\sigma_y = \frac{2}{3} \times 1450 = 966.67MPa$$

and

$$K_{IC} = 72 \frac{MN}{m^{3/2}}$$

Then (from $K_{\max} = 1.2\sigma\sqrt{\pi a}$),

$$72 \frac{MN}{m^{3/2}} = 1.2 \times 966.67 \frac{MN}{m^2} \times \sqrt{\pi \times a_{crit}}\, m^{1/2}$$

Therefore,

$$a_{crit} = \frac{1}{\pi}\left(\frac{72}{1.2 \times 966.67}\right)^2 = 1.226 \times 10^{-3} m = 1.226 mm$$

If the material was mild steel, with $\sigma_y = 210 MPa \; and \; K_{IC} = 200 \frac{MN}{m^{3/2}}$, then a_{crit} = 451mm, i.e., it is much more likely to be detected during inspection!

1.2.5 Fatigue crack growth

It has been shown by Paris and co-workers (1961) that, for a wide range of conditions, there is a logarithmic linear relationship between crack growth rate and the stress intensity factor range during cyclic loading of cracked components. Although this proposition had difficulty being accepted initially, it has become the basis of the damage tolerant approach to fatigue life estimation and is widely used both in industry and in research. Essentially, it means that crack growth can be modelled and estimated based on knowledge of crack and component geometry, loading conditions and using experimentally-measured crack growth data to furnish material constants. This section describes the basics of this approach.

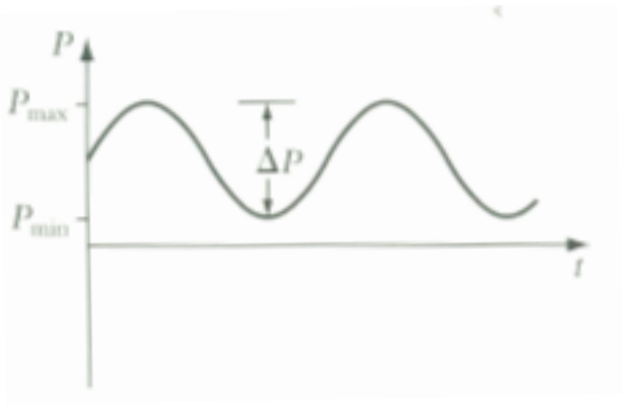

Figure 1.17: Variation of P (load) with t (time)

Considering a load cycle as shown in Figure 1.17 which gives rise to a load range acting on a cracked body:

$$\Delta P = P_{\max} - P_{\min}$$

The load range and crack geometry gives rises to a cyclic variation in stress intensity factor, which is given by:

$$\Delta K = K_{\max} - K_{\min}$$

Even though the stress intensity factor may be less than the critical stress intensity factor for unstable crack growth, stable crack growth may occur if the stress intensity range, ΔK, is greater than an empirically-determined material property called the *threshold stress intensity factor range*, designated ΔK_{th}. In addition, Paris showed that the subsequent crack growth can be represented by an empirical relationship as follows:

$$\frac{da}{dN} = C\,(\Delta K)^m$$

where *C* and *m* are empirically-determined material constants. This relationship is known as the Paris equation. Fatigue crack growth data is often plotted as the logarithm of crack growth per load cycle, d*a*/d*N*, and the logarithm of stress intensity factor range. There are

three stages, as shown in Figure 1.18. Below ΔK_{th}., no observable crack growth occurs; region II shows an essentially linear relationship between log(d*a*/d*N*) and log(ΔK), where *m* is the slope of the curve and *C* is the vertical axis intercept; in region III, rapid crack growth occurs and little life is involved. Region III is primarily controlled by K_c or K_{Ic}.

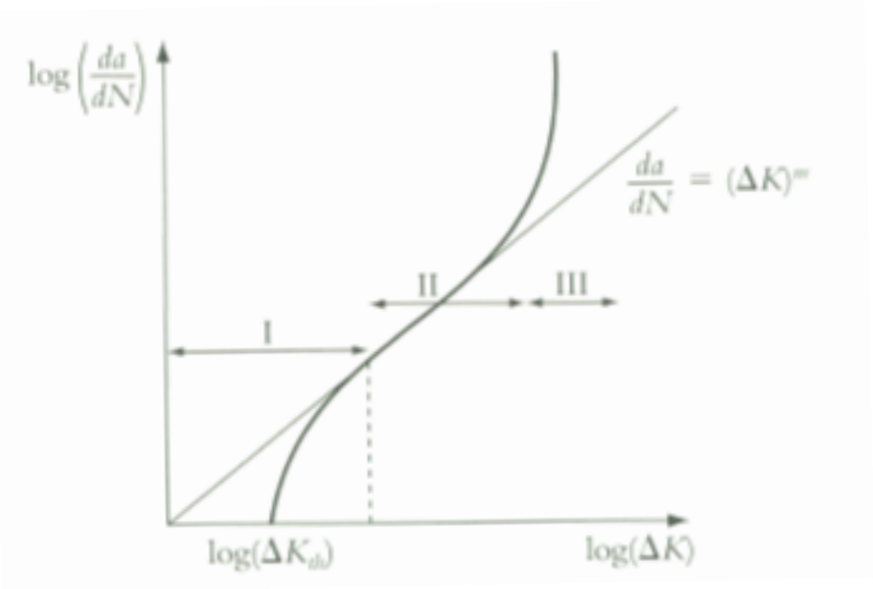

Figure 1.18: Typical (schematic) variation of log (da/dN) with log (ΔK)

The linear regime (Region II) is the region in which engineering components which fail by fatigue propagation occupy most of their life. Knowing the stress intensity factor expression for a given component and loading, the fatigue crack growth life of the component can be obtained by integrating the Paris Equation between the limits of initial crack size and final crack size.

For most materials, the constant *C* is found to be dependent on *R* where *R* is a measure of the mean stress defined as:

$$R = \frac{K_{\min}}{K_{\max}}$$

as shown below in Figure 1.19.

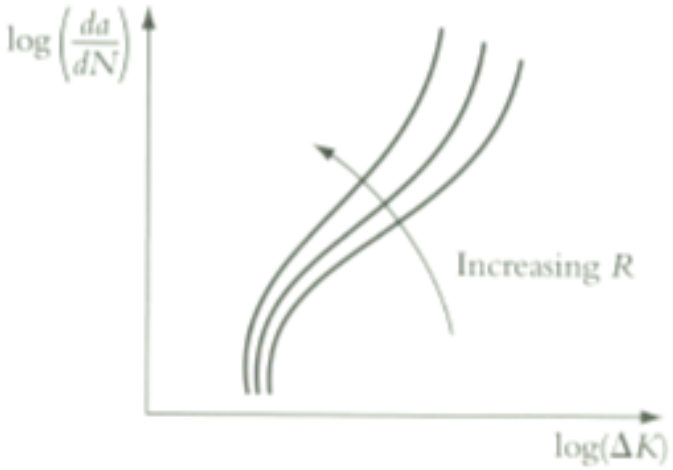

Figure 1.19: Effect of R on fatigue crack growth

Some typical fracture mechanics values for a range of materials are shown in Table 1.3.

Table 1.3: Typical values for ΔK_{th}, m and ΔK

Material	ΔK_{th} (MN/m$^{3/2}$)	m	ΔK (MN/m$^{3/2}$) for da/dN = 10^{-6} mm/cycle
Mild Steel	4 to 7	3.3	6.2
316 stainless steel	4 to 6	3.1	6.3
Aluminium	1 to 2	2.9	2.9
Copper	1 to 3	3.9	4.3
Brass	2 to 4	4.0	4.3 to 66.3
Nickel	4 to 8	4.0	8.8

From L.P. Pook, *J. Strain Analysis*, 1978, pp 114-135.

(N.B. The ΔK_{th} and ΔK (for da/dN = 10^{-6} mm/cycle) values depend on the R-value.)

3 Thermal Stress and Strain

Learning Summary

1. Recall that thermal strains arise when a change in temperature is applied to an unconstrained body (knowledge);
2. Recognise the cause of thermal strains and how 'thermal stresses' are caused by thermal strains (comprehension);
3. Solve problems involving both mechanical and thermal loading (application).

3.1 Introduction

Stresses and strains usually arise when mechanical loads are applied to a system. However, they can also exist when no mechanical loading is present. A typical example of this is when a temperature change occurs.

Changes of temperature in a body cause expansion/contraction. This phenomenon is quantified by the coefficient of thermal expansion, α. Some typical values of thermal expansion coefficient for some common engineering materials are presented in Table 1. For isotropic materials, α is the same for all directions.

Table 3.1

Material	Coefficient of Thermal Expansion, α, [°C^{-1}]
Concrete	10 x 10^{-6}
Steel	11 x 10^{-6}
Aluminium	23 x 10^{-6}
Nylon	144 x 10^{-6}
Rubber	162 x 10^{-6}

Uniform temperature change throughout an unrestrained body produces uniform strain but no stress, i.e. there is free expansion/contraction.

For a bar of length l, subjected to a temperature change ΔT, the change in length $\delta l_{thernal}$ due to the temperature change is given by:

$$\delta l_{thermal} = l\alpha\Delta T \tag{3.1}$$

The thermal strain due to this length change can be determined as follows:

$$\varepsilon_{thermal} = \frac{\delta l_{thermal}}{l} = \frac{l\alpha\Delta T}{l} = \alpha\Delta T \tag{3.2}$$

Using the principle of superposition, which states that:

$$\begin{bmatrix} The\ total\ effect\ of\ combined \\ loads\ applied\ to\ a\ body \end{bmatrix} = \sum \begin{bmatrix} The\ effects\ of\ the\ individual \\ loads\ applied\ spearately \end{bmatrix} \tag{3.3}$$

thermal extensions can simply be added to elastic (mechanical) extensions to give the total extension by:

$$\delta l_{total} = \delta l_{elastic} + \delta l_{thermal} \tag{3.4}$$

or, for an axial member:

$$\delta l_{total} = \frac{Fl}{AE} + l\alpha\Delta T \tag{3.5}$$

However, if the body is restrained, or the temperature is not uniform, thermal stresses are produced in the body.

3.2 Resistive Heating of a Bar

The bar shown in Figure 2.1 is subjected to a temperature rise of ΔT and restricted from expanding by constraints at each end.

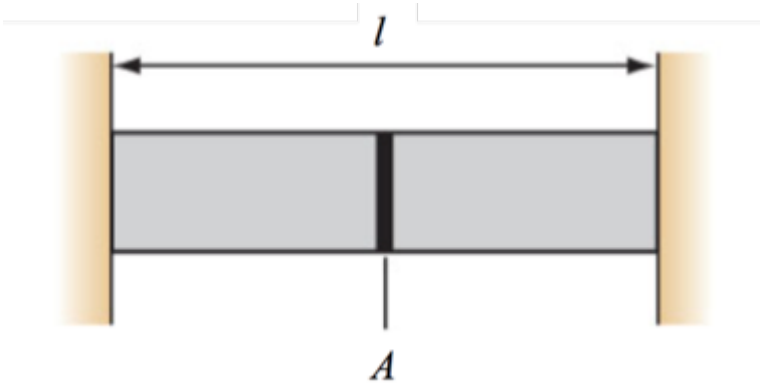

Figure 3.1

Since the bar cannot extend, applying Equation (3.4):

$$\delta l_{total} = \delta l_{elastic} + \delta l_{thermal} = 0 \tag{3.6}$$

or alternatively:

$$\delta l_{total} = \frac{Fl}{AE} + l\alpha\Delta T = 0 \tag{3.7}$$

Cancelling l in Equation (3.7) and rearranging to find the force F gives:

$$F = -AE\alpha\Delta T \tag{3.8}$$

and the stress in the bar, σ is:

$$\sigma = \frac{F}{A} = -E\alpha\Delta T \tag{3.9}$$

3.3 Compound Bar Assembly

A compound bar assembly consisting of one aluminium and one steel bar of the same dimensions between two rigid end plates which are able two slide without friction is shown in Figure 3.2.

If the whole assembly is subjected to a temperature change ΔT will the bars be in tension or compression?

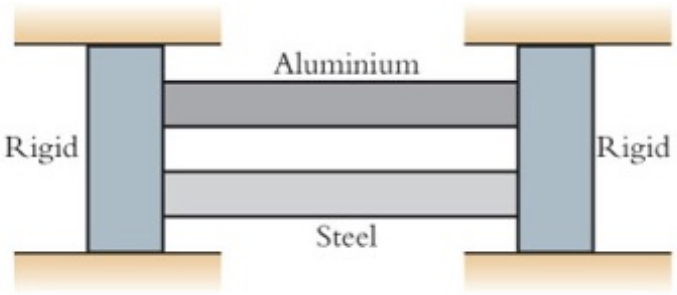

Figure 3.2

If we consider this 'intuitively', because of compatibility the extension of the bars must be identical, i.e.:

$$\delta l_{steel} = \delta l_{alu} \tag{3.10}$$

Referring to Table 3.1, we can see that $\alpha_{alu} > \alpha_{steel}$ therefore the aluminium bar will want to extend more than the steel bar but is constrained from doing so due to the rigid end blocks attached to the steel bar. This means that the **aluminium bar will be in compression**. The reverse is true of the steel bar, it wants to extend less than the aluminium bar but the rigid end blocks attached the aluminium bar forces it to extend further, therefore the **steel bar is in tension**. This is shown schematically in Figure 3.3, where the free expansion is compared to the constrained expansion.

We can consider an analytical solution to the same problem; again Equation (3.10) applies meaning that (from Equation (7)):

$$\frac{F_{steel}l}{A_{steel}E_{steel}} + l\alpha_{steel}\Delta T = \frac{F_{alu}l}{A_{alu}E_{alu}} + l\alpha_{alu}\Delta T \tag{3.11}$$

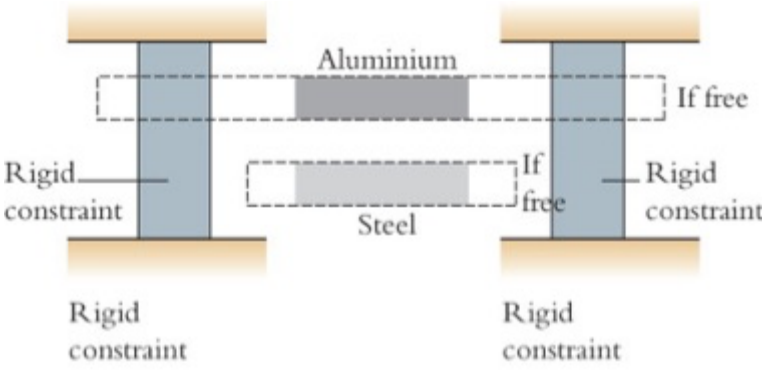

Figure 3.3

The equilibrium condition can be obtained from the FBD in Figure 3.4 as follows:

$$F_{steel} = -F_{alu} \tag{3.12}$$

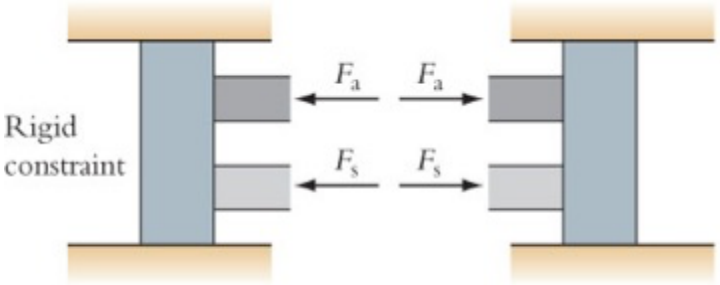

Figure 3.4

Substituting for F_{steel} from Equation (3.12) into Equation (3.11) gives:

$$l\Delta T(\alpha_{steel} - \alpha_{alu}) = F_{alu}l\left[\frac{1}{A_{alu}E_{alu}} + \frac{1}{A_{steel}E_{steel}}\right] \tag{3.13}$$

and therefore:

$$\sigma_{alu} = \frac{F_{alu}}{A_{alu}} = \frac{\Delta T(\alpha_{steel} - \alpha_{alu})}{\left[\frac{1}{E_{alu}} + \frac{A_{alu}}{A_{steel}E_{steel}}\right]} \tag{3.14}$$

As $\alpha_{steel} < \alpha_{alu}$ this means that $\sigma_{alu} < 0$ i.e. the **aluminium bar is in compression**.

If we consider that:

$$A_{alu}\sigma_{alu} = -A_{steel}\sigma_{steel} \tag{3.15}$$

Then:

$$\sigma_{steel} = -\frac{A_{alu}\sigma_{alu}}{A_{steel}} = -\frac{A_{alu}}{A_{steel}}\frac{\Delta T(\alpha_{alu} - \alpha_{steel})}{\left[\frac{1}{E_{steel}} + \frac{A_{steel}}{A_{alu}E_{alu}}\right]} \tag{3.16}$$

As $\alpha_{steel} < \alpha_{alu}$ this means that $\sigma_{steel} > 0$ i.e. the **steel bar is in tension**.

3.4 Generalised Hooke's Law in 3D

To incorporate thermal effects in 3D we add a thermal strain ($\alpha\Delta T$) term to the normal strains in Hooke's Law:

$$\varepsilon_x = \frac{1}{E}(\sigma_x - \nu[\sigma_y + \sigma_z]) + \alpha\Delta T \tag{3.17}$$

$$\varepsilon_y = \frac{1}{E}(\sigma_y - \nu[\sigma_x + \sigma_z]) + \alpha\Delta T \tag{3.18}$$

$$\varepsilon_z = \frac{1}{E}(\sigma_z - \nu[\sigma_x + \sigma_y]) + \alpha\Delta T \tag{3.19}$$

$$\gamma_{xy} = \tau_{xy} / G \tag{3.20}$$

$$\gamma_{yz} = \tau_{yz} / G \tag{3.21}$$

$$\gamma_{zx} = \tau_{zx} / G \tag{3.22}$$

where ΔT is the temperature at a point relative to some datum. There is no change to the shear stress-strain relationship as for linearly elastic, isotropic materials; a temperature change produces only normal strains.

By introducing these thermal strains into the generalised Hooke's Law we can obtain solutions to thermal stress problems which are often very important in, for example, power and chemical plant, aeroengines and internal combustion engines (e.g. pistons and cylinder walls) etc.

3.5 Case 1: An initially straight uniform beam

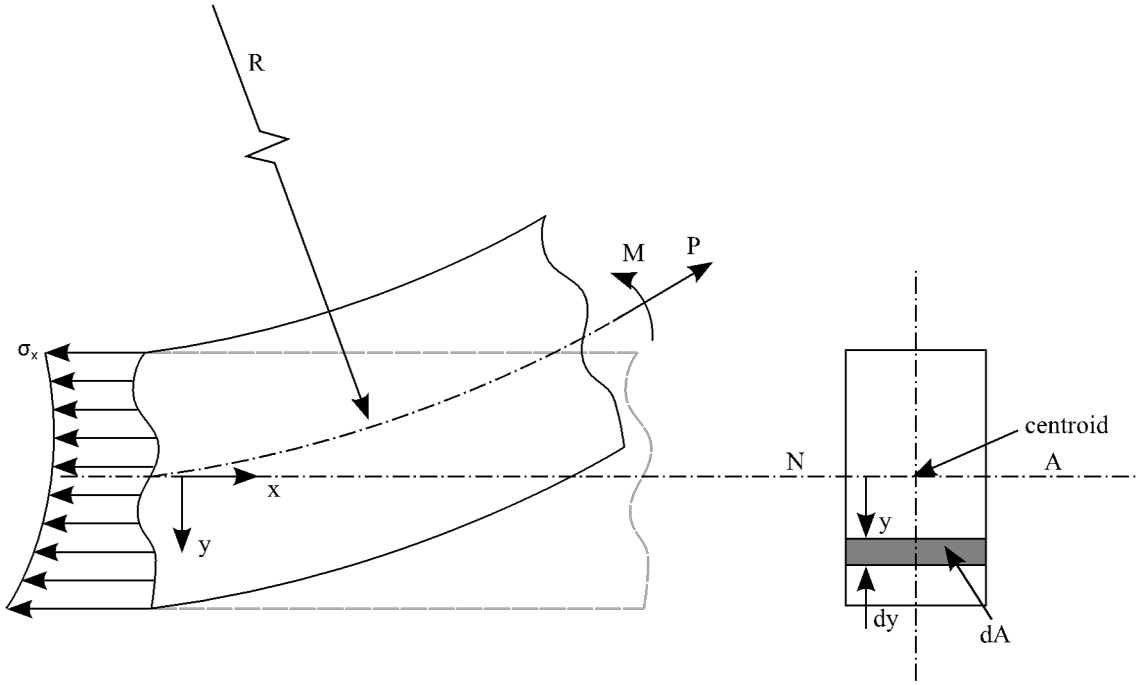

Figure 3.5

- Determine the deformations and stresses (small deformations)

The temperature variation is (assumed) purely a function of y, i.e. $\Delta T = \Delta T(y)$.

The coefficient of thermal expansion = α. Axial force P, and pure bending, about the z-z axis, M, are also applied.

$\sigma_z, \sigma_y, \tau_{xz}$, and τ_{yz}= 0 because the cross-sectional dimensions are small compared with the length.

Also τ_{yz} = 0, because M does not vary with x, $S = \frac{dM}{dx} = C$ (a constant value)

3.5.1 Compatibility

Remote from the ends, strain varies linearly with y,

$$\varepsilon_x = \bar{\varepsilon} + \frac{y}{R} \tag{3.23}$$

Where $\bar{\varepsilon}$ is the mean strain (at y = 0) and R is the radius of curvature.

3.5.2 Stress-strain

From the generalised Hooke's Law Equation (3.17) (as σ_y and σ_z are 0)

$$\varepsilon_x = \frac{\sigma_x}{E} + \alpha\Delta T \tag{3.24}$$

Substituting Equation (3.23) into Equation (3.24) and rearranging for σ_x gives:

$$\sigma_x = E\left(\bar{\varepsilon} + \frac{y}{R} - \alpha\Delta T\right) \tag{3.25}$$

3.5.3 Axial Equilibrium

$$P = \int_A \sigma_x dA \tag{3.26}$$

Substituting Equation (3.25) into Equation (3.26) gives:

$$P = E\int_A \left(\bar{\varepsilon} + \frac{y}{R} - \alpha\Delta T\right) dA \tag{3.27}$$

Multiplying out to give individual terms:

$$P = E\bar{\varepsilon}A + \frac{E}{R}\int_A y dA - E\alpha\int_A \Delta T dA \tag{3.28}$$

however, $\int_A y dA = 0$ because y is measured from an axis passing through the centroid, so Equation (3.28) reduces to:

$$P = E\bar{\varepsilon}A - E\alpha\int_A \Delta T dA \tag{3.29}$$

d

3.5.4 Moment Equilibrium

$$M = \int_A y\sigma_x dA \tag{3.30}$$

Substituting Equation (3.25) into Equation (3.30) gives

$$M = E\int_A \left(\bar{\varepsilon} + \frac{y}{R} - \alpha\Delta T\right) y dA \tag{3.31}$$

Multiplying out to give individual terms:

$$M = E\bar{\varepsilon}\int_A y dA + \frac{E}{R}\int_A y^2 dA - E\alpha\int_A \Delta T y dA \tag{3.32}$$

By definition $\int_A y^2 dA = I$ and $\int_A y dA = 0$ as before, therefore Equation (3.32) reduces to:

$$M = \frac{EI}{R} - E\alpha\int_A \Delta T y dA \tag{3.33}$$

3.5.5 Example 1

A rectangular beam, width b and depth d has a temperature variation given by:

$$\Delta T(y) = \Delta T_{\max}\left(1 - \frac{4y^2}{d^2}\right) \tag{3.34}$$

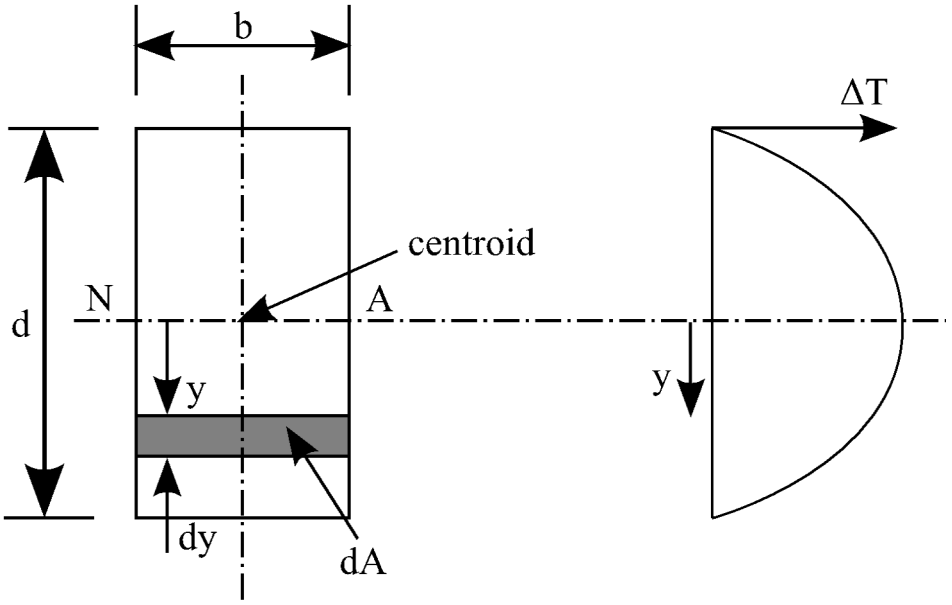

Figure 3.6

There is no restraint or applied loading (i.e. P = M = 0). Obtain the stress distribution.

Axial Force Equilibrium

Recalling Equation (3.29) and inserting the temperature variation, axial force and considering a rectangular cross-section from the problem gives:

$$0 = E\bar{\varepsilon}bd - E\alpha\int_{-\frac{d}{2}}^{\frac{d}{2}} \Delta T_{\max}\left(1 - \frac{4y^2}{d^2}\right)bdy \tag{3.35}$$

Rearranging for the mean strain, $\bar{\varepsilon}$ gives:

$$\bar{\varepsilon} = \frac{\alpha}{d}\Delta T_{\max}\int_{-\frac{d}{2}}^{\frac{d}{2}}\left(1-\frac{4y^2}{d^2}\right)dy \tag{3.36}$$

And evaluating the integral:

$$\bar{\varepsilon} = \frac{\alpha}{d}\Delta T_{\max}\left[y-\frac{4y^3}{3d^2}\right]_{-\frac{d}{2}}^{\frac{d}{2}} \tag{3.37}$$

Gives:

$$\bar{\varepsilon} = \frac{2}{3}\alpha\Delta T_{\max} \tag{3.38}$$

Moment Equilibrium

With M = *0* we can obtain 1/R from the moment equilibrium (Equation (3.33)) but from symmetry we can see that (1/R) = 0.

Stress Distribution

Using Equation (3.25) and substituting in the expression for mean strain (Equation (3.38)), 1/R and the temperature variation (Equation (3.34)) gives:

$$\sigma_x = E\left(\frac{2}{3}\alpha\Delta T_{\max}+0-\alpha\Delta T_{\max}\left(1-\frac{4y^2}{d^2}\right)\right) \tag{3.39}$$

Which reduces to:

$$\sigma_x = E\alpha\Delta T_{\max}\left(\frac{4y^2}{d^2}-\frac{1}{3}\right) \tag{3.40}$$

Evaluate Stress Distribution

At y = 0,

$$\sigma_x = E\alpha\Delta T_{\max}\left(\frac{4\times 0^2}{d^2}-\frac{1}{3}\right) \tag{3.41}$$

Which gives:

$$\sigma_x = \frac{-E\alpha\Delta T_{\max}}{3} \tag{3.42}$$

At y = ±d/2,

$$\sigma_x = E\alpha\Delta T_{\max}\left(\frac{4\left(\frac{d}{2}\right)^2}{d^2}-\frac{1}{3}\right) \tag{3.43}$$

Reduces to:

$$\sigma_x = E\alpha\Delta T_{\max}\left(1-\frac{1}{3}\right) \tag{3.44}$$

And then:

$$\sigma_x = \frac{2E\alpha\Delta T_{\max}}{3} \tag{3.45}$$

We can also evaluate the point at which the stress, σ_x = 0, i.e. when $\frac{4y^2}{d^2} = \frac{1}{3}$, from Equation (3.40) which gives:

$$y = \sqrt{\frac{1}{12}d^2} \tag{3.46}$$

Or y = ±0.287d

This is the stress distribution away from the ends. At the ends, σ_x = 0 and there is a gradual transition between the two.

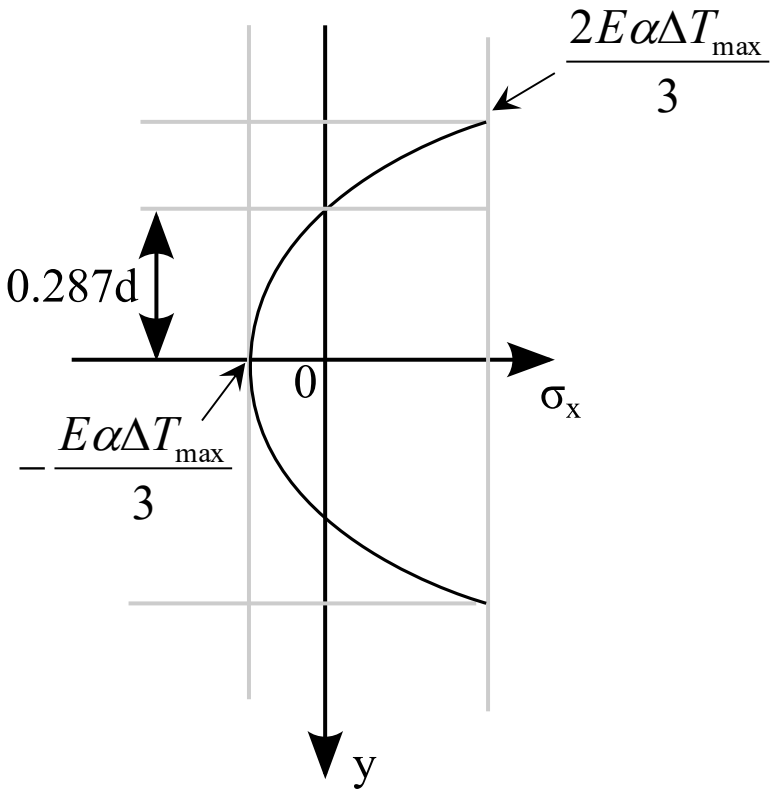

Figure 3.7

3.5.6 Example 2

A rectangular beam (again b x d), but with:

$$\Delta T(y) = \Delta T_{\max} \frac{2y}{d} \tag{3.47}$$

And the constrained so that ε = 0 and 1/R = 0.

Determine the stresses and restraints.

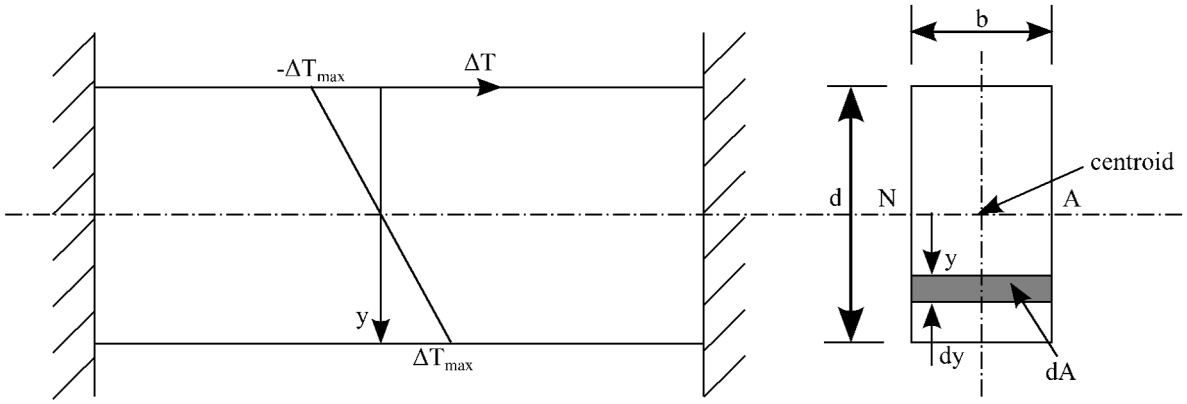

Figure 3.8

Axial Force Equilibrium

Recalling Equation (3.29) and substituting in for the temperature variation:

$$P = E\bar{\varepsilon}bd - E\alpha \int_{-\frac{d}{2}}^{\frac{d}{2}} \Delta T_{\max} \frac{2y}{d} b dy \tag{3.48}$$

Evaluate the integral:

$$\int_{-\frac{d}{2}}^{\frac{d}{2}} \Delta T_{\max} \frac{2y}{d} b dy = \frac{2\Delta T_{\max} b}{d} \int_{-\frac{d}{2}}^{\frac{d}{2}} y dy = \frac{2\Delta T_{\max} b}{d} \left[\frac{y^2}{2} \right]_{-\frac{d}{2}}^{\frac{d}{2}} = 0 \tag{3.49}$$

Also,

$\bar{\varepsilon} = 0 \qquad \therefore P$ = 0

Moment Equilibrium

Recalling Equation (3.31) and substituting in for the temperature variation and evaluating the integral:

$$\int_A \Delta T y dA = \frac{2\Delta T_{\max} b}{d} \int_{-\frac{d}{2}}^{\frac{d}{2}} y^2 dA = \frac{2\Delta T_{\max} b}{d} \left[\frac{y^3}{3} \right]_{-\frac{d}{2}}^{\frac{d}{2}}$$
$$= \frac{2\Delta T_{\max} b}{d} \left[\left(\frac{d^3}{24} \right) - \left(\frac{-d^3}{24} \right) \right] = \frac{\Delta T_{\max} b d^2}{6} \quad (3.50)$$

Also as $1/R = 0$, this gives

$$M = \frac{-E\alpha\Delta T_{\max} b d^2}{6} \quad (3.51)$$

Stress Distribution

Using Equation (3.25) with $\varepsilon = 1/R = 0$

$$\sigma_x = -E\alpha\Delta T \quad (3.52)$$

Substituting in for the temperature variation:

$$\sigma_x = -E\alpha\Delta T_{\max} \frac{2y}{d} \quad (3.53)$$

$$M = \frac{-E\alpha\Delta T_{\max} b d^2}{6} \quad (3.54)$$

At $y = d/2$,

$$\sigma_x = -E\alpha\Delta T_{\max} \quad (3.55)$$

At $y = -d/2$

$$\sigma_x = E\alpha\Delta T_{\max} \quad (3.56)$$

Evaluate Stress Distribution

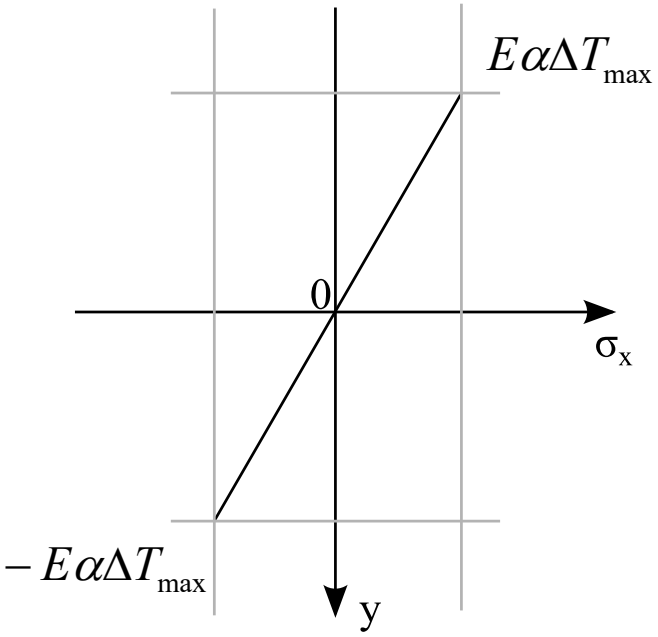

Figure 3.9

3.6 Case 2: Thin cylinders

Thin cylinders are in common use in power and chemical plant, e.g. pipes, pressure vessels, etc. Often temperature variations are approximately linear through the thickness. Considering positions remote from the ends, flanges, etc.

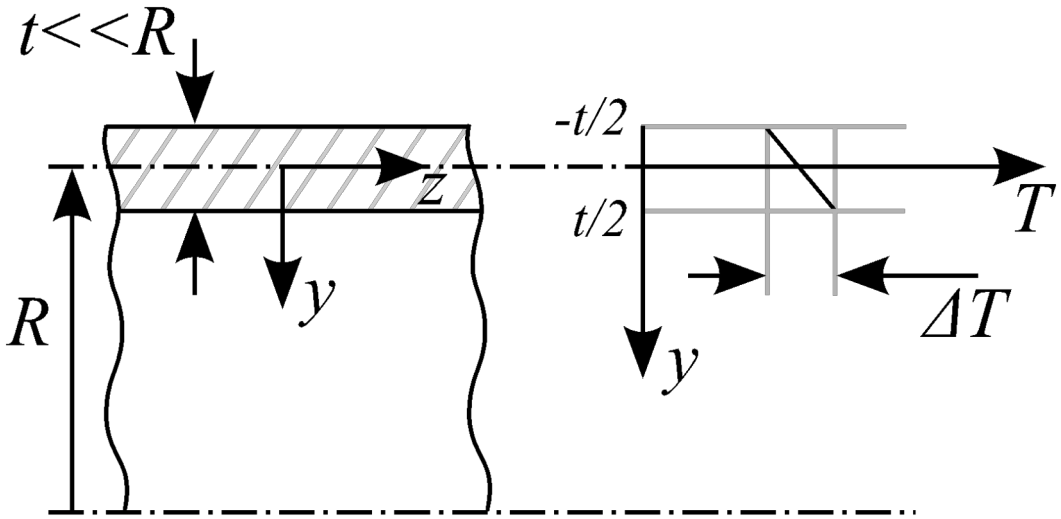

Figure 3.10

It is convenient to consider the effect of the uniform temperature change and the temperature gradient separately. If the cylinder is not restrained then the uniform temperature change causes overall dimensional changes, but no stress. The stresses due to axial restraint are easily calculated.

For the temperature gradient we have:

$$\Delta T = \Delta T_{wall} \frac{y}{t} \tag{3.57}$$

where ΔT_{wall} is the temperature difference across the wall.

For a thin cylinder:

$$\sigma_r \approx 0 \tag{3.58}$$

Now using a cylindrical coordinate system and substituting in for σ_r:

$$\varepsilon_\theta = \frac{1}{E}\left(\sigma_\theta - \nu\sigma_z\right) + \alpha\Delta T \tag{3.59}$$

And

$$\varepsilon_z = \frac{1}{E}\left(\sigma_z - \nu\sigma_\theta\right) + \alpha\Delta T \tag{3.60}$$

Remote from the ends of the cylinder sections remain plane and circular. Therefore, from compatibility considerations (with zero mean temperature change), the hoop and axial strains must both be zero. Therefore:

$$0 = \frac{1}{E}\left(\sigma_\theta - \nu\sigma_z\right) + \alpha\Delta T_{wall}\frac{y}{t} \tag{3.61}$$

And

$$0 = \frac{1}{E}\left(\sigma_z - \nu\sigma_\theta\right) + \alpha\Delta T_{wall}\frac{y}{t} \tag{3.62}$$

Solving, gives

$$\sigma_\theta = \sigma_z = \frac{-E\alpha\Delta T_{wall}}{\left(1-\nu\right)}\frac{y}{t} \tag{3.63}$$

2 Yield Criteria

Learning Summary

1. Recognise the difference between ductile and brittle failure, as illustrated by the behaviour of bars subjected to uniaxial tension and torsion (knowledge);
2. Describe the meaning of yield stress and proof stress, in uniaxial tension, for a material (comprehension);
3. Describe the Tresca (maximum shear stress) yield criterion and the 2D and 3D diagrammatic representations of it (comprehension);
4. Employ the Tresca yield criterion to determine whether yield has occurred in a structure (application);
5. Describe the von Mises (maximum shear strain energy) yield criterion and the 2D and 3D diagrammatic representations of it (comprehension);
6. Employ the von Mises yield criterion to determine whether yield has occurred in a structure (application).

2.1 Introduction

If a ductile material is subjected to uniaxial loading, as shown schematically in Figure 2.1(a), beyond a certain point (the initial yield stress, σ_{y0}) the stress-strain behaviour ceases to be linear (i.e. stress is no longer proportional to strain) as shown in Figure 2.1(b) and the material is said to have 'yielded'. Typical stress-strain curves for some materials are shown schematically in Figure 2.2. For some materials (such as the aluminium alloy in Figure 2.2), the yield stress is not easily discernible, in these cases an offset or proof stress is defined, commonly at 0.1 or 0.2% strain. This value is determined by drawing a line at the same gradient as the elastic portion of the stress-strain curve starting at at the value of strain at which the proof stress is to be determined, as shown in Figure 2.3. Loading past the yield stress, σ_{y0}, leads to permanent, unrecoverable deformation (permanent strain) of the material when the stress is removed, as shown by the quantity x in Figure 2.4.

Materials that can be subjected to large strains before failure, such as mild steel and the aluminium alloy in Figure 2.2, are known as ductile materials, these are good materials from an engineering perspective as they absorb a lot of energy and exhibit large deformations before failure. In contrast, grey cast iron is a brittle material and shows little or no yielding before failure.

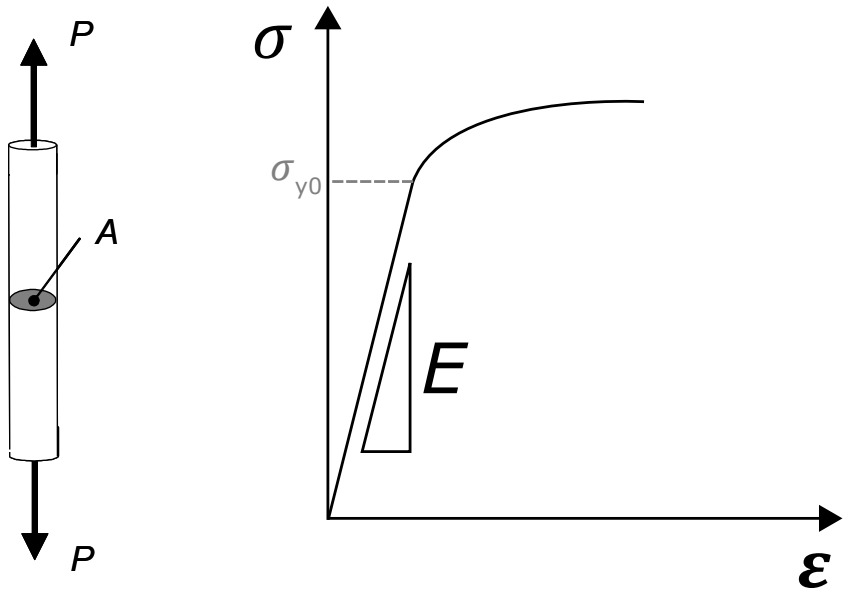

(a) (b)

Figure 2.1

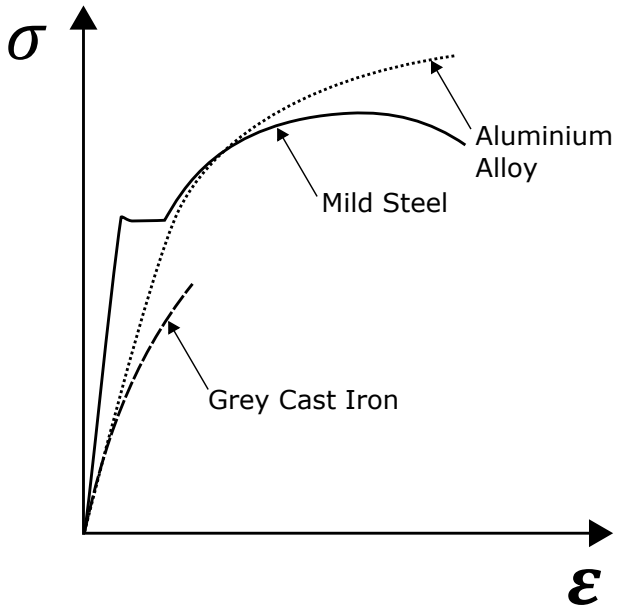

Figure 2.2

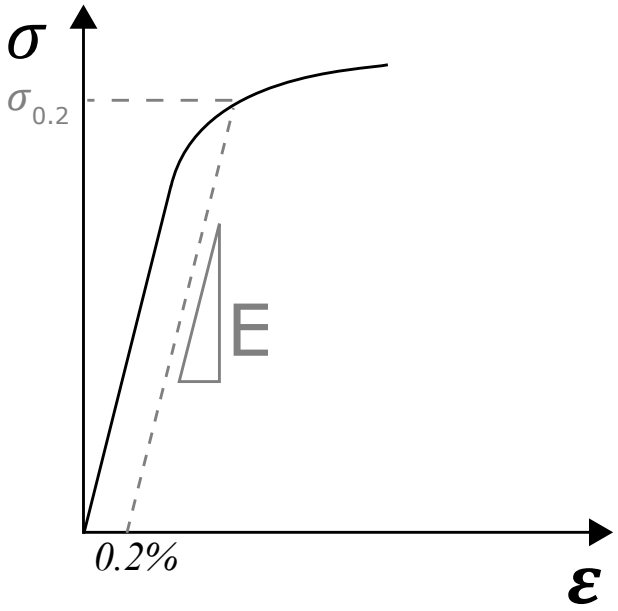

Figure 2.3

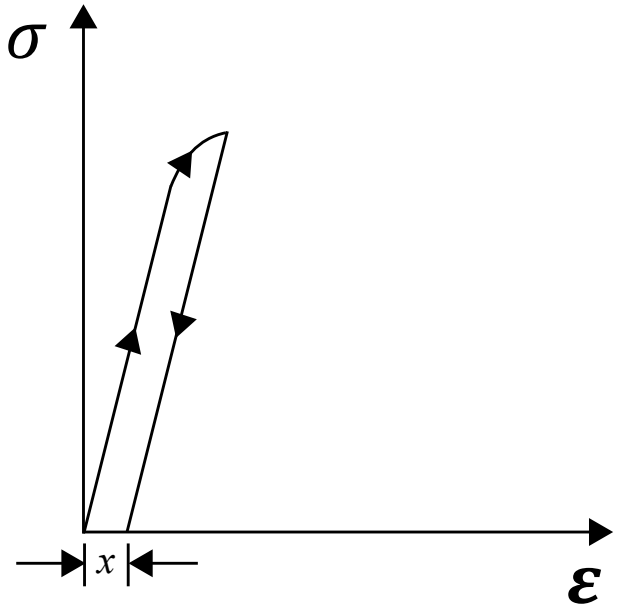

Figure 2.4

The ductility of a material is usually expressed as a percentage elongation or percentage reduction in area at failure. The percentage elongation is the failure strain of the sample expressed as a percent. If L_f is the final length of the specimen at failure and L_0 is the original length, the percent elengation is expressed as:

$$Percent\ elongation = \frac{L_f - L_0}{L_0}(100\%) \qquad (2.1)$$

The percentage reduction in area can be expressed as:

$$Percent\ reduction\ in\ area = \frac{A_0 - A_f}{A_0}(100\%) \qquad (2.2)$$

where A_0 and A_f are the initial and final cross sectional areas respectively.

2.2 Failure of Ductile Materials

The failure of a tensile test specimen of a ductile material, such as mild steel, tends to be a 'cup and cone' mode of failure as shown in Figure 2.5(a) with a cone angle of 45°. Analysis of the Mohr's circle for the loading condition, as shown in Figure 2.5(b) indicates that the 45° plane is the plane on which the maximum shear stress occurs.

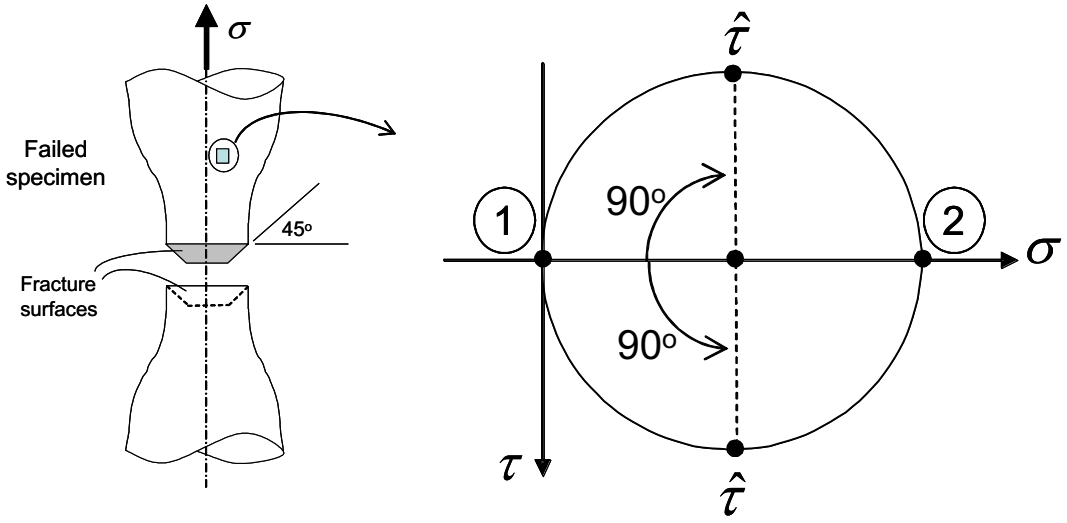

(a) (b)

Figure 2.5

If a circular cross section bar of ductile material (mild steel in this case) is subjected to torsional loading as shown in Figure 2.6(a), the torque-angle response is shown in Figure 2.6(b). For $T \leq T_y$, $T \propto \theta$ and the torque-angle behaviour is reversed on removal of the torque. If the torque is continuously increased until failure occurs, the fracture plane is transverse to the axis of the specimen as shown in Figure 2.7. A Mohr's circle for the torsion loading case, also shown, indicates that failure occurs on the maximum shear stress plane.

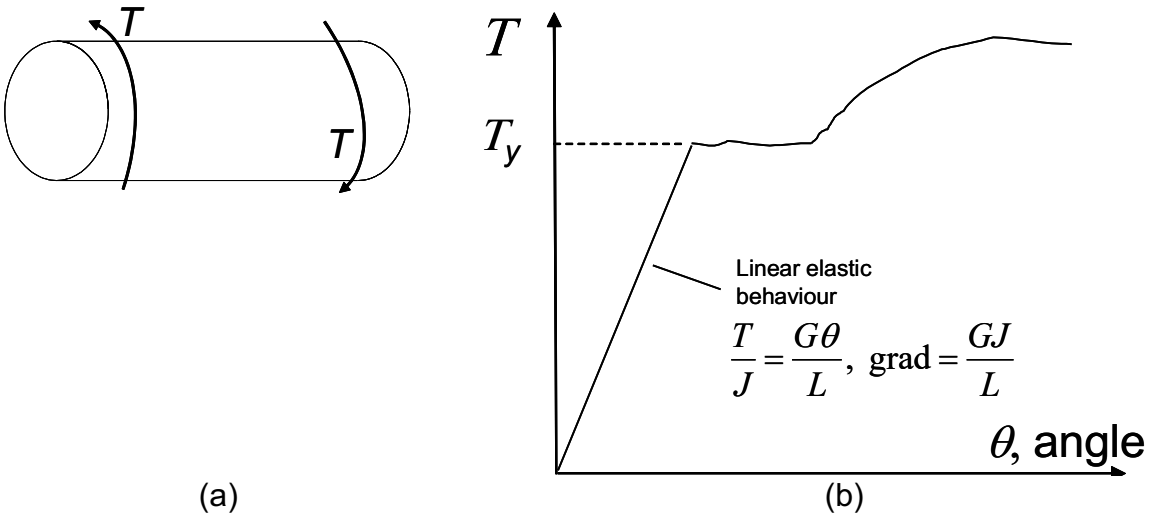

Figure 2.6

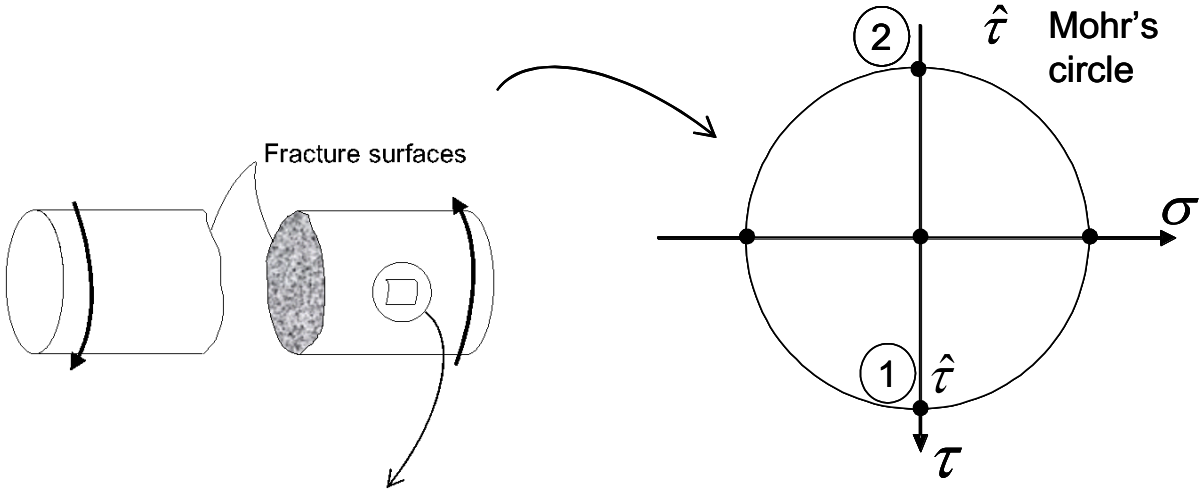

Figure 2.7

Therefore, the results of both the tension and the torsion tests indicate that failure occurs on the planes that contain the maximum shear stresses. This behaviour is similar to that of many "ductile" materials.

2.3 Failure of Brittle Materials

The failure of a tensile test of a brittle material, such as grey cast iron, will tend to be a flat fracture surface perpendicular to the loading direction, as shown in Figure 2.8. As previously mentioned there is little or no plastic deformation and the crack propagation across the fracture surface is very fast.

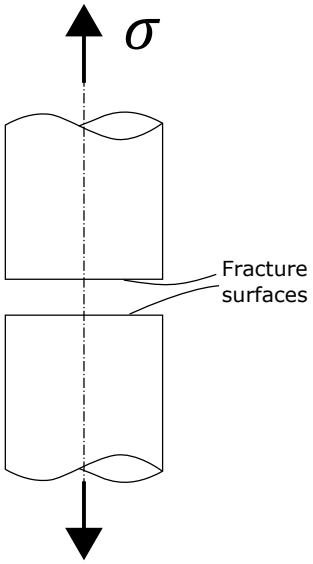

Figure 2.8

A torsion test on a brittle material will lead to a torque-angle response as shown in Figure 2.9 and will lead to a 45° helical failure in the specimen as shown in Figure 2.10.

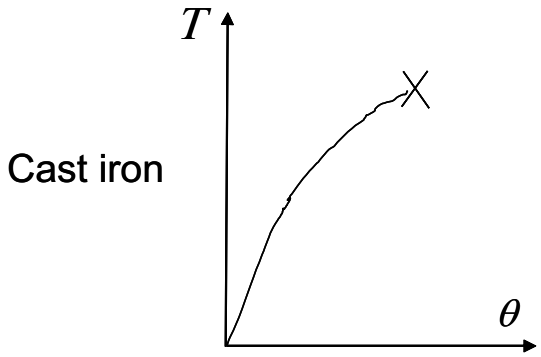

Figure 2.9

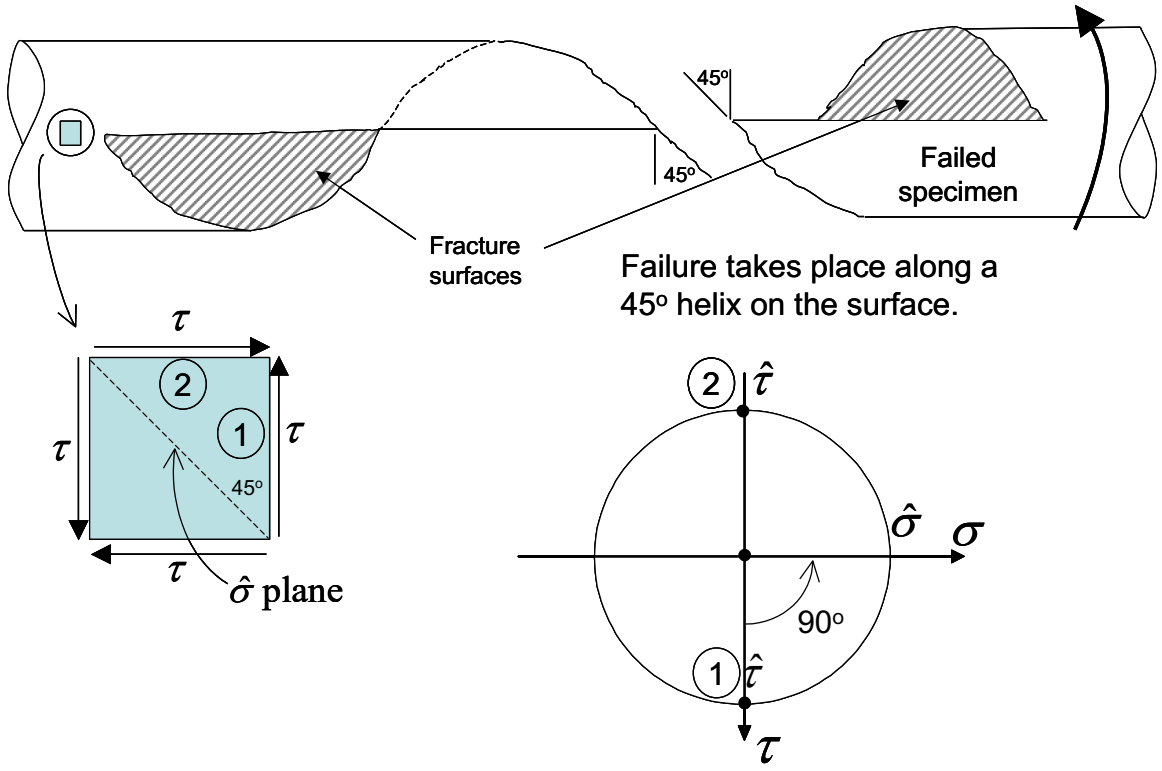

Figure 2.10

A Mohr's circle for this loading condition, also shown in Figure 2.10, shows that the point on the Mohr's circle associated with the maximum principal stress is 90° (ccw) from point 1. Therefore, this represents a plane at 45° from plane 1 on the element. This maximum principal stress, $\hat{\sigma}$, plane corresponds to the 45° helix angle of the fracture on the surface. This indicates that failure in this material has occurred on a plane on which the maximum principal stress exists.

The tests and stress states used to come to the above conclusions for "ductile" and "brittle" failures are very simple and it would therefore be unwise to base failure criteria on this evidence alone.

2.4 Yielding of Ductile Materials

The topic of "Yield Criteria" is limited to the prediction of the initiation of yielding in "ductile" materials.

Two criteria that generally provide a good indication of yield that are widely used in elastic-plastic analysis are the maximum shear stress (Tresca) criterion and the maximum shear strain energy (von Mises) criterion.

2.5 The Maximum Shear Stress (Tresca) Yield Criterion

If σ_1, σ_2 and σ_3 are the principal stresses in three-dimensions ($\sigma_1 > \sigma_2 > \sigma_2$) then as shown in the Mohr's circle in Figure 2.11:

$$\tau_{max} = \frac{\sigma_3 - \sigma_1}{2} \tag{2.3}$$

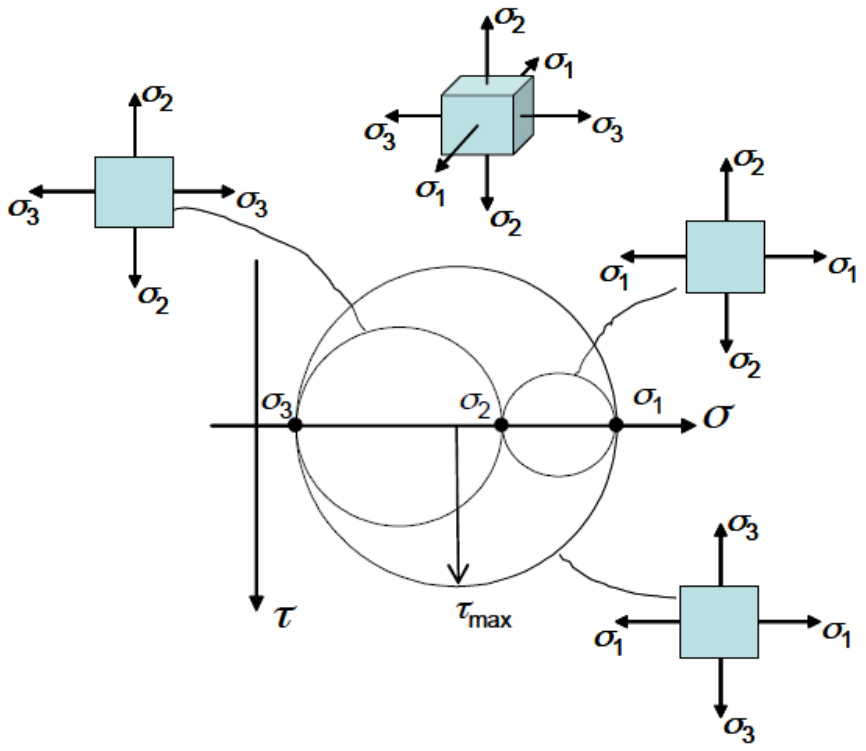

Figure 2.11

The Tresca yield criterion states that the material will yield when the maximum shear stress in the material exceeds a limiting value, this limiting value can be related to the uniaxial yield stress, σ_y when $\sigma_1 = \sigma_y$, σ_2 σ_3 = 0

$$\tau_{max} = \frac{\sigma_y - 0}{2} = \frac{\sigma_y}{2} \tag{2.4}$$

The Tresca (or τ_{max}) yield criterion therefore states that the material will yield if

$$\sigma_1 - \sigma_3 \geq \sigma_y \text{ for } \sigma_1 > \sigma_2 > \sigma_3 \quad (2.5)$$

2.6 The Maximum Shear Strain Energy (von Mises) Yield Criterion

The von Mises yield criterion states that the material will yield when the maximum shear strain energy (per unit volume) exceeds a limiting value. If σ_1, σ_2 and σ_3 are the three principal stresses ($\sigma_1 > \sigma_2 > \sigma_3$) then:

$$\frac{\text{shear strain energy}}{\text{unit volume}} = \frac{1}{12G}\{(\sigma_1 - \sigma_2)^2 + (\sigma_2 - \sigma_3)^2 + (\sigma_3 - \sigma_1)^2\} \quad (2.6)$$

Again, the limiting value can be related to the uniaxial yield stress, σ_y, obtained from a uniaxial tensile test. Thus, at yield when $\sigma_1 = \sigma_y$, σ_2 σ_3 = 0:

$$\frac{\text{shear strain energy}}{\text{unit volume}} = \frac{1}{12G}\{2{\sigma_y}^2\} \quad (2.7)$$

The von Mises yield criterion can thus be expressed as follows:

$$\frac{1}{12G}\{(\sigma_1 - \sigma_2)^2 + (\sigma_2 - \sigma_3)^2 + (\sigma_3 - \sigma_1)^2\} \geq \frac{1}{12G}\{2{\sigma_y}^2\} \quad (2.8)$$

which can be reduced to the following, more common expression for the onset of yield, according to the von Mises yield criterion:

$$(\sigma_1 - \sigma_2)^2 + (\sigma_2 - \sigma_3)^2 + (\sigma_3 - \sigma_1)^2 \geq 2{\sigma_y}^2 \quad (2.9)$$

2.7 Two-dimensional Stress Systems (i.e. $\sigma_3 = 0$)

The yield boundaries for both the Tresca and von Mises in a two-dimensional stress-state are shown in Figure 2.12. For plotting purposes here, σ_1 and σ_2 can take on any values, i.e. σ_1 is not necessarily always greater than σ_2.

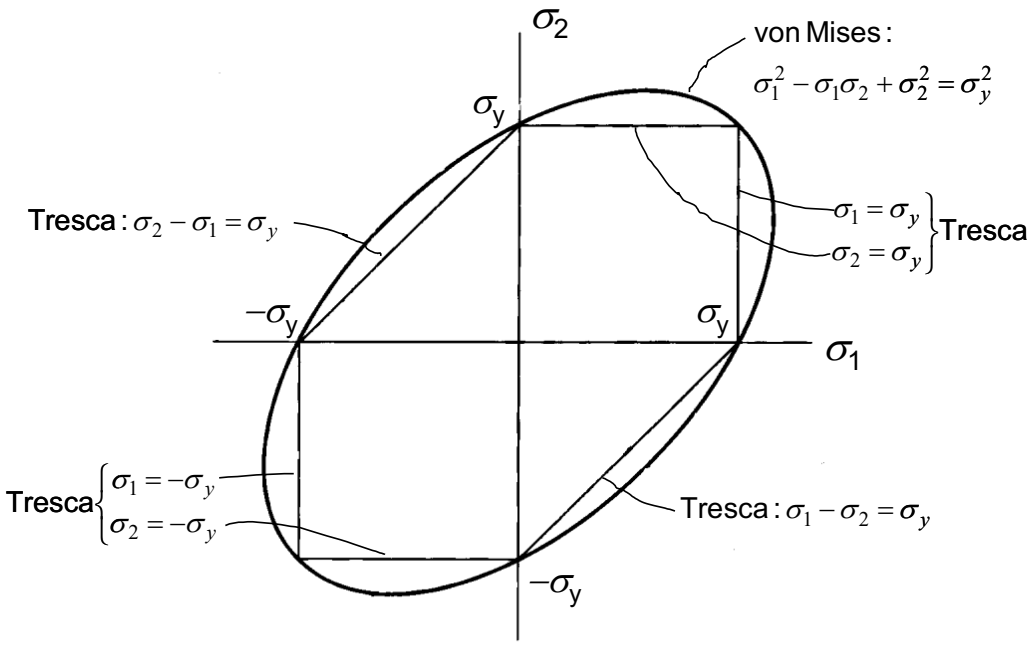

Figure 2.12

In general, the von Mises yield criterion is easier to handle analytically because it is continuous. This is particularly important for the calculation of incremental plastic strains, since the plastic strains are related to the normal to the yield surface and at the corners of the Tresca yield locus there is ambiguity about the directions of the normal, whereas there is no such ambiguity about the von Mises yield locus.

2.8 Three-dimensional Stress Systems

The Tresca and von Mises yield criterion are not altered if a constant stress component (σ) is added to each stress component:

$$(\sigma_1 + \sigma) - (\sigma_3 + \sigma) = \sigma_1 - \sigma_3 = \sigma_y \qquad (2.10)$$

and

$$\begin{aligned}&\big((\sigma_1+\sigma)-(\sigma_2+\sigma)\big)^2+\big((\sigma_2+\sigma)-(\sigma_3+\sigma)\big)^2\\&\quad+\big((\sigma_3+\sigma)-(\sigma_1+\sigma)\big)^2\\&\quad=(\sigma_1-\sigma_2)^2+(\sigma_2-\sigma_3)^2+(\sigma_3-\sigma_1)^2=2{\sigma_y}^2\end{aligned}\qquad(2.11)$$

This implies that the addition of a "hydrostatic stress state", i.e. $\sigma_1 = \sigma_2 = \sigma_3 = \sigma$ does not change the shapes of the yield surfaces shown in the section on two-dimensional stress systems.

The mean principal stress $\sigma_h = \frac{1}{3}(\sigma_1 + \sigma_2 + \sigma_3)$, which is known as the *hydrostatic stress* for a given stress state ($\sigma_1, \sigma_2, \sigma_3$), is the stress which causes volume change. Now, the independence of the yield criteria with respect to hydrostatic stress means that the three-dimensional yield criteria are prismatic surfaces with the axes of the prisms in each case being the line $\sigma_1 = \sigma_2 = \sigma_3$. This is called the *hydrostatic line* in 3D stress space (Haigh-Westergaard stress space) and it has direction cosines $(\frac{1}{\sqrt{3}}, \frac{1}{\sqrt{3}}, \frac{1}{\sqrt{3}})$. The yield boundaries can thus move any distance in the direction $\sigma_1 = \sigma_2 = \sigma_3$. The yield surfaces for both the von Mises and Tresca yield criteria therefore have a constant oblique section and hence a constant perpendicular cross-section, whose true shape can be seen in the view along the line $\sigma_1 = \sigma_2 = \sigma_3$. Any arbitrary stress 'vector' ($\sigma_1, \sigma_2, \sigma_3$), e.g. $\overrightarrow{OB}$ and$\overrightarrow{OD}$, (Figure 2.13), in the stress space can be decomposed into two components, one parallel to the hydrostatic line, e.g. $\overrightarrow{OA}$ and $\overrightarrow{OC}$, and one perpendicular to the hydrostatic line, e.g. $\overrightarrow{AB}$ and $\overrightarrow{CD}$. The oblique planes which are perpendicular to the hydrostatic line are called deviatoric planes and are given by equations of the form $\sigma_1 + \sigma_2 + \sigma_3 = const$, each representing a different level of hydrostatic stress. The deviatoric plane with $\sigma_1 + \sigma_2 + \sigma_3 = 0$ is known as the π-plane. It can be shown that the component of ($\sigma_1, \sigma_2, \sigma_3$) parallel to the hydrostatic line is ($\sigma_h, \sigma_h, \sigma_h$), e.g. $\overrightarrow{OA}$ and $\overrightarrow{OC}$, while the component parallel to the deviatoric planes is $(\sigma_1 - \sigma_h, \sigma_2 - \sigma_h, \sigma_3 - \sigma_h)$, $\overrightarrow{AB}$ and $\overrightarrow{CD}$. Only the latter component of stress is important in determining yield according to the von Mises and Tresca criteria.

The representation of yield surfaces for a three-dimensional stress state and the decomposition of the stress into hydrostatic and deviatoric components are shown in Figure 2.13.

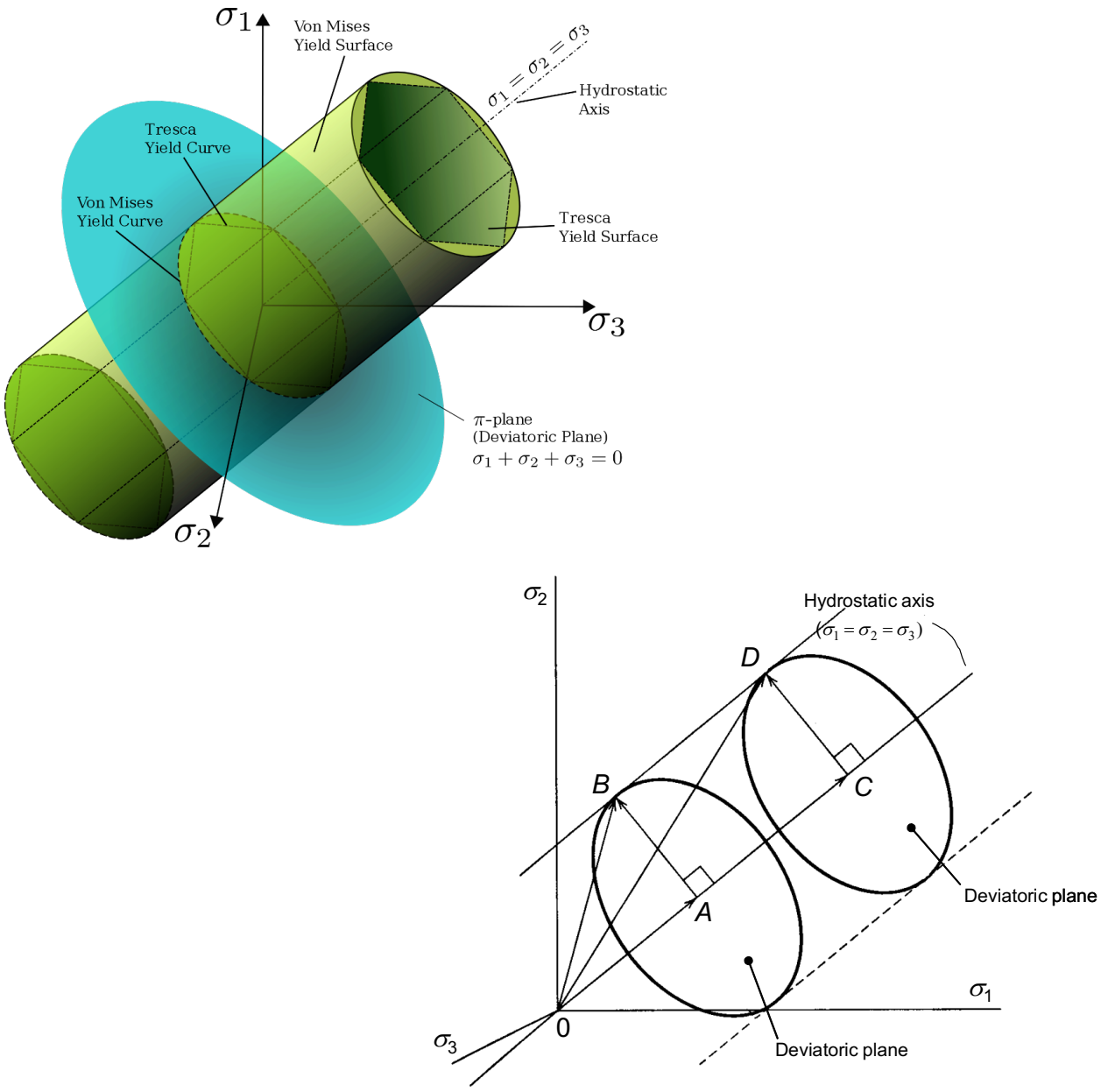

Figure 2.13

The view along the $\sigma_1 = \sigma_2 = \sigma_3$ line of the von Mises and Tresca yield criteria is an isometric view showing the three axes included at 120° intervals. This is sometimes called a view on the π-plane, as shown in Figure 2.14 on which the Tresca yield surface is a hexagon and the von Mises yield surface is a circle. Therefore, large principal stresses do not necessarily result in yield; it is the stress differences and the route to the final stress

state that govern whether yielding will occur.

Figure 2.14 can be used, instead of the equations, to decide whether a certain stress state will be safe. Simply plot on the diagram each of the three principal stresses parallel to each of the three axes and see whether the final point lies inside the appropriate yield surface.

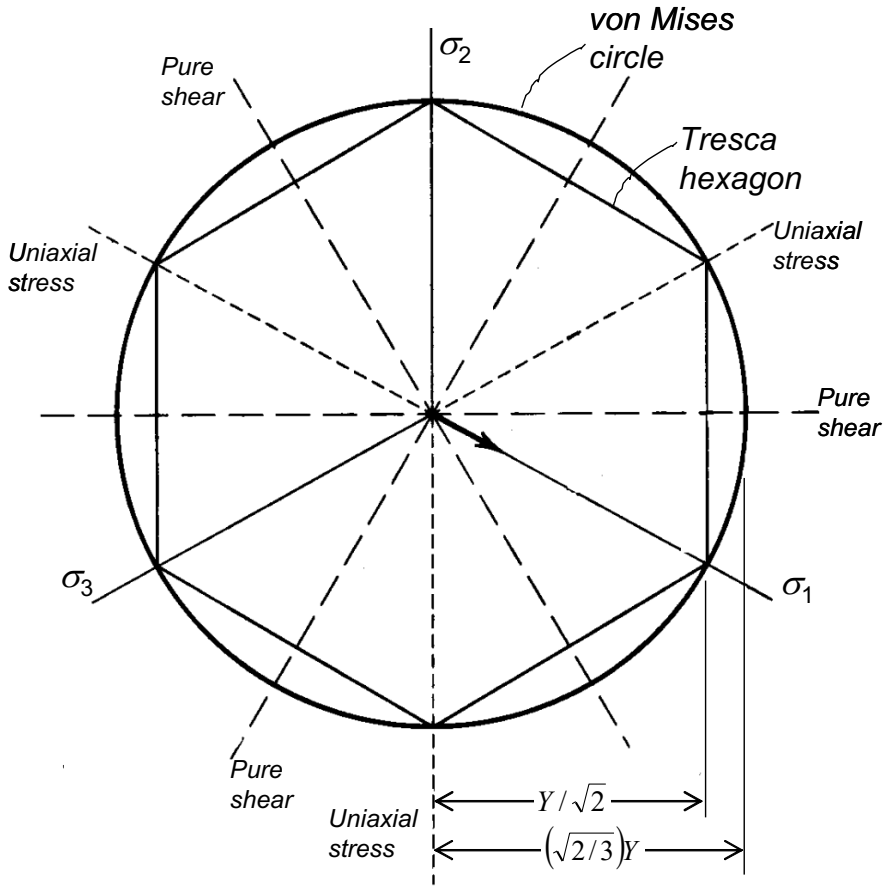

Figure 2.14

NB:

(i) The yield condition can be examined by either using the appropriate equation, i.e.

Tresca: $\sigma_1 - \sigma_3 = \sigma_y \ \ (\sigma_1 > \sigma_2 > \sigma_3)$

von Mises: $(\sigma_1 - \sigma_2)^2 + (\sigma_2 - \sigma_3)^2 + (\sigma_3 - \sigma_1)^2 = 2{\sigma_y}^2$

or by plotting principal stresses on the π-plane.

(ii) All three principal stresses are important. At free surfaces the normal stress is usually zero, but it may be important, particularly if the other two principal stresses are of the same sign.

Note: The last three figures are taken from Boresi, Schmidt and Sidebottom, “Advanced Mechanics of Materials”, 5th Ed, Wiley & Sons, 1993.